Universitat Autònoma de Barcelona

Plant Species Climatic Niche and its Relationship with Population Responses to Extreme Drought

Maria Ángeles Pérez Navarro

Plant Species Climatic Niche and its Relationship with Population Responses to Extreme Drought

DOCTORADO EN ECOLOGIA TERRESTRE

Centre de Recerca Ecològica i Aplicacions Forestals

Universistat Autònoma de Barcelona

PhD Thesis Maria Ángeles Pérez Navarro

Advisors: Francisco Lloret Maya

Miguel Ángel Esteve Selma

December 2019

Acknowledgements

A pesar de ser firme defensora de que la tesis no supone un mérito excepcional digno de especiales reconocimientos, no desperdiciaré la oportunidad de agradecer todo lo vivido durante estos años y dejar grabado lo mucho que deben estas páginas a las personas que me rodean.

Durante esta etapa, que empezó cuando llegué a Barcelona, he tenido la suerte de encontrar a personas maravillosas, de viajar por el mundo y de aprender sobre diferentes aspectos de la vida. Quiero agradecer en primer lugar, a la que fue mi primera familia en Catalunya, mis compañeros de máster, en especial a Estrella, Aida, Alba, Aina, Carla, Enrique, John y Gustavo y a mis compañeros de piso Laura y Josan. Gracias por los ratos en el césped, las visitas a Mataró y las noches arreglando el mundo en el *Cop de ma*, gracias, en definitiva, por hacerme sentir en casa.

Cuando una empieza la tesis le dicen que debería preocuparse de escoger bien a sus directores porque son personas con las que tendrá que compartir cuatro años y ver más a menudo que a sus propios padres. Yo con Paco apenas tuve dos reuniones antes de solicitar el doctorado. Después de estos más de cuatro años trabajando juntos sé que si volviese atrás volvería a elegirte. Gracias Paco por el ejemplo, por las charlas en los viajes, por tu forma de pensar tan crítica y profunda, por enseñarme tanto más allá de lo estrictamente académico... A Miguel Ángel lo conocía más. Fui su alumna durante la carrera y sé que pocas personas tienen un conocimiento más holístico de la naturaleza murciana, mayor integridad y devoción por su trabajo. Gracias por aportar siempre la perspectiva más naturalista y aplicada, gracias por las charlas de política y las explicaciones sobre el Mar Menor. Durante estos años he crecido con y gracias a vosotros, y no podría sentirme más afortunada.

Además esta tesis no hubiese tenido los mismos resultados sino hubiese compartido las dudas, preocupaciones, alegrías y el desánimo con tantos buenos compañeros.

Gracias a los compañeros de despacho, a Anna, Javi, Judit, Carlos, Manu, Marta, Pere y Pol. Sin duda las penas han sido menos penas con vosotros y las fiestas, almuerzos y barbacoas mucho más divertidas. Gracias por las risas y la terapia de grupo. No me acostumbro a pensar en un trabajo sin vosotros.

Gracias también a los compañeros de grupo. Enric, Jordi, Luciana y Nuria, el *phoskitos lab* no podría tener mejor plantilla. Con vosotros se demuestra que hacer ciencia no está reñido con un ambiente laboral de calidad, colaborativo, respetuoso y divertido. Gracias por tantos buenos momentos, por las salidas a la montaña y las jornadas de convivencia en los congresos. Quiero agradecer también a mis compañeros de departamento en Murcia. Gracias a Paqui, Jose Miguel y Pablo por el trabajo de campo y de despacho, por las discusiones académicas y las no tan académicas, por no haber dudado en ayudar siempre que lo he necesitado. Gracias también a Guillem por las semanas de trabajo y convivencia en Murcia y tus dosis de amabilidad y optimismo, a Pep Serra y Gerard Sapes por los sabios consejos y la inspiración.

Durante estos últimos años también he tenido la oportunidad de librarme de los calurosos veranos catalanes y murcianos escapándome de estancia a otros países. Gracias a Jens-Christian por la acogida en Aarhus y a Antoine y Olivier por la estancia en Suiza. Me quedo con el recuerdo de los paseos en bici por Dinamarca y la estampa de los Alpes por la ventana del despacho y las barbacoas en el lago Leman. Gracias también a los que han estado siempre ahí, a los amigos de toda la vida, Jose, Maria José, Mari Nieves, Maria Victoria, Álvaro y Pedro. Gracias por estar tan cerca a pesar de los kilómetros, gracias por las visitas, por aguantar con paciencia mis quejas sobre política y ciencia, por los cafés, las terapias y el consuelo. Gracias también a Victor M. por el tiempo que hemos pasado juntos en Barcelona, por las horas de desahogo mutuo y los planes culturales.

Quiero agradecer también a mi hermano mayor, por plantar la semilla del amor por la naturaleza, sin tu ejemplo no hubiese dado los primeros pasos del camino que ahora completo. Gracias también a mi hermano mellizo por la ayuda incondicional e implicación, llegando incluso a armarte con botas y cinta métrica para echar una mano en el trabajo de campo.

Gracias sobre todo a quien desde hace más de tres años es mucho más que un compañero de despacho. Gracias Víctor por tu compresión, tu paciencia, tus consejos

y buenas ideas. Gracias literalmente por tu ayuda. Gracias por animarme y hacerme ver siempre el vaso medio lleno. Por darme una segunda familia en Catalunya.

Gracias finalmente a mis padres, a quienes una época cruel y la falta de recursos les despojó de la oportunidad para completar etapas académicas más allá de los estudios más elementales. Sabed que habría sido posible llegar hasta aquí sin vosotros.

Table of Contents

List of Tables

List of Figures

Abstract

Understanding how climate affects species' distribution and performance is a central issue in ecology since its origins. In last decades, however, the interest in this question has been reactivated by the current context of climate change. Species Niche Modelling has been widely used to assess shifts in species distribution and to test the relationship between species' climatic niche and species physiological and demographic performance, implicitly assuming that species occurrence portrays the environmental and biotic species' suitable conditions. Nevertheless it is still largely undetermined whether these models can portray population and community responses, particularly in relation to extreme climatic episodes.

In this thesis I aim at exploring the capacity of niche modelling to predict species decay under extreme climatic conditions, particularly droughts, addressing some constraints of this approach and proposing possible solutions. To achieve this goal, I counted with 3 vegetation decay datasets measured in the Spanish SE after the extreme drought year 2013-2014. Two of these datasets were based on defoliation sampling of individual plants belonging to more than 40 semiarid shrubland species (chapters 2, 4 and 5), while the other one was based on regional compiled data of *Pinus halepensis* L. affectation in plots of $1km^2$ (chapter 3). In second chapter I used different Species Distribution Model (SDMs) algorithms to estimate species' climatic suitability before (1950-2000) and during the extreme drought, in order to test the possible correlation between suitability and decay, and whether the existence of this relationship depended on the applied SDM algorithm. I consistently found a positive correlation between remaining green canopy and species' climatic suitability before the event, suggesting that populations historically living closer to their species' tolerance limits are more vulnerable to drought. Contrastingly, decreased climatic suitability during the drought period did not correlate with remaining green canopy, likely because of extremely low climatic suitability values achieved during the exceptional

climatic episode. In order to test whether this extremely low suitability values could derive as a consequence of only considering climatic averages when calibrating SDMs, in the third chapter I developed a method to include inter-annual climatic variability into niche characterization. I then compared the respective capacities of climatic suitabilities obtained from averaged-based and from inter-annual variability-based niches to explain demographic responses to extreme climatic events. I found that climatic suitability obtained from both niches quantifications significantly explained species demographic responses. However, climatic suitability from inter-annual variability-based niches showed higher explanatory capacity, especially for populations that tend to be more geographically marginal. In the fourth chapter I tried to overcome the inability of the SDMs to predict populations decay during extreme conditions, as observed in the second chapter, by using Euclidean distances to species' niche in the environmental space. I compared the capacities of both population distances in the climatic environmental space and population climatic suitability derived from SDMs to explain population observed physiological and demographic responses to an extreme event. Additionally, I tested such relationship in populations located in three different bedrock sites, corresponding to a gradient of water availability. I found that SDMs-derived suitability failed to explain population decay while distances to the niche centroid and limit significantly explained population die-off, highlighting that population displaced farther from species' niche during the extreme episode showed higher vulnerability to drought. The results also suggested a relevant role of some bedrocks buffering species decay responses to extreme drought events mainly according to soil water holding capacity. Finally, in the fifth chapter, I used species niche characterizations in the environmental space and demographic data to address the impact of extreme events at community level. Particularly, I estimated the community climatic disequilibrium before and after a drought episode along a gradient of water availability in three bedrock types. Disequilibrium was computed as the difference between observed climate and community-inferred climate, which was calculated as the mean of species' climatic optimum weighted by species abundance collected in field surveys. I found that extreme drought nested within a decadal trend of increasingly aridity led to a reduction in community climatic disequilibrium, particularly when combined with low water-retention bedrocks. In addition, community climatic disequilibrium also varied before the extreme event across bedrock types, according to soils water-retention capacity. In conclusion, by developing different techniques, de-

rived from species distribution, that characterize climatic accuracy at population and community level, this work reveals the capacity of species climatic niche to explain demographic responses under climate change-induced episodes of extreme drought.

1

Introduction

1.1 Understanding species distribution in a changing climate

1.1.1 Climate as driver of species distributions

The current context of anthropogenic climate change has recently fueled the attention given to climate in ecological studies. However, the interest on knowing the effect of climate in species distribution is an old issue. More than two centuries ago, Alexander von Humboldt realized that the vast diversity of plant forms was frequently distributed following specific patterns along altitudinal and latitudinal gradients, from dense forest on lowlands and low latitudes to grasses and lichens on high elevations and latitudes (Morueta-Holme & Svenning, 2018; von Humboldt & Bonpland, 1807 (2009)). Although other authors have previously perceived the possible relationship between climate and vegetation (Lomolino et al. 2004, Jackson 2009), Humboldt was the first on reporting causation by systematically inventorying plant distributions and recording information on environmental parameters. That approach could be considered as a kind of early correlative distribution model and laid the foundations of biogeography science. Since Humboldt essay, climate has been widely recognized as a key factor on plant species distribution (von Humboldt and Bonpland 1807 (2009), Woodward 1987). Nevertheless, other factors such as soils, biotic interactions, perturbations or herbivory have since been recognized as relevant drivers (Morueta-Holme and Svenning 2018, Pausas and Bond 2018).

As a consequence of this coupling between vegetation and climate, it is inferred that plant species could respond to changes in climate mainly in three different ways: by changing their distribution according to the speed and direction of change in climate, therefore migrating; by maintaining their distribution but modifying the way they interact with climate, being able to survive under conditions previously unsuitable for their survivorship, therefore adapting; or by disappearing if migration and adaptation rates do not match the climate change climate velocity, therefore becoming extinct. While paleoecological records along the last Quaternary glacial-interglacial periods strongly support species capacity to track the climate (Huntley and Webb 1989, Webb III 1992, Hewitt 2000, Davis and Shaw 2001), past evidences of plant species adaptations to changing environments are less frequent (Davis and

Shaw 2001). This suggests that plant species shift their distribution more readily than they evolve to tolerate new environmental conditions, although both processes are not mutually exclusive (Ackerly 2003, Aitken et al. 2008).

To properly track the climate at a given temporal scale, plant species are supposed to successfully establish in the new climatically favorable regions (leading edge) and disappear from regions that have become unfavorable (trailing edge) (Svenning and Sandel 2013) with a velocity according with the rate of climate change. Conversely, if climate change rate exceeds species dispersal capacities to arrive to new accurate locations, or species have large persistence time which retard populations extinction in the trailing edge, species will be in disequilibrium with climate (Blonder et al. 2017). Importantly, this capacity to track the climate is species-dependent, since each species responds to climate change with a particular rate and direction. As a consequence, communities composition do not remain constant during shifting climate processes (Ackerly 2003).

Current climate is changing with a velocity comparable to that observed during periods of maximum change during the Quaternary (Svenning and Sandel 2013). Human population growth and the increase in per-capita consumption rates after the industrial revolution are disrupting global natural systems at an unprecedented pace. Anthropic greenhouse gas emissions are responsible for the ongoing rapid climate change, with global average temperatures that could increase up to 4 degrees above the average for the period 1986-2005 by the end of this century (IPCC Working Group 1 2014). In addition to increase in global temperature, climate change is also leading to rainfall reductions in subtropical latitudes as well as increases in climate variability, which implies an increment in extreme events such as heat waves and severe droughts (Giorgi and Lionello 2008, IPCC Working Group 1 2014). Plant responses to these changes are already noticeable, from species migrations upward in elevation and poleward in latitude (Lenoir et al. 2008, Devictor et al. 2012), to increasing decay and mortality episodes in lowlands and in the equatorial range edge of species distribution (Allen and Breshears 1998, Jump et al. 2009). The contemporary environmental scenario poses a double threat for species' persistence, since rapid climate change is combined with the anthropogenic land surface transformation, which have generated artificial barriers that reduce species' dispersal capacity and increase the genetic isolation of populations.

Thus, knowing the factors that govern species distributions is as relevant today as it was in Humboldt's days, since understanding these forces is crucial to face the current environmental challenge, allowing us to predict the future species distribution and community composition, to anticipate population, species or ecosystems' vulnerability, as well as to correctly guide efforts in conservation to avoid severe losses in ecosystem services.

1.1.2 The niche concept

Humboldt progresses on linking organisms and environmental factors and his influence on further researchers probably constituted the germ for the emergence of the niche concept. This concept deeply permeates different fields of biology and environmental sciences, from ecology to evolution.

Since its birth, the niche concept has evolved and incorporated advances from others ecological theories, and its meaning has varied depending on time and author. The niche concept emerged in the first third of the 20th century and it is independently attributed to Joseph Grinell (1917) and Charles Elton (1927). Grinnell (1917) was the first explicitly coining the term, and described the niche as the set of environmental conditions that determines species distribution (that is what species require), while Elton (1927), apparently without influences from Grinnell's concept (Colwell and Rangel 2009), defined the niche as the species functional role in the biotic community, mostly referred to trophic level or food webs (that is, how species impact their community). In spite of the different orientation of each author, both definitions shared noticeable similarities, as in both cases the niche was a property of the environment, a place that exist independently of its occupant, that is, without been necessarily occupied by species.

Inspired by both two authors and by the principle of competitive exclusion (Volterra 1926, Gause 1934), Hutchinson formalized his niche concept in 1957 (Hutchinson 1957) as the n-dimensional hypervolume defined by the environmental dimensions within which species can survive and reproduce, permitting species to exist indefinitely. He also distinguished between fundamental niche, as the set of environmental conditions that allows species persistence in absence of competition, and realized niche, as the subset of the fundamental niche in which species can

persist in the presence of competitors. Although this is probably Hutchison's most famous and cited contribution, his richest and most innovative view about niche did not come until 1978 (Hutchinson 1978). Whereas his predecessors described the niche as a property of the environment, Hutchinson attributed the niche to species, which truly constitutes a theoretical advance, since in this way it is forced the separation of the physical space and the environmental space (i.e., an abstract space that describes the set of requirements of a species). From this duality physical space-environmental space (or niche-biotope sensu Colwell and Rangel 2009), it is inferred that species' distribution ranges are just the geographical translation of species' environmental requirements in the abstract hyperspace, as long as the combination of variables that constitute the species fundamental niche exists in the geographical space and competitors do not impede the species presence. This entails that the realized niche is not only constrained by the effects of species interactions (as stated by Hutchinson), but also implicitly by the lack of contemporary environments corresponding to parts of the fundamental niche (Colwell and Rangel 2009), see Figure 1.1a. This duality and the reciprocal correspondence between physical and environmental spaces constitute the core of species distribution models (SDMs), since they calibrate species niche in the environmental space from georeferenced occurrence data and then re-project back the distribution into the physical geographic space (Colwell and Rangel 2009).

The large weight of interspecific competition in Hutchinson's niche concept, possibly as a consequence of the relevance of competitive exclusion in contemporary theories (Pulliam 2000, Araújo and Guisan 2006, Colwell and Rangel 2009), hindered an accurate consideration of the role of species' dispersal limitations in causing species' absence in determined portions of the fundamental niche (Araújo and Guisan 2006). Pulliam (2000) integrated the niche concept with metapopulation theory (Hanski 1999), source-sink theory (Pulliam 1988) and dispersal limitation, emphasizing the relationship between species' niche and fitness, specifically population growth rate, which allow to identify species fundamental niche with those environmental conditions allowing for a positive intrinsic growth. According to him, species may frequently be present in unsuitable sites where environmental conditions do not permit indefinite persistence in absence of continued immigration (sink habitats). Alternatively, species could be absent from suitable habitats due to local extirpation or species dispersal

limitations. These situations points that estimating species suitability from habitat occupancy could be an oversimplification (Franklin 2010). These ideas crystallized in the conceptual model of Soberón (2007) that joins the set of dimensions that affect species distribution in the geographic space: abiotic factors (A), biotic factors (B), and accessible area given species' dispersal capacity (M), see Figure 1.1b. Species may be found in different combinations of these three dimensions, but population growth rate will only be positive at the triple intersection (source habitat). Subsets of the three dimensions where only M and B or M and A intersect will have negative growth rate (sink habitats). In addition, intersection between A and B (potential habitat) corresponds to suitable habitat that is unoccupied due to dispersal limitations.

A central premise to argue for stasis in paleoecological records is the evolutionary conservatism of species environmental tolerances, in other words, species' trend to maintain niches unchanged along evolutionary periods (Wiens and Graham 2005). Niche conservatism implies that functional links between environment and species demography will remain constant in different time periods and space regions. Even though it has been demonstrated that this assumption does not always hold -particularly when species ability to migrate is limited (Ackerly 2003) or during biological invasions (Broennimann and Guisan 2008)- it is implicitly assumed when forecasting future species distributions, since most distribution models extrapolate current links between species and environment. When considering precisely the prevalence of niche conservatism over niche shifts, it its inferred that species commonly respond to changes in climate by changing their distribution. This does not mean, however, that species respond simultaneously to changes in climate, so species observed ranges are not necessarily in close equilibrium with their environmental optimum conditions (Svenning and Sandel 2013). Therefore, inferring species requirements and tolerances assuming that species are in equilibrium with climate at a given time, may lead to niche characterization' misinterpretations.

After the above mentioned evolution in the niche theory, and despite this fell from grace during the late 70s and early 80s -probably due to the crisis of the interspecific competition concept, to which niche concept was closely related (Wiens et al. 2009)-, the niche theory is now suffering a kind of renaissance (Colwell and Rangel 2009), driven precisely by the growing use of species distribution models in the current context of climate change and their application in conservation biology.

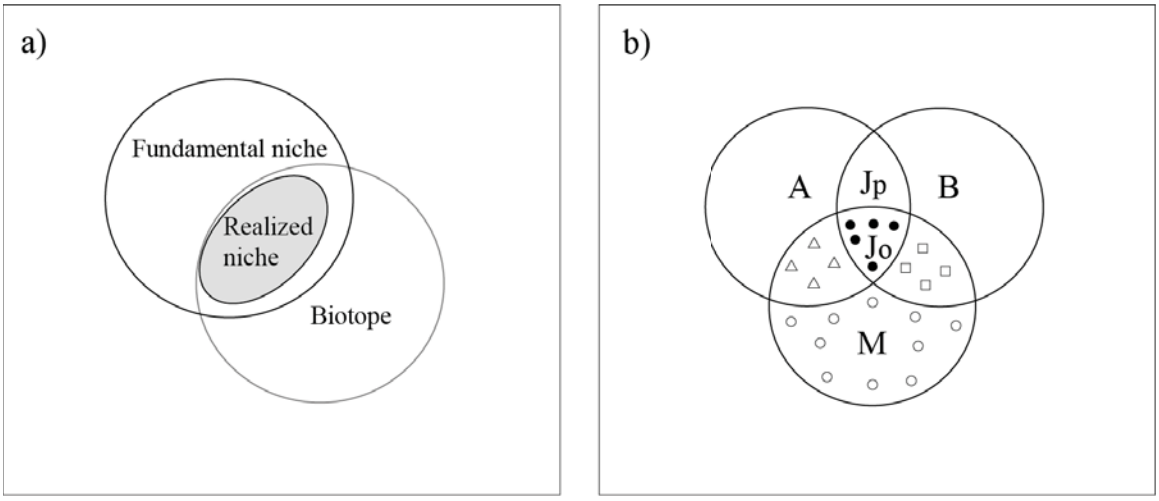

Figure 1.1: a) Hutchinson niche concept. The biotope constitutes the range of environmental variables that occur in a given geographic area. The fundamental niche corresponds to the set of environmental conditions that allows species persistence. The realized niche is a subset of the environmental space which constitute the fundamental niche coinciding with the availability of environmental conditions of the geographical space, discarding those areas where competitors impede the species presence. (Figure modified from Franklin 2010). b) Diagram of the three dimensions determining species geographic distribution. A represents the geographical area where abiotic conditions allow for a species' positive intrinsic growth rate. B represents the geographical area where the species can exclude or coexist with competitors. M represents the total area accessible to the species given it dispersal capacity. Solid circles represent occupied area with source populations. Open triangles are sink due to competitive exclusion. Open squares represent sink populations due to the lack of accurate abiotic conditions. Open circles are sink populations due to combinations of this previous two (abiotic and biotic conditions). J_o is the occupied area and J_p is the potential occupied area, where only species dispersal capacity limit the species presence. Figure simplified from (Soberón 2007).

1.1.3 Species niche and community assembly

Niche differences enable species to coexist explaining a substantial proportion of the diversity patterns observed in communities. It is widely acknowledged that variations in biodiversity patterns derives from multiple assembly processes whose relative importance varies between communities (Takahashi and Tanaka 2016, Li et al. 2018). These processes determining community composition include: drift (neutral and stochastic processes, Hubbell 2001), selection (niche processes, including both environmental and biotic filtering, Macarthur and Levins 1967, Keddy 1992), disper-

sal (a combination of stochastic and trait-dependent processes, Belyea and Lancaster 1999, Vellend 2010) and speciation (Ricklefs 2008, Vellend 2010). In addition, it is generally recognized that these processes are arranged as hierarchical filters that allow or impede the entry of each prospective community member (Pearson et al. 2018). Speciation is the responsible of the global species pool and dispersal filter determine which biological units are able to colonize the local community (Belyea and Lancaster 1999, Weiher et al. 2011, Pearson et al. 2018). Then, niche processes select the species subset with appropriate niches for persisting after environmental and biotic filtering. First, environmental filtering removes those species unsuited to a specified set of environmental conditions (Keddy 1992) and causes overall similarity in the coexisting species niches. Later, biotic filtering (mainly competition) acts promoting niche differenciation, and therefore, reduces niche similarity and overlap (Weiher et al. 2011, Li et al. 2018). Nevertheless, these filters could act simultaneous and interactively (Adler et al. 2013), varying its relative weight across communities and time periods. All these drivers, in addition to demographic stochasticity and neutral dynamics, make community assembly a complex and context-dependent process (Pearson et al. 2018).

Despite this complexity, niche based processes (environmental and biotic filters) can still have substantial power to explain community structure, and its relevance could be measured and quantified, taking into account the spatial scale at which each filter is detectable (Weiher et al. 2011). Among other analyses, depicting species niches in the environmental space allows to assess the relative importance of these filtering processes, whether total community niche volume is lower than randomly expected combined with lower niches' dissimilarity than random (in order to test environmental filtering), or whether species niche volume and dissimilarity are higher than randomly expected (in order to test similarity limitations, due, for instance, to competition) (Li et al. 2018). Furthermore, it could be particularly useful to assess community changes occurring along with temporal changes in climate. For example, showing whether new climatic conditions are filtering community composition by reducing total niche volume or by reducing distances between community climatic optimum and occurring climate, linked to extinction or decreasing more unsuited species and increases or immigration of species with more accurate traits to the new climate.

1.2 Predicting species distribution

1.2.1 Species distribution modelling

Species distribution models (SDMs), also known as ecological niche models or predictive habitat distribution models, are widely used in ecology, evolutionary biology, and conservation plans (Franklin 2010, Guisan et al. 2013). A common characteristic of SDMs is that they are deeply rooted on the niche concept (Guisan and Zimmermann 2000). Generally, SDMs could be classify in two main different categories: correlative SDMs and mechanistic or process-based SDMs. Correlative SDMs statistically relate species occurrences or abundances with the environmental conditions of the sites where species occur to, then, project species potential distribution back in the geographic space, not explicitly accounting for the ecological and physiological processes underpinning this relationship. It is widely assumed that these SDMs estimate the species realized niche, since they implicitly include biotic interactions and cannot represent the regions of the fundamental niche that do not correspond to environmental combinations of the biotope (Kearney 2006, Colwell and Rangel 2009). In contrast, mechanistic SDMs use species' performance responses to environmental gradients (taken from controlled field or laboratory studies) to determine the range of species distribution knowing the environmental conditions in the physical space (Kearney and Porter 2009). Since these models allow to characterize the species' physiological tolerance limits to environmental variables, it is assumed that these mechanistic SDMs approximate the species fundamental niche (Kearney 2006). Nevertheless, due to the high requirements of knowledge of species' biology and the labor intensity of parametrizing species physiological responses (Holt 2009, Schurr et al. 2012), mechanistic SDMs are not widely used across species, particularly for those poorly studied ones. Since correlative models are the most widespread SDMs in literature and were used in the present thesis analyses, I will only detail correlative model procedures, referred as SDMs hereafter.

From the SDMs work flow (Figure 1.2) it is deduced that the reliability of SDMs estimates will depend on the quality of species occurrence data and environmental variables, as well as on the selected algorithm to calibrate the relationship between them. In addition, model accuracy could be assessed by using different evaluation

indices.

Species occurrence data used in SDMs are frequently included as presence/absence. As other statistical analyses, SDMs assumes that data used for calibration are random representative samples of the studied population. In particular, since SDMs aim to detect the species-habitat associations, the samples of occurrences must be representative from an environmental space view which not necessarily equate to geographical representativeness. Although random stratified and systematic sampling exist for some species (as national forest inventories or "gradsect sampling", Wessels et al. 1998, Mauri et al. 2017), which provide data on both species' presence and absence, this is usually not the case for the vast majority of species. Instead of that, most species only account for presence-only records from natural history surveys and museum collections, or from independent research studies, often compiled in global databases such as the Global Biodiversity Information Facility (GBIF, `http://www.gbif.org/`). In addition, these datasets are frequently biased in the geographical space in favor of spatially accessible areas. This bias could be translated into the environmental space and lead to misleading assessment of the relationship between species occurrence and environmental variables (Araújo and Guisan 2006, Franklin 2010). Anyway, even if representative samples with presence-absence data were reachable for most species, these data would also have some limitations, such us the equilibrium assumption (see previous section), since most species have still not reached their optimal conditions (Svenning and Skov 2004), the impact of management practice, favoring or hindering species presence in determined habitats, or the lack of population fitness information, so leading to not exclude sink populations (which have negative growth rate and are outside of species realized niche) from niche estimations. Indeed, these binary datasets (presence-absence) are worse proxies of species requirements than continuous records such as species abundance (Colwell and Rangel 2009) which allow to discriminate species habitat preferences within suitable areas.

On the other hand, these models include environmental variables recognized to be relevant determining species distribution, such as climate, soil, topography, disturbances, etc. (Franklin 2010). The values of these variables for occurrence localities are generally extracted from maps rather than from in situ measurements, given the

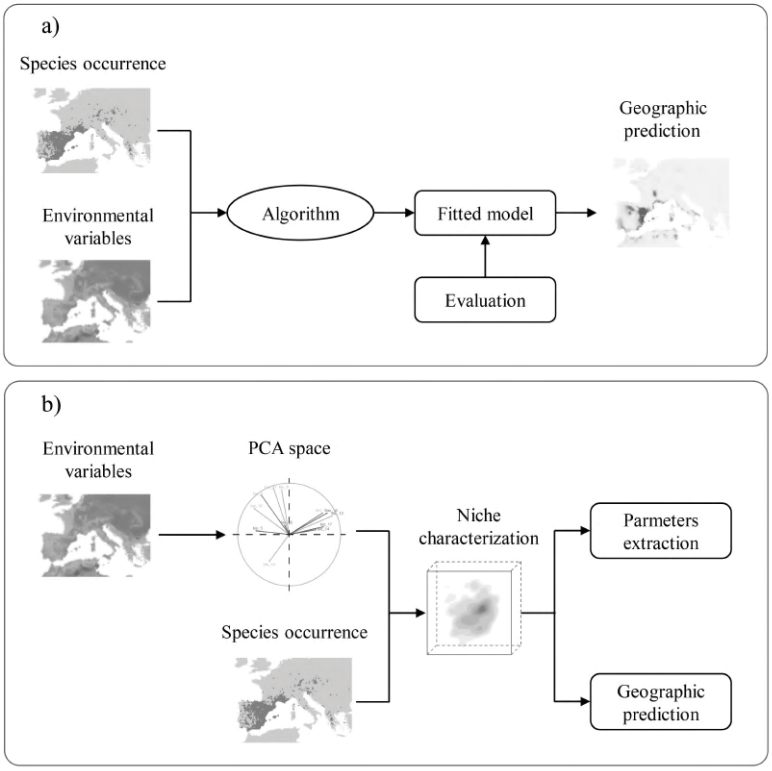

Figure 1.2: Workflow of SDMs (a) and niche characterization (b), illustrated on a study area representing the Mediterranean basin. a) Species observations are georeferenced on the field and the attributes of a set of environmental maps could be extracted for each one of them. Statistical model algorithm relates species observations to the environmental conditions observed in occurrences sites, fitting species response curves to each environmental predictor. The fitted model could be then applied over initial environmental maps projecting contemporary geographic distribution, or over new environmental conditions not used for model calibration (for example, by projecting future distribution under climate change). Fitted model is commonly evaluated by comparing model predictions with a subset of species occurrence not used during model fitting. b) Environmental conditions of each pixel of a region are used to build a principal component analyses (PCA) converting multiple correlated environmental conditions into a small number of uncorrelated variables. Then the environmental space is defined by the selected axis of the PCA (three in this case). Species occurrences could be then translated into this space, where kernel density functions allow to determine smooth density of every cell of the environmental space, determining species realized niche. This niche representation allows to obtain different parameters such as species niche centroid, limit, etc., as well as to convert niche density into environmental suitability, which could be translated again into the geographic space obtaining species geographic distribution maps.

volume of data and the geographic extent of most species ranges. In spite of the variety of potentially relevant variables in species distribution, SDMs frequently rely exclusively on climate predictors due to their primacy controlling species ranges but also due to the lack of fine grain resolution of other important environmental variables with high spatial heterogeneity such as soils (Franklin 2010). These climatic datasets are frequently inferred from a limited number of weather stations which become scarcer as they go back in time. In addition, the resolution of the most frequent global databases does not exceed 1 km^2 (Karger et al. 2017, Fick and Hijmans 2017) -although the spatial resolution of regional climatic databases may be considerably high (Ninyerola et al. 2007) -. These considerations imply that the climate experienced by organisms at ground level (microclimate) can substantially differ from dataset-inferred macroclimate, particularly in regions with elevated land cover and terrain variation (De Frenne et al. 2013). Linking species occurrence to climate values other than those really perceived by species could lead to errors characterizing species niche, which will be propagated when projecting species distribution both into past or future conditions. Less attention has been paid, however, to temporal resolution of climatic datasets. Generally, climatic variables are included as monthly and annual averages of reference periods of 30 or 50 years (Hijmans et al. 2005, Karger et al. 2017, Fick and Hijmans 2017), in most cases, irrespective of species lifespan. Using climatic averages instead of the total climatic variability could lead to constraints in niche characterization and underestimations in species distribution ranges.

Since the appearance of the first computer-based predictive modelling of species distribution in the mid-1970s (Austin 1971), an impressive diversity of modelling algorithms has increasingly become available (Guisan and Thuiller 2005). According to their functioning (and more or less coinciding with their emergence in chronological order), SDM algorithms could be classified as envelope and distance methods (such as BIOCLIM or mahalanobis distance), classical statistical approaches (such as GLM, GAM or MARS) and machine learning (such as random forest or MaxEnt) (Franklin 2010), representing, in addition, a gradient of growing complexity. The former group required presence-only species records, while the two latter groups require presence-absence or presence-pseudoabsence data (when real absences are not available). These variety of algorithms vary in how they deal with categorical variables, allow for predictor interactions, define smoothness of fitted response curves, adopt different statisti-

cal assumptions, weight variable contributions, predict species ranges and extrapolate species distribution in novel environments (Elith 2006, Franklin 2010). Some of the simplest models such as Mahalanobis distance assume that predictors are equally weighted, follow normal distribution and only consider linear relationships between them (Franklin 2010), whereas others more complex models such as MaxEnt can include high-order interaction terms and different degree of response curve smoothness, although they do not allow to deliberate and exactly control predictor interactions and the complexity of response curves, as statistical models do (Phillips and Dudík 2008, Elith and Graham 2009, Elith and Leathwick 2009). Generally, model outputs are ranged between 0 and 1, and are interpreted as environmental suitability or species' occurrence probability, though some algorithm outputs require to be transformed to obtain probability values. In addition, regarding the variety of methodological considerations, different algorithms also imply different predictions of species distributions. It has been suggested that simplest models are more suitable for extrapolation, while more complex models are supposed to be more suitable for interpolation (Franklin 2010, but see Elith et al. 2010). Nevertheless, there is still no clear consensus on which model best determines species distribution (Araújo and New 2007), instead model algorithm is selected depending on each particular study characteristics.

Although error and uncertainty can be evaluated at different steps of the modeling process, in case of SDMs model evaluation is typically synonymous with model performance and validity (Franklin 2010). Commonly, it consists on dividing the occurrence dataset on a training set to calibrate the model, and a test set to evaluate predictions' accuracy. In addition, differently from other statistical-model evaluations, SDMs accuracy measures are applied to categorical or probabilistic predictions referred to a categorical variable (presence-absence), which requires dedicated evaluation metrics (Guisan et al. 2017). There are different alternative accuracy indexes depending on the relevance of omission or commission errors, the necessity of using probability threshold or the dataset used for evaluation (presence-absence or presence-only). Area Under ROC Curve (AUC) is probably the most frequently used metric, based on the relationship between true and false positives which does not require threshold selection. Furthermore, it allows to compare different models predictive capacity provided that it could be affected by species prevalence (Segurado and Araújo 2004). Other indexes such as sensitivity, specificity, or boyce index could be useful in

cases that requires to particularly measure false negative rate, false positive rate or model accuracy using presence-only as test set, respectively.

Here details of numerous aspects about SDMs' data and implementation are not explained, since entering into more details is an overwhelming task that largely exceeds the boundaries of this introduction. I will refer the reader to Franklin 2010 and Guisan et al. 2017 for a complete explanation about species distribution modelling.

1.2.2 Environmental niche characterization

Both species occurrences and environmental variables (with their strengths and their weaknesses, as previously described) could also be used to characterize species niche directly in the environmental space (which constitute the "hutchinsonian duality" sensu Colwell and Rangel 2009). Differently from SDMs, niche characterization in the hyperspace allows to obtain niches parameters and estimates other than niche suitability, such as niche breadth or niche optimum. In this case, the workflow basically consists on estimating species' occurrence density along the environmental axes of a multivariate space (Figure 1.2). Throughout ordinations techniques such as Principal Component Analysis (PCA), environmental space of multiple correlated environmental variables could be converted into a small number of uncorrelated linear combinations of the original variables. Then, the environmental space will be defined by the selected axes of the ordination analysis (Broennimann et al. 2012), normally in a number of 2 or 3, due to limitations for representation and interpretation of more dimensions (but see Blonder et al. 2014). This environmental space or volume could be divided into a grid of a selected number of cells, each one of them corresponding to a unique vector of n dimensions (V 1-n) equivalent to number of selected PCA axes, which correspond to the environmental conditions observed at one or more sites in the geographical space. PCA could be either build with the environmental conditions of every pixel of an entire region, or just with the environmental values observed at species' occurrences sites. Species occurrences could be then translated into this environmental space, from which Kernel density function could be applied to determine the smoothed density of occurrences in each cell of the hyperspace (Broennimann et al. 2012). Finally, quantile thresholds could be applied to remove possible occurrence of outliers.

These density values could be then ranged between 0 and 1 in order to obtain habitat suitability values, which could be then translated back to the geographical space. In addition, this and other similar frameworks (Blonder et al. 2014 n-dymensional hypervolume), allows to estimate other niche parameters not reachable with conventional SDMs, such as species niche centroid estimation (as niche center of mass), species boundaries delineation according to selected density percentile, measurements of distances between population locations and niche limit or centroid, as well as to estimations of niche similarity and overlap when comparing different species or population niches (Broennimann et al. 2012, Blonder et al. 2014). In addition, these niche parameters could be also scaled up at community level, allowing to characterize the global community position in the environmental space and its volume (see Community Inferred Climate and Community Volume in Blonder et al. 2015), and to test niche-based assembly processes (environmental and biotic filtering) as well as changes in community assembly over time.

1.3 Thesis aims and scope

1.3.1 Setting the scene: the impact of extreme events

As previously developed, changes in climate over time will lead to both shifts in species distribution and changes in species niche structure. Actually, under the current climate change scenario, different plants species adaptations, mostly related to warm and dry climate tolerances, are being reported (Franks et al. 2014), as well as an increase in species die-off events worldwide (Allen et al. 2010). Vegetation decay episodes often occur as a consequence of extreme climatic events such as heat waves or extreme droughts, both induced by the increase of climatic variability driven by climate change. Nevertheless, several mechanisms could impede or reduce species decay in these situations, such as: favorable local microclimate, positive species interactions or accurate soil and topographic conditions (Cornwell and Ackerly 2009, Svenning and Sandel 2013, De Frenne et al. 2013).

Regions with high historical climatic variability which are also predicted to become more variable in future, such as the Mediterranean basin (IPCC Working Group 1 2014), are specially prone to suffer this kind of decay events. In this context, the

southeast of the Iberian Peninsula has recently experienced its driest year on record (AEMET, 2014), causing extensive die-off across different vegetation communities, including *Pinus halepensis* L. forests and areas dominated by shrublands (Esteve-Selma et al. 2015). This climatic and biologically exceptional situation was used as a study system to develop the following objectives.

1.3.2 Objectives

In this thesis I address the question of why some species or populations decay while other persist under extreme climatic events from a species niche perspective, assuming the correspondence between population fitness and species niche (Pulliam 2000, Sexton et al. 2009), and so generally hypothesizing that populations closer to their species climatic tolerance limit will be more affected. Particularly, I aim to understand the capacity of niche-based indices to predict species and population responses to extreme events, to assess the relevance of inter-annual climatic variability when characterizing species niches, to evaluate the importance of local environmental variables, and to test the environmental filtering role of extreme climatic event by reducing communities climatic mismatch. I address these objectives both at species level (chapters 2, 3 and 4), basing on field decay data of co-occurring shrubland species and *Pinus halepensis* L. forests, and at community level (chapter 5) by scaling up co-occurring shrubland species responses. The specific objectives for each chapter are listed below:

Chapter 2: To test the correlation between species decay response to an extreme drought event with species climatic suitability derived from different SDMs. Here I addressed the possible correlation between species climatic suitability and remaining green canopy of shrubland co-occurring species after an extreme drought event. In addition, given the considerable amount of uncertainty existing with respect to SDMs techniques, I estimated the climatic suitability by using four different SDM algorithms, following a gradient of model complexity. Particularly, I examined (i) whether those species with lower climatic suitability showed higher decay responses to extreme events and (ii) whether this relationship was algorithm-dependent.

Chapter 3: To include climatic variability in niche characterization in order to improve the analysis of drought-induced mortality based on species climatic suitability. In this chapter, I estimated the correlation between mortality of more of 4000

km^2 of *Pinus halepensis* L. forests during an extreme event and climatic suitability obtained from niches characterized only with climatic averages and with the complete inter-annual climatic resolution. In addition, I compared the differences between average-based niches and inter-annual variability-based niches for species with different distribution ranges. Specifically, I aimed to test (i) whether inter-annual climatic variability improve niche characterization and the relationship between demographic responses and niche suitability and (ii) whether those species with narrower distribution ranges increased more their niche space when considering inter-annual climatic variability.

Chapter 4: To use species environmental niche characterization to assess species decay responses to climatic extremes.
Here I proposed the use of niches parameters directly measured in the environmental space, such as euclidean distance to the centroid and limits of species niche, which allow to obtain continuous values even when climatic suitability is zero, to assess species decay driven by an extreme climatic event. Then, I compared the predictive capacity of niche-based distances and climatic suitabilities derived from SDM when predicting co-occurring shrubland decay under a drought episode. In addition, I analyzed the effect of local bedrock type, which determines soil water capacity, on the observed decay. Here, I examined (i) whether niche-based distances in the environmental spaces better predict decay responses to extreme events than climatic suitability, and (ii) whether some bedrock types could buffer or exacerbates species die-off under similar extreme climatic conditions.

Chapter 5: To test the environmental filtering effect of extreme climatic events and bedrock type in Community Climatic Disequilibrium. Finally, I used species niche characterizations in the environmental space and demographic data measured in shrubland communities before and after an extreme drought episode in order to estimate the Community Inferred Climate before and after the event. I also considered the effect of different bedrock types, determining a gradient of soil water capacity. The distance between Community Inferred Climate and the observed climate corresponds to the Community Climatic Disequilibrium. Then, I compared the climatic disequilibrium of these shrubland communities before and after drought and between bedrock types, allowing to test (i) whether extreme drought events reduce

the climatic disequilibrium of communities, acting as an environmental filter, and (ii) whether bedrock types with low water retention capacities exacerbated this filtering effect.

2

Climatic suitability derived from species distribution models captures community responses to an extreme drought episode

Pérez-Navarro M.A., Sapes G., Batllori E., Serra-Diaz J.M., Esteve M.A., Lloret F.

2.1 Abstract

The differential responses of co-occurring species in rich communities to climate change - particularly to drought episodes - have fairly been unexplored. Species Distribution Models (SDMs) are used to assess changes in species suitability under environmental shifts, but whether they can portray population and community responses is largely undetermined, especially in relation to extreme events. Here we studied a shrubland community in SE Spain since this region constitute an ecotone between the Mediterranean biome and subtropical arid areas, and it has recently suffered its driest hydrological year on record. We used four different modelling algorithms (Mahalanobis distance, GAM, BRT and MAXENT) to estimate species' climatic suitability before (1950-2000) and during the extreme drought. For each SDM, we correlated species' climatic suitability with their remaining green canopy as a proxy for species resistance to drought. We consistently found a positive correlation between remaining green canopy and species' climatic suitability before the event. This relationship supports the hypothesis of a higher vulnerability of populations living closer to their species' limits of aridity tolerance. Contrastingly, climatic suitability during the drought did not correlate with remaining green canopy, likely because of the exceptional episode led to almost zero suitability values. Overall, our approach highlights climatic niche modelling as a robust approach to standardizing and comparing the behavior of different co-occurring species facing strong climatic fluctuations. Although many processes contribute to resistance to climatic extremes, the results confirm the relevance of populations' position in the species' climatic niche for explaining sensitivity to climate change.

2.2 Introduction

The climatic trends observed over the last decades are promoting vegetation shifts (Parmesan and Yohe 2003), phenological changes (Zavaleta et al. 2003) and modifications to disturbance regimes (Mouillot et al. 2002, Allen et al. 2015), as well as altering the interactions between these processes (Franklin et al. 2016). However, the adjustment of populations to changing climatic conditions may be more influenced by the extremes of climatic variability than by average climate trends. For instance, mortality and recruitment processes – which shape species' distributions and ranges – may be largely conditioned by pulses of extreme climatic conditions such as extreme drought events (del Cacho and Lloret 2012, Greenwood et al. 2017).

Vegetation mortality and die-off processes associated with climatic warming have often been observed at ecotones corresponding to the rear edge of species' distributions (Allen and Breshears 1998, Bigler et al. 2006, Jump et al. 2006, Lesica and Crone 2016), supporting the assumption that a decline in plant populations may be more significant at their equatorial latitudinal or lowland altitudinal margins (Thomas et al. 2004). Translated into the perspective of a plant community, marked by the coexistence of species that have adapted differently to environmental conditions, mortality processes would have a greater influence on the populations of species located close to their tolerance limits, to the benefit of other species that find the new environment more suitable (Martínez-Vilalta and Lloret 2016). This hypothesis implicitly correspond to the biogeographic paradigm that species perform better in their geographical center of distribution than they do in the margins (Centre-Periphery hypothesis, see Sexton et al. 2009; but see Dallas et al. 2017), with the further assumption that geographical and environmental spaces are mostly concordant (Pironon et al. 2015).

Species Distribution Models (SDMs) have been used to test the relationship between species' climatic niche and their physiological or demographic performance (Serra-Diaz et al. 2013, Pironon et al. 2015, van der Maaten et al. 2017). These are statistical models that relate the location of species occurrences to the environmental data on these sites (Franklin 2010). The SDM approach is based on the assumption that species occurrence portrays the environmental and biotic conditions that are

suitable for species to survive and reproduce (i.e. the realized niche: Pulliam 2000, Soberón 2007, Peterson et al. 2011), and so model outputs are interpreted as a species-specific index of relative suitability or habitat suitability. Accordingly, SDMs have been widely used under average climatic conditions (climatic norms) to predict past or future distributional changes of species (Elith and Leathwick 2009). However, it is not yet known whether these models are able to capture the impact of extreme climatic events (e.g. droughts), especially in relation to community dynamics.

In the Mediterranean basin, vegetation has developed different strategies for dealing with variable rainfall, such as shallow roots and deciduous summer leaves (Valladares et al. 2004, Zunzunegui et al. 2005). Nevertheless, these adaptive syndromes may not be enough under the predicted scenarios of increased climatic extremes (IPCC 2013). In this context, the southeast of the Iberian Peninsula has recently experienced the driest year on record (AEMET 2014), causing an extensive vegetation die-off event in areas dominated by shrubland (Esteve-Selma et al. 2015). This Iberian region represents the ecotone between the Mediterranean biome and subtropical shrublands of arid lands (Esteve-Selma et al. 2010). This recent drought-induced mortality event therefore offers the possiblity to assess community dynamics in relation to biogeographical paradigms at the limits – in this case, the aridity margin - of the biome's distribution, which are areas considered to be very sensitive to climate change (Guiot and Cramer 2016).

In this study, we use a shrubland community at the arid southern limit of the Mediterranean biome to assess the differential response of coexisting species to an extreme drought event according to species' climatic suitability, as determined from SDMs. Specifically, we test whether populations living close to the edge of their species' climatic niche (i.e. lower suitability values compared to the niche's optimal value) are more vulnerable to such extreme events than populations living closer to their niche center. We use the remaining green canopy of species after the drought event to examine the correlation between drought-induced die-off and species' climatic suitability, considering both the historical suitability, as inferred from historical climatic series, and the drought episode suitability, as reflected by the conditions during the drought event. Given the considerable amount of uncertainty existing with respect to the various SDM techniques, which use model-specific algorithms (Araújo

and New 2007), we also test whether the relationship between species' die-off and their climatic suitability depends on the SDM algorithm applied. For this purpose, we applied four SDMs with highly contrasting approaches (Mahalanobis distance, Generalized Additive Models –GAM–, Boosted Regression Trees –BRT–, and Maximum Entropy approaches –MaxEnt–) to determine species suitability, that was later correlated to species' die-off.

2.3 Material and methods

Study area

The study was carried out in two semi-arid shrubland areas in the province of Murcia (southeast of the Iberian Peninsula) (Figure 2.1), Campo de Cagitán (38° 06' N, 1° 32' W) and Oro Mountain (38° 11' N, 01° 30'W), 10 km apart but with similar soil characteristics and climatic conditions. The Campo de Cagitán site was covered by a small expanse of scrubland embedded in an agricultural matrix, and the Oro Mountain site was occupied by shrubland close to an open pine forest on a hill slope. The overall sampled area amounted to 19 hm^2.

The potential vegetation comprises an open forest of *Pinus halepensis* L. and a sclerophyllous shrubland (garrigue) dominated by *Quercus coccifera* L., *Pistacia lentiscus* L., *Olea europea* L., *Rhamnus lycioides* L. and *Juniperus oxycedrus* L., along with a highly diverse range of small shrubs, such as *Thymus hyemalis* Lange and *Helianthemum* spp. (Braun-Blanquet and Bolòs 1957). The current landscape in these regions is a highly fragmented cropland that is either in use or recently abandoned, with small patches of forest or shrubland interspersed between the crops. The steep slopes in some areas preclude the presence of agricultural crops but they are instead covered by scrublands, often containing the tussock grass *Stipa tenacissima* L. (which was cultivated for fibers until the 1960s) and occasional open pine forests.

The region is included within the Mesomediterranean thermoclimatic belt and the Mediterranean xeric bioclimatic region (Rivas-Martínez et al. 2011), characterized by annual mean temperatures of 18.5 °C and an annual rainfall of 200-350 mm. Precipitation in the area is low and mainly concentrated in the fall, with great variability between years. During the hydrological year 2013-2014 the Region of Murcia

suffered the worst drought on record since 1941, demonstrating the extreme conditions of the event. During the drought event a mean regional rainfall of 146.5 mm was recorded; this corresponds to just 46% of the average value for the period 1971-2000 (Figure 2.1, AEMET 2014). This episode led to high mortality and defoliation in different forests and shrublands (Esteve-Selma et al. 2015).

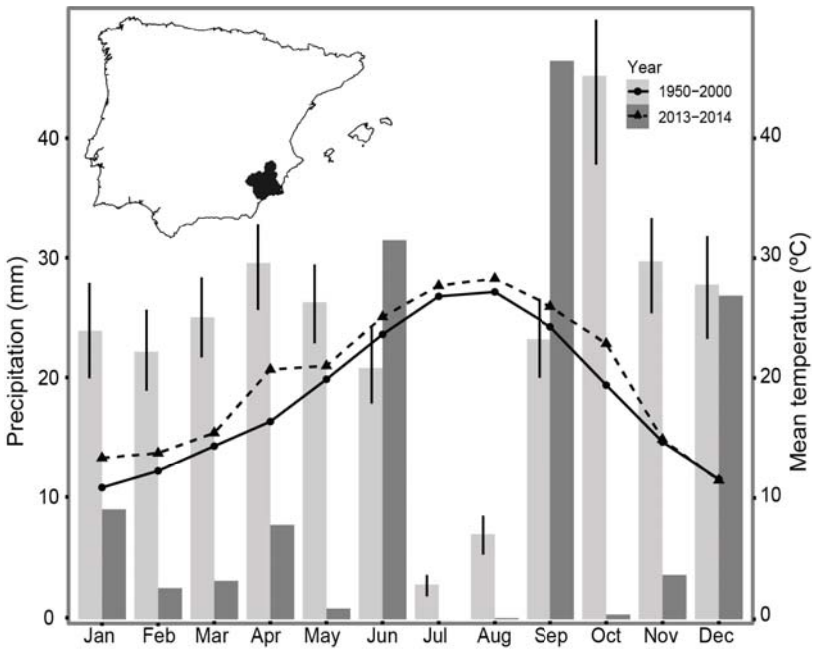

Figure 2.1: Study region within the Iberian Peninsula (Murcia region: black shading in the inset, upper left map) and monthly temperature (lines) and precipitation (bars) data during the historical 1950-2000 period (light grey bars and dots) and the 2013-2014 hydrological year (anomaly period; dark grey bars and triangles).

Field sampling

In March 2015, a set of ten $50m^2$ replicate plots were established in the study region, three in the Campo de Cagitán and seven in the Oro Mountain, according to the shrubland surface area available on each site. This sampling design reflects the region's highly fragmented habitat, which prevented us from establishing ten replicates in a single location.

Sampling plots were established with the following criteria: 1) shrubland with no signs of recent disturbance, with high species richness, different life forms, and low S. tenacissima density; and 2) low pine presence, in order to avoid wetter microenvironments caused by the shade of tree canopies, which could affect the moisture in

the air and soil. Each plot consisted of two linear transects of 25 meters long by 1 wide. On each plot, we recorded the total number of individuals per woody species, estimated their size by measuring two perpendicular diameters crossing at the center of each individual and visually estimated the proportion of remaining green canopy (RGC) per individual. A total of 22 species were sampled (Table 2.2). RGC levels were visually estimated as a proxy for the species response to drought (die-off) as the percentage of green leaves present relative to the amount in healthy individuals found in the study area (Sapes et al. 2017). To ensure that the green cover loss resulted from the drought of the previous year, we avoided individuals with signs of older decay (e.g., stumps, decomposed stems, branches with no thin tips). To determine the reliability of the visual RGC estimate, we also measured the length (cm) of the segments occupied by green leaves and dry leaves (including segments with no leaves) along a linear path from the tip to the base of two representative branches of ten individuals per species, on every plot where a species was present. Then, a directly measured RGC value was calculated per individual as [branch length with green leaves (cm)/total branch length (cm)]*100. When ten individuals per species were not found within a given plot, we measured the closest individuals to the sampled transects until ten replicates were attained. Pearson's correlation between direct and visually estimated values of RGC was calculated for plants from each species, always resulting in values higher than 0.7 (Appendix A Table A.1). These analyses support the use of visual estimate of RGC as a proxy for die-off (Sapes et al. 2017). Considering this high correlation and the limited number of individuals with real measures of defoliation (10 per species and plot), we used the visually estimated RGC (made for every individual) for the statistical analyses.

The variables described above were then scaled to the landscape level. First, we calculated the following information for each plot: average percentage of visually estimated RGC for each species; species frequency (the number of plots where each species was found over the total number of plots) and the average size of each species (as the product of the two diameters measured in the plants), since RGC could be affected by species size or relative abundance (Lloret et al. 2016, Sapes et al. 2017). The values of species' RGC and size were then averaged across plots. Finally, to account for the different species' strategies in relation to leaf longevity and annual seasonality (Valladares et al. 2004), all the species were classified into one of the

following foliar strategies: 1-evergreen, 2- semi-deciduous, 3-summer deciduous, and 4-retamoid or leafless species.

Climatic suitability modelling

For the 22 sampled species, we built SDMs using four different algorithms - Mahalanobis distance, GAM, BRT, and MaxEnt - to assess the robustness of the potential relationships between visual estimates of RGC and the climatic suitability output of these models. These models represent four highly differentiated modelling methods: distance-based models (Mahalanobis distance), regression-based models (GAM), decision tree-based methods (BRT) and a machine-learning technique based on the principle of maximum entropy (MaxEnt). Therefore, they represent a gradient of complexity, where some models such as Mahalanobis distance only consider linear relationships between predictors (Franklin 2010) whereas others such as MaxEnt and BRT can include high-order interaction terms (Elith et al. 2008, Phillips and Dudík 2008).

The geographical occurrence data for each species were obtained from GBIF (Global Biodiversity Information Facility: <www.gbif.org>). Occurrence data were filtered in order to remove taxonomic and geographic inconsistencies and reduce dense local sampling by randomly thinning species' records to one observation per 1x1 km grid cell. We considered the whole distributional range of species; thus, the available number of occurrences was considerably different from one species to the next, ranging from 200 to 6,000 after filtering. For each set of filtered occurrences, 70% of presences were reserved for fitting the model (training data) and the other 30% for the validation set (testing data), according to the number of environmental predictors selected in our models and following the rule described by Huberty 1994 for determining the optimum partitioning of training and test data. To improve the models' performance accuracy (Barbet-Massin et al. 2012), 100,000 random background points were simulated for each species to fit both GAM and MaxEnt algorithms, and a random set of pseudo-absences equivalent to the number of each species occurrences was simulated for BRT. Since Mahalanobis distance works without simulated absences, no background points were used in this case. The background extension was delineated in order to represent the current or past available geographical space for the selected species (M dimension

sensu Soberón 2007). In our case, the geographical region used to establish species background was the Mediterranean basin.

Six climatic variables representative of Mediterranean climate were used as predictors to calibrate the suitability models: isothermality (mean diurnal temperature range/temperature annual range), temperature seasonality, mean temperature of wettest quarter, mean temperature of driest quarter, annual precipitation and precipitation seasonality, all of them with 1 by 1 Km resolution. These variables were selected from the 19 bioclimatic variables available in Worldclim.org (version 1.4) for the period 1950-2000 (Hijmans et al. 2005), according to the knowledge of the species' ecological requirements and in order to reduce variables' collinearity. Pearson correlation and variation inflation factor (VIF) among variables were always less than 0.75 and 5, respectively. Additionally, we used monthly precipitation and maximum, minimum and mean temperature records over the 2013-2014 period from between 68 and 114 weather stations of the Spanish Meteorological Agency (AEMET) to elaborate the climatic layers during the drought event (also in 1 by 1 km resolution), following Ninyerola et al. (2000), and using the 'biovars' function (dismo package; Hijmans et. al 2016). To minimize differences in the climatic interpolation methods between Worldclim and Ninyerola et al. (2000), only latitude, longitude and elevation were used as explanatory variables for climatic data. In addition, we applied MESS analysis between these two data set over the Spanish territory (where AEMET data are available) during the 1950-2000 period to assess dataset dissimilarities, showing the high concordance and comparability of both climatic interpolation methods over the entire extension and particularly over the study region (Appendix A Figure A.1). Finally, species' historic climatic suitability (HCS) was estimated projecting the models over the climatic layers for the period 1950-2000, whereas species' climatic suitability during the drought event (episode climatic suitability, ECS) was estimated by projecting the calibrated models over the climate layers of the anomaly period 2013-2014.

Table 2.1: Main settings used in the different SDM modeling approaches.

Method	Key reference and main settings
Mahal Mahalanobis distance	adehabitatHS package (Calenge, 2015). Modification of the original function mahasuhab in order to obtain distance and probability values from other layers not used to calculate variables mean vector. This function makes it possible to determine probability values, assuming that under multivariate normality, squared Mahalanobis distance is approximately distributed as Chi-square with n-1 degrees of freedom, which makes it possible to calculate p-value maps (Clark et al., 1993).
GAM Generalized Additive Models	mgcv package v.1.8-16 (Wood, 2011). Weighted background number: 100,000 points. The optimal number of edf for each variable was selected between 1 and 4 by cross-validation, using gam function. The number of knots for those species where response curves being biologically counterintuitive was also reduced.
BRT Boosted Regression Tree	gbm package v. 2.1.1 (Ridgeway, 2007). Pseudoabsence number equivalent to presence species data. Tree complexity of 5 for those species with more than 250 occurrences and 3 for those species with less than 250. The learning rate of 0.005 was chosen because it made it possible to achieve at least 1,000 trees in every case, following Elith and others (2008).
MaxEnt Maximum entropy	MaxEnt v. 3.3.1 (Phillips and Dudik, 2008b) used with default setting with the exception of: 100,000 background points, 10-fold cross-validation, regularization multiplier of 3, and threshold feature unselect in order to produce smoother response curves.

For the four implemented SDM algorithms, model settings were selected following recommendations from the literature, and partial dependence plots and predictive maps were assessed to exclude those settings that produced unreliable response curves or distribution maps. The final selected settings and main literature are showed in Table 2.1. To make all the model outputs comparable (between 0 and 1 probability values), log raw output transformation was applied for MaxEnt models (Phillips and Dudík 2008) and distance transformation into p-values was applied for Mahalanobis distances (Clark et al. 1993). Each model's predictive performance was assessed by comparing model predictions with testing data, using the Area Under Receiver Operating-characteristic Curve (AUC, Fielding and Bell 1997) and the Boyce index (Boyce et al. 2002, Hirzel et al. 2006). These evaluation methods are considered a reliable approach for our models and allowing comparison among them, since all the

models were fitted with the same species data set and environmental extension of layers (Hirzel et al. 2006, Franklin 2010). Finally, multivariate environmental similarity surface (MESS, Elith et al. 2010) analyses were carried out to measure the similarity between historical climate and the extreme drought period in the occurrence locations; these analyses allowed to identify extrapolation for predictions during the anomalous period as areas with high climatic dissimilarities.

Table 2.2: Main species information and attributes used in statistical analyses. See methods for details about foliar strategy, RGC (Remaining Green Canopy), Size and Frequency.

Family	Species	Code	Life form	Foliar strategy	RGC (%)	$Size(cm^2)$	Frequency
Anacardiaceae	Pistacia lentiscus	PLE	Microphanerophyte	Evergreen	25.33	0.083	0.5
Asparagaceae	Asparagus horridus	AHO	Chamaephyte	Leafless	15.00	0.029	0.1
Asteraceae	Artemisia barrelieri	ABA	Chamaephyte	Semideciduous	44.29	0.004	0.9
	Artemisia campestris	ACA	Chamaephyte	Semideciduous	13.33	0.012	0.1
Boraginaceae	Lithodora fruticosa	LFR	Nanophanerophyte	Semideciduous	47.27	0.029	0.1
Chenopodiaceae	Salsola genistoides	SGE	Nanophanerophyte	Leafless	6.67	0.080	0.2
Cistaceae	Cistus albidus	CAL	Nanophanerophyte	Semideciduous	77.50	0.045	0.2
	Cistus clusii	CCL	Nanophanerophyte	Semideciduous	44.77	0.046	0.9
	Helianthemum syriacum	HSY	Chamaephyte	Semideciduous	61.39	0.002	0.3
Cupressaceae	Juniperus oxycedrus	JOX	Microphanerophyte	Evergreen	56.69	0.550	0.6
	Juniperus phoenicea	JPH	Microphanerophyte	Evergreen	60.00	0.074	0.1
Fagaceae	Quercus coccifera	QCO	Microphanerophyte	Evergreen	33.10	0.009	0.7
Lamiaceae	Rosmarinus officinalis	ROF	Nanophanerophyte	Semideciduous	53.00	0.235	1.0
	Sideritis leucantha	SLE	Nanophanerophyte	Semideciduous	44.77	3.029	0.2
	Teucrium capitatum	TCA	Chamaephyte	Semideciduous	68.00	2.019	0.6
	Thymus hyemalis	THY	Chamaephyte	Semideciduous	45.28	0.389	1.0
Leguminosae	Anthyllis cytisoides	ACY	Nanophanerophyte	Semideciduous	21.46	0.378	0.6
	Dorycnium pentaphyllum	DPE	Nanophanerophyte	Semideciduous	21.54	0.577	0.5
	Ononis fruticosa	OFR	Nanophanerophyte	Semideciduous	10.11	0.474	0.4
Poaceae	Stipa tenacissima	STE	Hemicryptophyte	Evergreen	61.89	0.009	1.0
Rhamnaceae	Rhamnus lycioides	RLY	Microphanerophyte	Semideciduous	8.75	0.056	0.3
Timeleaceae	Daphne gnidium	DGN	Nanophanerophyte	Semideciduous	15.00	0.004	0.2

Statistical analyses

Generalized Linear Models (GLM) with normal distributions were performed to assess the relationship between SDM-inferred HCS and ECS for each species and their die-off recorded in the field. The visually estimated species RGC was used as a response variable whereas HCS, ECS, the interaction between HCS and ECS, species size (logarithmically transformed), species frequency, and species foliar category were introduced as explanatory variables. Difference between HCS and ECS was discarded

as an explanatory variable in the models, due to the high correlation with ECS which produced same models results.

The final models were selected according to stepwise selection based on AIC (Akaike Information Criterion) (Table 2.3). In addition, Phylogenetic Generalized Linear Models (PGLS) using Phylomatic distances (Webb and Donoghue 2005) were performed in order to assess the potential effect of phylogenetic species relationships in the selected model (Freckleton et al. 2002). This PGLS was finally discarded from the final analyses since phylogeny was not significant in any case (lambda =0). Finally, consistency in the climatic suitability estimates (HCS, ECS) obtained from each of the four implemented SDMs was tested by pairwise comparisons, using Pearson correlation tests. All statistical analyses were carried out with R version 3.3.2 (R Core Team 2016).

2.4 Results

All the four SDMs algorithms developed showed high performance accuracy values with AUC values higher than 0.75 and Boyce index' values being always positive and higher than 0.5 (Elith et al. 2002, Hirzel et al. 2006, Appendix A Figure A.2). Particularly AUC mean values were 0.96±0.02 and Boyce index mean values were 0.93±0.07 MESS analyses showed that precipitation seasonality exhibited high dissimilarity between extreme event climatic data and training predictor data near the coastal region. However, the values corresponding to the drought episode were never outside training boundary values for the study locations (Appendix A Figure A.3). Climatic suitability dropped dramatically during the drought episode for all species, irrespective of the SDM method, as shown by the comparison between the respective HCS and ECS values (Figure 2.2, Appendix A Table A.2).

For the majority of SDM algorithms the stepwise GLM model selection determined that the most parsimonious models explaining species' RGC were those including HCS, foliar category and species size as explanatory variables. Only in the case of Mahalanobis distance did the stepwise GLM model selection fail to remove any explanatory variables from the saturated model. There was some variation in the significant variables associated with RGC in the different SDM algorithms. All the

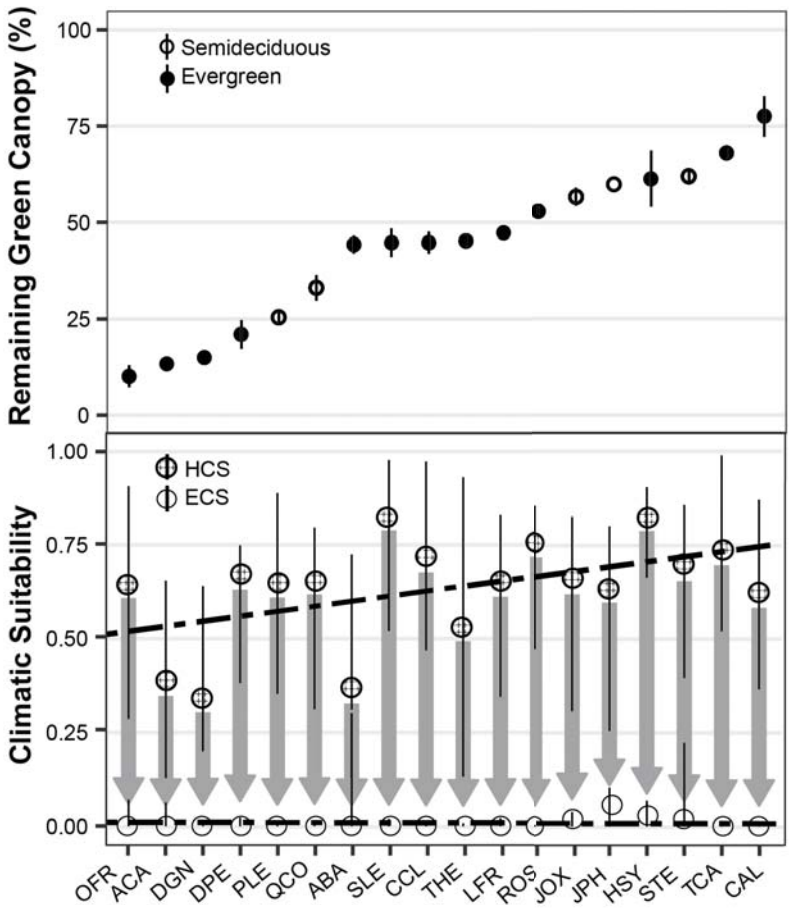

Figure 2.2: Averaged proportion of Remaining Green Canopy (RGC) in shrub species with foliar strategies 1 and 2 (top graph) for the ten studied plots. Species' RGC values are sorted in increasing order (x-axis) and error bars are shown. Red and blue dots represent foliar strategies. The lower graph shows the Historical Climatic Suitability (HCS) and the drought Episode Climatic Suitability (ECS) values for each species. Blue and red dots represent median suitability values of HCS and ECS, respectively, and the error bars correspond to the range between maximum and minimum suitability values predicted by the four applied SDM algorithms (see text for details).

selected variables were significant in BRT, while in MaxEnt HCS and foliar category were significant, in GAM foliar category was significant and HCS was only marginally significant, and in Mahalanobis only HCS and foliar category were marginally significant (Table 2.4).

In all cases RGC was positively related to HCS (Figure 2.2 and 2.3). Foliar categories 3 (summer deciduous species) and 4 (leafless species) presented a signifi-

cant, negative correlation with RGC in BRT, GAM and MaxEnt models, while in the Mahalanobis distance model, foliar category 3 was only marginally significant. Finally, species size was only significantly negatively related with RGC in BRT models (Table 2.4). Species frequency, ECS or the interaction between HCS and ECS were not significant in any model (Table 2.4).

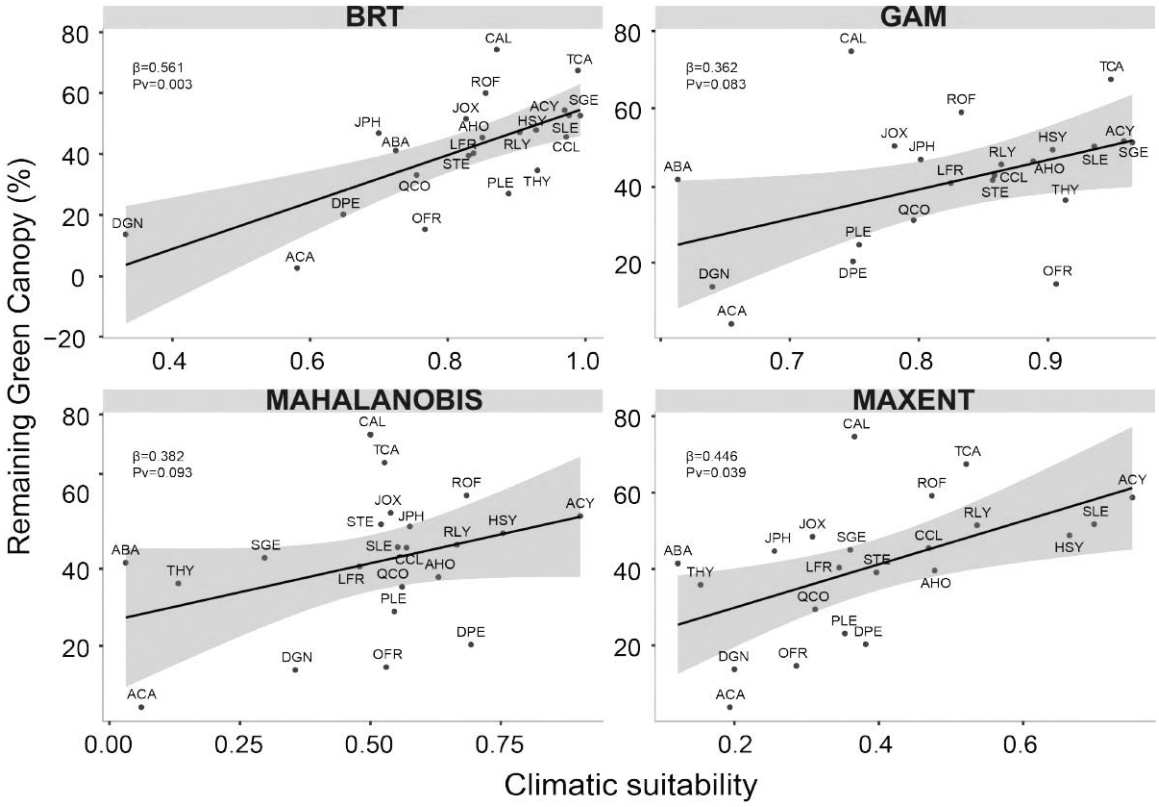

Figure 2.3: Partial residual plot of RGC (Remaining Green Canopy) in relation to HCS (Historical Climatic Suitability) obtained for each SDM model. β (standardized estimate value) and P values for HCS in these models are shown in the left corner of each plot. Species codes are shown in Table 2.2.

The values of species' HCS varied from model to model. BRT predicted the highest suitability values for a given species and MaxEnt the lowest ones. This pattern was consistent for almost all species (Appendix A Figure A.4). For all species, the majority of pairwise Pearson correlations between the HCS values inferred from the different SDM algorithms were significant, with correlation values ranging between 0.45 and 0.78 (Appendix A Figure A.5). However, the correlation between Mahalanobis distance and BRT was not significant (Appendix A Figure A.5). In contrast, most pairwise correlations between models were not significant for ECS, likely

due to the extremely low ECS values exhibited by most species; in this case, when a significant correlation was found, the relationship was driven by a single outlier value (Appendix A Figure A.6).

Table 2.3: AIC and Adjusted $R^2$of GLMs explaining remaining green canopy as a function of foliar strategy, size, frequency, HCS (Historical Climatic Suitability), ECS (Episode Climatic Suitability) and the interaction between the latter two (HCS:ECS) calculated from four different SDMs (Mahalabonis distance, GAM, BRT, MaxEnt). AIC stepwise selection was applied to obtain the final models.

	Mahalanobis distance	GAM	BRT	MaxEnt
AIC	197.97	196.1	187.33	194.15
R2 adj	0.32	0.33	0.55	0.39

Table 2.4: Results of GLMs explaining remaining green canopy as a function of foliar strategy, size, frequency, HCS (Historical Climatic Suitability), ECS (Episode Climatic Suitability) and the interaction between the latter two (HCS:ECS) calculated from four different SDMs (Mahalabonis distance, GAM, BRT, MaxEnt). AIC stepwise selection was applied to obtain the final models.

	Mahalanobis distance			GAM			BRT			MaxEnt		
	β	Std.Error	P.value	β	Std.Error	P.value	β	Std.Error	P.value	β	Std.Error	P.value
Intercept (Foliar.STR 1)	0	0	0.939	0	0	0.61	0	0	0.324	0	0	0.051
HCS	0.382	0.213	0.096	0.362	0.196	0.083	0.561	0.157	0.003	0.446	0.199	0.039
Foliar.STR 2	0.062	0.299	0.838	-0.317	0.241	0.207	-0.317	0.198	0.13	-0.364	0.234	0.139
Foliar.STR 3	-0.435	0.23	0.081	-0.563	0.21	0.016	-0.618	0.172	0.002	-0.706	0.223	0.006
Foliar.STR 4	-0.254	0.254	0.336	-0.688	0.218	0.006	-0.69	0.173	0.001	-0.628	0.199	0.006
Log(size)	-0.244	0.212	0.271	-0.318	0.201	0.133	-0.373	0.167	0.039	-0.33	0.1934	0.107
FREQUENCY	0.369	0.225	0.125									
ECS	27.618	18.64	0.162									
HCS:ECS	-27.36	18.59	0.165									

2.5 Discussion

We found a clear relationship between field measurements of species performance under an extreme drought episode and the historical climatic suitability (HCS) of species derived from SDMs. Within the studied community, co-occurring species living closer to their climatic tolerance limit -identified by low HCS values compared to the optimal value of the distribution range- proved more vulnerable to the extreme drought episode. This climatic limit corresponds to the aridity margin of species' climatic niche (Appendix A figures A.7 to A.11). These results are consistent with the relationship observed between the decay of shrubland and woodland species and the decrease in climatic suitability in other semi-arid areas in Spain (Sapes et al. 2017) and Southwestern North America (Lloret and Kitzberger 2018). This relationship is also consistent with other studies which suggest that species' sensitivity to climate change is related to niche characteristics such as mean niche position and niche breadth (Thuiller et al. 2005, Broennimann et al. 2006). Species in the climatic niche margins are generally assumed to exhibit lower survivorship and recruitment and higher extinction risk because of the less favorable environmental conditions (Weber et al. 2016). Precisely in these situations of the environmental space closest to the physiological tolerance limits of the species, the effect of climate variability is probably more severe (Zimmermann et al. 2009), promoting species' decline or range shifts at the trailing edge of species distribution (Bigler et al. 2006, Walther et al. 2009).

Species' drought responses and climatic suitability

Studies that compare habitat suitability with different species' performances (population density, growth, recruitment, fecundity, etc.) along the species distribution gradient are scarce and still not fully conclusive with respect to general biogeographic paradigms (Centre-Periphery hypothesis, Wright et al. 2006, Sexton et al. 2009, Thuiller et al. 2010, Abeli et al. 2014, Csergő et al. 2017). Likely species interaction, local variables or adaptation mechanisms underlie the limited evidence of the relationship between species' performance and climate suitability (Sexton et al. 2009, 2014, Dallas et al. 2017, Lloret and Kitzberger 2018). Our results throw some light in this sense as they support the relationship between species' performance when cli-

matic conditions are extreme and climatically-based descriptions of their suitability (i.e. HCS).

We also expected that populations experiencing higher displacement of climatic suitability during the extreme event (low ECS) would experience greater leaf loses and higher mortality rates. However, contrary to our expectations, we found that species' suitability during the extreme episode (ECS) did not significantly explain species leaf loses in the studied community. Our extremely low ECS levels observed for all species probably made it impossible to obtain contrasted values of ECS among them. These low values indicate that the climatic episode was extreme enough to displace all the studied populations far from their climatic optimum, even for those species that were closer to this optimum during the historical period (Figure 2.2). In addition to the exceptionality of the extreme event, the extremely low ECS values may derive from 1) the averaged climatic data used for calibrating the models, which does not reflect the variability or annual extremes during the considered 50-year period and 2) the limited ability of models to predict suitability under climatic scenarios that are highly different from the period used to fit the models (Elith et al. 2010), as shown by the low MESS values, particularly for precipitation seasonality –*bio 15*- (although these were not negative in the study site) (Appendix A Figure A.3). This situation may also amplify the differences between different algorithms and species' prevalence data in the predictions (Thuiller 2004, Pearson et al. 2006), as supported by the low correlations between the ECS predicted by the different models (Appendix A Figure A.6).

In addition to HCS, foliar categories were also significant in explaining the observed species' RGC, suggesting that leaf strategy and seasonal senescence play a major role in understanding species performance under strong drought conditions, at least in Mediterranean type ecosystems. Our results show that summer-deciduous and leafless species always present significantly lower values of RGC. This result is in part expected due to the general strategy in Mediterranean species of dropping leaves during the dry, hot season to limit evapotranspiration and water loss (de la Riva et al. 2016a). In the Mediterranean basin this semideciduous mechanism typically appears in combination with shallow roots and low water potentials as an anisohydric syndrome, in contrast to species with hydrostable syndromes, which present sclerophyllous leaves, more sensitive stomatal control and deeper roots (Zunzunegui et al.

2005, de la Riva et al. 2016b). Thus, estimates of RGC as a proxy of drought resistance can be misleading if these foliar strategies are not considered (Lloret et al. 2016). In addition to foliar strategies, other physiological features and local factors may modulate the interspecific variability of responses to a given drought episode. For instance, species-specific resistance to hydraulic failure and carbon economy (McDowell et al. 2008, Anderegg et al. 2012, Adams et al. 2017) and mutualistic and antagonistic biotic interactions (Lloret et al. 2012, Valladares et al. 2014).

SDM algorithms and demographic performance

Despite all these potential sources of variability, the four different SDM algorithms used in our approach highlighted the positive relationship between climatic suitability (HCS) and resistance to drought (RGC). These results were consistent across species, as shown by the high correlation between the different models' HCS values (Appendix A Figure A.5). The agreement holds despite the wide variety of the modeling approaches. However, the 'simplest' models (Mahalanobis distance and GAM) showed the lowest performance explaining species' RGC compared to 'complex' ones (BRT and MaxEnt). This difference in algorithm performance highlight the importance of the interactions between climatic variables and non-linear relationships when assessing species' responses to climate, and thus, supporting the use of SDMs versus simpler approaches based on univariate or multivariate correlations of demographic performance with climatic variables. Moreover, algorithms that are generally calibrated to produce smoother response curves, such as GLMs and GAMs, would be more accurate to predict habitat suitability under new conditions (Elith et al. 2010, Merow et al. 2014), while models based on presence-only data are more appropriate for predicting the lowest suitability values in these scenarios (Pearson et al. 2006). There is no general agreement, however, about the most accurate algorithm in relation to situations of range shift because even simpler models can lead to erroneous outputs (Elith et al. 2010, Merow et al. 2014). We therefore urge ecologists to assess the degree of model complexity needed to use SDMs as a proxy of ecological mechanisms, such as defoliation in this case.

Caution should also be taken when interpreting SDM predictions, given the assumptions that these kind of models implicitly include (Pearson and Dawson 2003). Among other limitations, these models commonly use only climatic predictors with

a broad resolution (~1 km^2), disregarding other meaningful abiotic factors, and they are also unable to capture microclimatic effects at small spatial scales (Lenoir et al. 2013, Franklin et al. 2013, D'Amen et al. 2017). Microsite factors could be particularly important for our study, given that soil features and depth, slope and orientation are especially relevant to species survival under extreme drought (Colwell et al. 2008, Hamerlynck and McAuliffe 2008). Furthermore, SDMs assume that species respond homogeneously to climate change across their range, not including intraspecific genetic variability and phenotypic plasticity, which may also favor species' local adaptation under unfavorable conditions (Benito Garzón et al. 2011, Lloret and García 2016).

The drought episode experienced in the Region of Murcia in 2013-2014 was extraordinary in historical terms, but these climatic situations are expected to become more frequent in the future (Sheffield and Wood 2008). The ability of plant communities to withstand these events and subsequently recover their green canopy will depend on both physiological traits related to the adaptive syndromes of Mediterranean species (Peñuelas et al. 2001) and the balance between demographic processes such as mortality, growth, and recruitment (Lloret et al. 2012). Under drier climatic scenarios, leafless and semi-deciduous species with shallow roots (xerophytic malacophyllous) would be expected to be to take more advantage of scarce and irregular rainfalls than sclerophyllous species with deeper roots. This is consistent with the particularly high HCS values obtained for malacophyllous species (Figure 2.2 and 2.3). These potential changes in species dominance within the community will likely lead to less productive shrublands dominated by smaller species (Valladares et al. 2004). Since species' climatic suitability is broadly related to both physiological and demographic species performance (Martinez-Meyer et al. 2013), indexes describing climatic suitability can provide rough estimates of species' vulnerability to extreme climatic episodes. While community resistance and resilience could minimize ecological changes, the recurrence of these extreme drought events could lead these Mediterranean communities to cross thresholds beyond which they could collapse (Vicente-Serrano et al. 2013, Valladares et al. 2014). This depletion of resilience in semi-arid shrubland communities could promote transitions to desert-like ecosystems, as has been predicted by some climate change scenarios for southern areas of Europe (Guiot and Cramer 2016). Accordingly, this study shows the impact of extreme drought

events even on communities supposedly well adapted to drought conditions (Lázaro et al. 2001, Sapes et al. 2017).

Conclusion

This study confirms the role of population position within its species climatic niche in explaining populations' vulnerability to extreme climatic events. In the studied semi-arid shrubland, species closer to their climatic tolerance limit were more vulnerable to extreme drought. Thus, the predicted recurrence of severe drought events could reduce the community resilience, increasing the risk of desertification in these arid lands. Our study empirically concurs with the trends foreseen by theoretical models, based on predicted suitability and correlations with drought response. This concurrence supports the use of SDMs to assess the impact of climate change on plant communities, particularly in extreme climatic conditions. This approach, which links species performance with regional biogeographic patterns, can probably be applied to other processes heavily determined by strong climatic fluctuations.

3

Temporal variability is key to model the climatic niche

Perez-Navarro M.A., Guisan A., Broennimann O., Esteve M.A., Moya-Perez J.M., Carreño M.F., Lloret F.

3.1 Abstract

Niche-based species distribution modelling (SDM) has become one of the most pervasive tools in ecology and biogeography. SDM relate species occurrences with the environmental conditions found at these sites. Climatic variables are usually included in SDMs as averages of a reference period (30-50 years). To date, the impact of not including climatic variability when estimating species niche and predicting species distributions has been scarcely considered. Here we first develop a method to include inter-annual climatic variability in niche characterization. We then compare climatic suitability obtained from averaged-based and from inter-annual variability-based niches by analyzing their respective capacities to explain demographic responses to extreme climatic events. Furthermore, we assessed the relative differences in niche space when including climatic variability in species with different distribution ranges. We found that climatic suitability obtained from both niches quantifications significantly explained species demographic responses. However, climatic suitability from inter-annual variability-based niches showed higher explanatory capacity, especially for populations located in the non-overlapping area between the two types of niches that tend to be geographically marginal populations. In addition, species with restricted distribution ranges increased relatively more their niche space, when considering climatic variability, probably because in widely distributed species, spatial variability compensates for temporal variability. According to our results, the common use of climatic averages when characterizing species niches could lead to overestimations of species extinction risk, underestimations of species distribution areas and risk of species invasions, or errors in conservation plans derived from SDM. From our study, we highlight that including climatic variability in SDM is particularly important when dealing with species with restricted distribution and populations at the margin of their niche.

3.2 Introduction

In recent years Species Distribution Modelling has become a very active field in biogeography, ecology and conservation sciences (Guisan et al. 2013, Araújo et al. 2019). This technique has been widely used for many purposes, such as niche quantification (Austin et al. 1990, Breiner et al. 2017), test of ecological and evolutionary hypotheses (Leathwick 1998, Anderson et al. 2002, Graham et al. 2004, Mellert et al. 2011), prediction of the effects of global change on biodiversity (Thomas et al. 2004, Thuiller et al. 2005), support of conservation plans (Hannah et al. 2007, Tulloch et al. 2016), or estimation of invasive species risk (Peterson and Vieglais 2001, Petitpierre et al. 2012).

Species Distribution Models (SDMs) are generally correlative models that statistically relate species' presences with the environmental conditions of sites where species occur (Franklin 2010, Peterson 2011, Guisan et al. 2017). These models are deeply founded on the Hutchinson's ecological niche concept (Guisan and Zimmermann 2000), what implies that species' observed ranges are the geographical translation of species' environmental requirements in the n-dimensional space - defined by these requirements-, discarding the areas where competitors impede the species presence (Soberón and Nakamura 2009). Several limitations of this method have been recognized, linked to both the underpinning theory and the commonly used methodologies. Some of the most criticized limitations include: the equilibrium assumption (Guisan and Thuiller 2005), which neglect any lag between climate changes and species distributions (Svenning and Skov 2004, Blonder et al. 2015); the lack of inclusion of biotic interactions or migration rates (Guisan and Thuiller 2005, Barve et al. 2011) due to the difficulty to report this information in a broad geographic scale; the niche conservatism assumption (Pearman et al. 2008), since these models implicitly consider that the niche remains constant over time when projected in time and space (Guisan et al. 2017); or the frequent use of exclusively climatic predictors (Franklin 2010, Thuiller 2013), partly encouraged by their widespread availability in contrast to the lack of fine grain resolution of other important environmental variables (e.g., soils in plant distributions). Furthermore, climatic variables are usually included as monthly or annual average of reference periods of 30 to 50 years (Hijmans et al. 2005, Karger et al. 2017, Fick and Hijmans 2017), in most cases, irrespective of

whether modeled species' lifespan is significantly longer or shorter than these periods.

From a theoretical view, characterizing the environmental requirements which constitute the Hutchinsonian niche (Soberón 2007), using exclusively historical averages could be constraining to a greater or lesser extent the real volume of species' niche in the n-dimensional space. By not accounting for climate variability, it is assumed that, for example, two species living under the same mean average temperature for a given period have the same thermal niche, even if one of them live under a yearly constant climate while the other suffer wide fluctuations in temperatures between years. Accordingly, it could be expected that the impact of including inter-annual variability in niche modelling could not be very important for species inhabiting areas with little temporal climatic variability. However, differences between the niche characterized with climatic averages and the niche characterized with inter-annual variability is likely substantial for those species living in habitats submitted to wide inter-annual climatic variability. In a similar way, it could be expected that species with small distribution ranges will have greater increases in the estimation of their niche size when we include inter-annual variability in relation to those species with larger geographic distribution areas, where spatial variability could compensate for temporal variability.

The potential distortion in niche size caused by the non-inclusion of the inter-annual climate variability would have implications on different facets of ecology and biogeography. For example, we could have been underestimating the present and future potential species distribution areas. Furthermore, if niche suitability and population dynamics are theoretically related (Pulliam 2000), niche breadth underestimation could contribute, among other ecological implications, to decouple macroclimatic suitability and demographic processes (Thuiller et al. 2014, Csergő et al. 2017). For instance, niche suitability estimated from average climate could predict population absence or decline in some environmental areas where the population intrinsic growth rate is still positive. Particularly, considering climatic variability could be especially relevant when predicting biodiversity changes under current climate change scenario in which both recurrence of climatic extremes and temperature climate means are increasing (Coumou and Rahmstorf 2012, IPCC Working Group 1 2014). Depending on the magnitude of extreme climatic events, these could promote populations changes

in their position in the environmental space, that may even push them outside of the species niche, a situation that would correspond to reduced populations capacity to survive if these conditions persists. But if niches are wider than traditionally considered, for a given change in climatic conditions the probability of populations to be pushed out of the niche size would be reduced. Accordingly, neglecting temporal climatic variability in SDMs could have led to the overestimation of population and species extinction risk under climate change.

Despite these substantial implications, inter-annual variability has been scarcely considered in SDMs (Zimmermann et al. 2009). Studies that have accounted for it, have included the inter-year variability as a new dimension of the environmental hyperspace (Zimmermann et al. 2009) or have considered the standard deviation of the climatic suitability over different years when explaining demographic responses (Lloret and Kitzberger 2018). However, in any case there is a clear assessment of the direct impact of including inter-annual climatic variability on niche breadth.

Here, we (1) developed a procedure to include yearly climatic resolution in species niche characterization, and (2) assessed whether this inclusion of inter-annual variability improves the expected correspondence between niche suitability and population-level processes, which in our case correspond to populations responses to an extreme climatic event. Particularly, we used decay data across more than 4,000 km^2 of *Pinus halepensis* L. forests affected by an extreme drought year in the Spanish southeast (Esteve-Selma et al. 2015). In addition, (3) we quantified the relative change in niche size when considering inter-annual climatic variability respect to only considering average climate, for species with different extent of their distribution areas across the Mediterranean basin, which corresponds to contrasting climatic ranges.

3.3 Material and methods

Here we infer species niches by projecting geographic occurrences into two-dimensions environmental space and then estimating kernel densities (Broennimann et al. 2012, Blonder et al. 2014). Considering all the yearly climatic records of every species' occurrences for a given period, we obtain the "inter-annual variability-based" niche

while by considering only the average climate of every species' occurrences we obtain the species "average-based" niche.

Niche suitability and demographic responses in *Pinus halepenis*

Demographic response data

The study was carried out across forests of *Pinus halepensis* in the Region of Murcia (Spanish southeast) (Figure 3.1), an area which represents the arid limit of the species distribution. The average climate of this region is characterized by annual mean temperature of 18° C, and annual rainfall ranging from 240 to 400 mm (Worldclim v 2.0, Fick and Hijmans 2017). During the hydrological year 2013-2014 the Iberian southeast suffered the most intense drought on records, recording on average less than 50 % of the average precipitation for the period 1970-2000 (AEMET 2014)(Appendix B Figure B.1) and causing an extensive die-off and plant mortality in forest and woodlands ecosystems (Esteve-Selma et al. 2015).

Pinus halepensis decay data were collected for the whole Region of Murcia after the extreme drought episode by the Health Forest Unit of the Agriculture and Water Council of Murcia. Data were recorded and translated to raster format of 1 km^2 considering two categories: highly affected forests and unaffected forests, covering a total of 4378 km^2. Around 20% of the forest surface of the region was highly affected. In addition, from this total surface, 264 plots were selected to measure the percentage of affectation from satellite imagery in order to have also a continuous data set which offer more information than the binary one. These decay percentage values were then contrasted in the field for 14 plots, obtaining a correlation of 0.79. Therefore, we used two databases, one with binary data and other with continuous values in order to better contrast our hypotheses (Figure 3.1).

Species niche characterization based on climate average vs inter-annual variability

Pinus halepensis occurrences dataset used to characterize species niche were collected from the third Spanish National Forest Inventory (IFN3 2007). Summarizing a total of 9959 occurrences along the whole country after removing *Pinus* plantations. This occurrence dataset already covers most of the *Pinus halepensis* climatic range (Mauri et al. 2016).

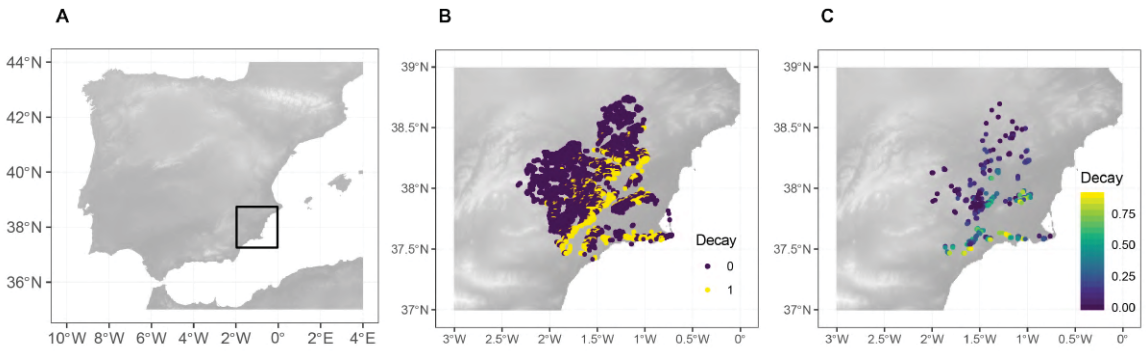

Figure 3.1: A) Location of the study site in the SE of the Iberian Peninsula. B) Location of *Pinus halepensis* decay plots with binary records (1-highly affected – 0-unaffected). Blue colors show not affected plot during the extreme year while yellow ones show highly affected plots. C) Location of *Pinus halepensis* decay plots with continuous records, blue colors show lowest percentages of affectation while yellow one show higher percentages of affectation.

As climatic dataset we used 12 bioclimatic variables for every year of the period 1979-2007 (Chelsa database, Karger et al 2017): bio 1 (annual mean temperature), bio 4 (temperature seasonality), bio 5 (maximum temperature of warmest month), bio 6 (minimum temperature of coldest month), bio 10 (mean temperature of warmest quarter), bio 11 (mean temperature of coldest quarter), bio 12 (annual precipitation), bio 13 (precipitation of wettest month), bio 14 (precipitation of driest month), bio 15 (precipitation seasonality -coefficient of variation), bio 16 (precipitation of wettest quarter) and bio 17 (precipitation of driest quarter); all of them with 1 km^2 resolution. The period of time was selected in order to use the most accurate climatic layers, i.e. after 1979 (Karger et al. 2017), and to be in concordance with the occurrence database, i.e. until 2007, when IFN3 was carried on.

From these 12 bioclimatic variables, we obtained an inter-annual climatic dataset by extracting the climatic values of *Pinus* occurrences locations for every year of the period 1979-2007 (that is, 9959 occurrences x 28 years) and an average climatic dataset by estimating the mean climate of the 28-year period for every occurrence location. From the inter-annual climatic dataset we built the environmental space by using a PCA to reduce the climatic space of the 12 variables into a two dimensional space (Broennimann et al. 2012).

This two-dimension environmental space was used to represent both the *Pinus* averaged-based niche and the *Pinus* inter-annual variability-based niche by trans-

lating the climatic values of *Pinus* occurrences into this environmental space. We then used kernel density function to determine the *Pinus* density for each cell of the two-dimensional environmental space, by applying Gaussian kernel, selecting optimal bandwidth by cross-validation (Duong and Hazelton 2005) and removing values under the 0.05 percentile. Finally, niche suitability was estimated by dividing each niche density value by the maximum density value of the niche, obtaining values ranging between 0 and 1.

We then obtained the climatic suitability of *Pinus* populations affected by drought, after translating the climatic conditions of each population during the extreme year into the two-dimensional environmental space. Climatic conditions of the extreme year 2013–2014 were obtained from monthly precipitation and maximum, minimum, and mean temperature records from between 68 and 114 weather stations of the Spanish Meteorological Agency (AEMET). This climatic dataset was translated into 1 km^2 resolution-maps following Ninyerola et al. (2000) with latitude, longitude and elevation as explanatory variables for climate. Then we applied the "biovars" function (dismo package; Hijmans et al. 2016) to convert them into the final bioclimatic variables format. Finally, we selected the same 12 bioclimatic variables as used for niche characterization.

Suitability-decay analyses

We applied GLM models with populations decay (binary or continuous) as response variable, and populations niche suitability during the extreme year (estimated from inter-annual variability or average based niches) as explanatory variable. We produced four alternative GLM models: binary decay vs. niche suitability from averaged based-model, binary decay vs. niche suitability from inter-annual variability-based model, continuous decay vs. niche suitability from averaged-based model, continuous decay vs. niche suitability from inter-annual variability-based model. Every model used binomial error distribution. These models allow us to compare the accuracy of the relationship between populations decay and niche suitability depending on niche characterization approach (inter-annual or average based).

In order to know whether this possible difference in accuracy varied in relation to populations location within the species niche size, we simulated 30,000 decay

datasets by sub setting the continuous dataset. Particularly, niche suitability differences are expected to be maximum in the not shared space by both niches, based respectively on average and inter-annual variability (Appendix B Figure B.3), since average-based niche predict 0 suitability while inter-annual variability-based niche predict positive suitability values. So, we randomly simulated different percentages of populations located in the non-shared space ranging from 0% to 100% with a population size ranging from 118 to 263 in order to maximize the total number of populations in each case. Then we compared the explained R^2 and p-value obtained from GLM models with population continuous decay as response variable and average or inter-annual niche-based suitability as response variable (see above explanation) and population size for each population simulated dataset (in order to correct the possible low performance of dataset with les number of populations).

Change in niche size and species climatic range

Species niche characterization based on climate average vs inter-annual variability

We characterized the niche of 42 Mediterranean species with distribution areas ranging from the whole Mediterranean basin to endemic species (i.e. mediterranean, occidental mediterrean, iberoafrican and Iberian Peninsula SE endemic species, Appendix B Table B.1) using the average and the inter-annual variability-based approaches. Species occurrence data were collected from (GBIF 2019, `http://www.gbif.org`) and herbarium of Jardí Botànic de Barcelona. Then, species' occurrence records were filtered to remove taxonomic inconsistencies as well as to reduce possible sampling bias by reducing observed occurrences to 1 per 1 km^2 grid cell. Final datasets ranged from 200 to 10,000 observations per species.

Average and inter-annual climatic datasets were obtained from CHELSA database (Karger et al. 2017) for the period 1979-2013. We selected the same 12 bioclimatic variables as selected above for *P. halepensis*. We obtained the environmental space by using a PCA built using inter-annual climatic data from all the occurrences of all 42 analyzed species (Broennimann et al. 2012) (Appendix B Table B.1). We estimated averaged and inter-annual variability-based niches by translating each species occurrences into the environmental space and using kernel density functions as described above.

Change in niche area –climatic range analyses

From these niches, we calculated the ratio between the niche size (area) determined with the inter-annual-based approach and the average-based approach. Finally, we used linear models (lm) with niches' ratio as response variable and average-based niche size logarithmically transformed and species distribution range as response variables.

3.4 Results

Niche suitability and demographic responses

The two first PCA axes explained 60% of the variability of the 12 climatic variables (Appendix B Figure B.2). The niche of *P. halepensis* characterized with inter-annual variability (inter-annual variability-based niche) was 42% larger than the niche estimated with the average dataset (average-based niche). These differences implied that during the extreme climatic year, 93.3% of unaffected forests and 63.3% of highly affected forests were inside the *P. halepensis* niche estimated with inter-annual variability. These values diminished to 52.8% for unaffected forests and 21.2% for highly affected ones when niche was calculated with average climate (Figure 3.2).

Models which relate species decay with species niche suitability during the extreme year obtained with both average-based and inter-annual variability-based niches, show that populations suitability significantly explained species decay irrespective of the decay dataset (binary or continuous) (Figure 3.3, Appendix B Table B.1). However, models with inter-annual variability-based niche suitability had a better fit explaining decay records and had considerably lower AIC (particularly for continuous dataset, see Figure 3.3).

The explanatory capacity of models that include suitability from inter-annual variability-based niche was always higher than that of models including average-based niche suitability, independently of the proportion of populations located in the non-shared area by both niches. Difference between the two models predictive capacity increased as the percentage of populations located in the non-shared area increased (Appendix B Figure B.4 and Table B.2).

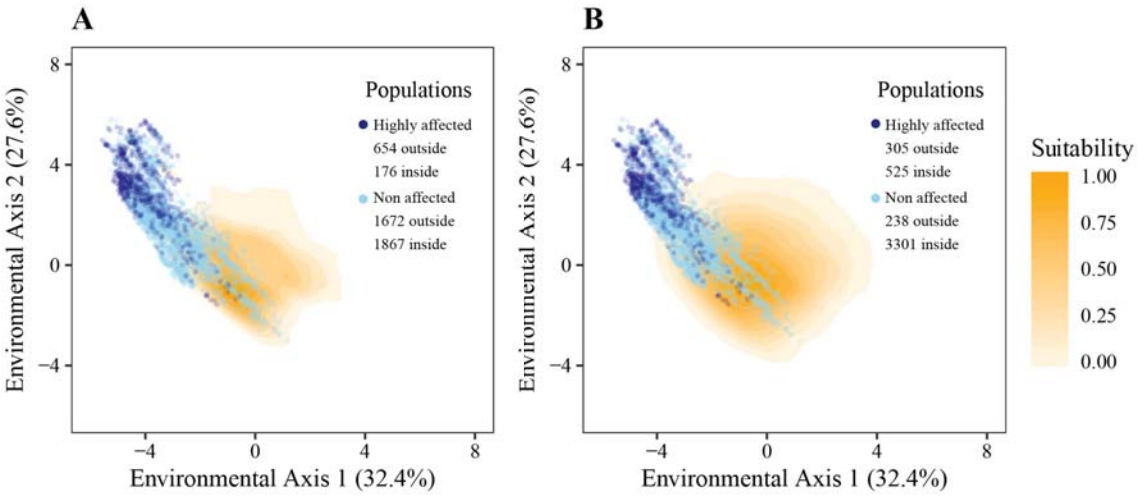

Figure 3.2: *P. halepensis* niche determined by two PCA environmental axis calculated from climatic data and location of highly affected and unaffected populations based on A) average climate and B) inter-annual climatic variability. Dark blue dots represent highly affected *P. halepensis* populations after the extreme event, while light blue dots represent unaffected *P. halepensis* population after the extreme event. Orange palette indicate *P. halepensis* climatic suitability.

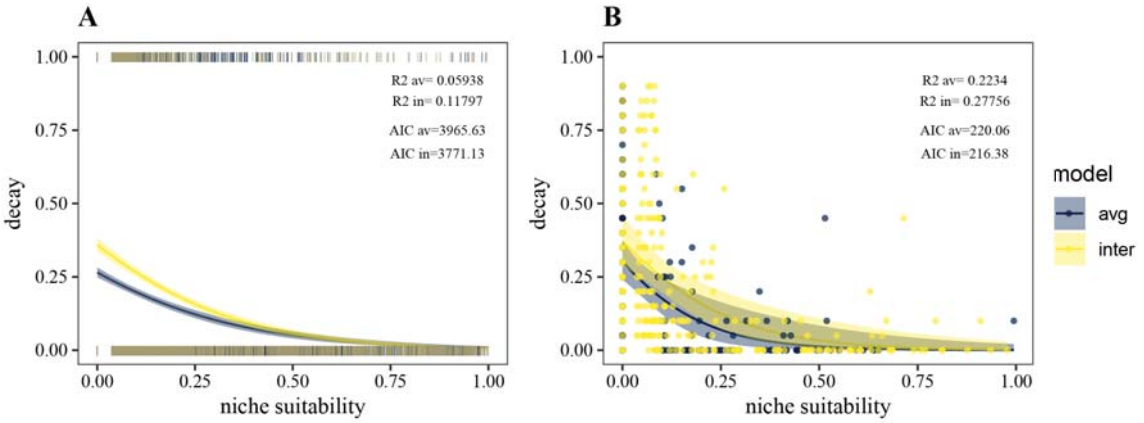

Figure 3.3: Drought-induced affectation in *P. halepensis* populations in relation to population niche suitability estimated from average climate (dark-blue color, avg) and from inter-annual climatic variability (yellow color, inter). Models considered drought-induced affectation as A) a binary response variable (highly affected vs unaffected) or as B) continuous response variable (percentage of affectation in plots).

Change in niche size and species climatic range

The two first PCA axes explained 60.8% of the variability of the 12 climatic variables (Appendix B Figure B.5). Lm models across species with different distribution ranges showed that species with smaller average-based niche area, which correspond

to species with more restricted distribution range, increased more their niche area when considering inter-annual climatic suitability than species with larger average-based niche area and wider distribution ranges (Figure 3.4 and Appendix B Table B.3). In addition, there were no differences between distribution range groups in the relationship of niche area ratio with area of average-based species' niche (Appendix B Table B.3).

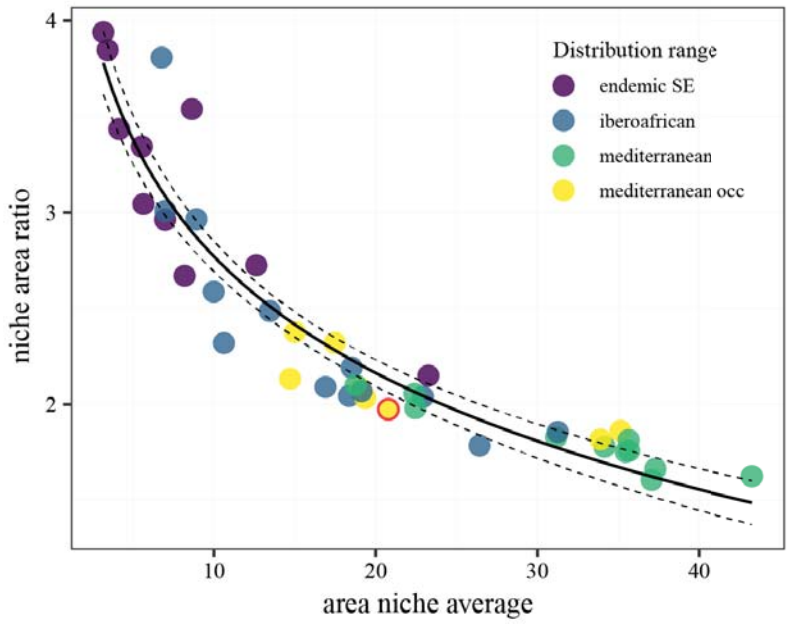

Figure 3.4: Species niche area ratio (niche area estimated with inter-annual variability / niche area estimated with average climate) in relation to species niche area estimated with average climate; this niche area corresponds to distinct distribution ranges across the Mediterranean basin. Green color represents species widely distributed along the Mediterranean basin, yellow color represents species mostly distributed in West Mediterranean basin, light blue color represents iberoafrican species, mostly distributed in North Africa and South Iberian Peninsula and dark blue color represents species distributed in South East Iberian Peninsula. Red circle corresponds to *Pinus halepensis*.

3.5 Discussion

Including inter-annual variability in niche characterization

This study brings out some limitations of the prevalent niche characterization based on average climate. Accounting for the temporal climatic variability in the locations

where species occur increases the range and resolution of species climatic requirements constituting the climatic niche, leading to an increase of niche size respect to the typical use of climate averages. Differently from other studies which include climatic extremes or standard deviation of inter-year climate as a new dimension of the environmental hyperspace (Zimmermann et al. 2009) in addition to climatic means, we included the whole distribution of climatic data across time for all occurrence sites, not adding new dimensions. This procedure allowed effectively quantify differences in niche size. Among all the time that a population has remained at a given site, climate likely have exceeded the species tolerance limits in some years. But these macroclimatic extreme conditions do not necessarily result in population extinction, due to more favorable conditions in microsites, species local adaptation or facilitation species interactions (Benito Garzón et al. 2011, De Frenne et al. 2013, Svenning and Sandel 2013), particularly for long-lived species. Including macroclimatic conditions that overpass the species tolerance limits could lead to overestimate species climatic niche size. This problem can be dealt by removing certain percentile of niche density (in our case, the 5% percentile) when delimiting niche size. In spite of this consideration, our approach presumably distorts niche size less than accounting only for average climate. Inter-annual variability could be also incorporated in different SDMs algorithms allowing for a hierarchical data structure (Wang and Maintainer 2016, Kuznetsova et al. 2017). Finally, including climatic variability when building SDMs is particularly promising under the current climate scenario since it supposes a more conservative approach to determine future species distribution in changing climates.

Climatic variability improves the relationship between macroclimatic suitability and demography

Our results emphasize the relevance of accounting climatic variability to explain the relationship between demographic processes and macroclimatic suitability, specifically under extreme climatic events. We found that *P. halepensis* climatic suitability estimated from niches characterized by inter-annual climatic variability better predicted species decay in comparison to climatic suitability estimated from niches that only considered climatic average (Figure 3.3) under extreme events. It is theoretically assumed that if species niche is properly represented, there should be a correspon-

dence between population demographic processes (such as growth or mortality rates) and niche parameters (Pulliam 2000, Thuiller et al. 2014, Csergő et al. 2017). Multiple studies have tried to assess this relationship (Thuiller et al. 2014, Csergő et al. 2017), particularly under extreme events (Lloret and Kitzberger, 2018, Pérez Navarro et al. 2018, Sapes et al. 2017), however this correspondence does not always emerge (Thuiller et al. 2014, van der Maaten et al. 2017). Very often these niche-demography relationships, particularly in case of parameters related to growth, are affected by many local aspects that impede identifying a clear relationship between niche and population performance (Csergő et al. 2017). Nevertheless, the presence of decoupling factors does not override the potential impact of climatic variability when estimating population dynamics from species niche. Actually, neglecting temporal variability in this kind of studies could introduce a substantial error when predicting population performance in fluctuating environments (Niehaus et al. 2012). Although suitability derived from average-based niche may be robust enough to explain dramatic demographic responses under extreme climatic episodes, as showed in our results (see also Lloret and Kitzberger 2018, Pérez Navarro et al. 2018, Sapes et al. 2017), the better the characterization of the niche, the better the species fitness' predictions.

In addition, the inclusion of inter-annual variability when predicting species responses is especially relevant for populations located in the non-overlapping space between the two niche margins (i.e. corona, between inter-annual and average-based niches) (Appendix B Figure B.4). This area of the species niche (when considering a two-dimensions of the space niche) corresponds to unsuitable climatic conditions according to average-based niche but suitable climatic conditions when including climatic variability in niche characterization. Therefore, average-based niche in this non-shared area does not have predictive capacity for demographic responses. Thus, if the locations' sample was composed only by populations from this area, the only model using climatic suitability that would predict populations response correctly and significantly would be the inter-annual-based one (Appendix B Figure B.5). This mismatch would also imply that populations located in this area, which in many cases correspond to populations sited at the geographic range margin, would be wrongfully located out of the niche size when using average-based species niche.

Change in niche size across species with different climatic and distribution ranges

These abovementioned implications of including inter-year variability could be even more important for species with narrow distribution ranges, which implies smaller average-based niche, comparing with those with broader distribution. Our results showed that, in the Mediterranean basin, species with smaller average-based niche areas increased relatively more their niche area when considering inter-annual climatic variability (Figure 3.4), probably because in species with narrow distribution ranges, spatial climatic variability do not compensate for temporal variability. Therefore, endemic and rare species probably would increase more their niche size, particularly when inhabiting highly fluctuating climates.

Other implications of inter-annual variability vs average-based climatic models

This study highlights some limitations that have been barely considered to date of using climatic averaged datasets of 30-50 years' periods (Hijmans et al. 2005, Karger et al. 2017, Fick and Hijmans 2017) when modelling species niche (Zimmermann et al. 2009). Not accounting for the whole temporal climatic resolution of species occurrences when modelling climatic niche could result in errors affecting from the characterization of species geographical distribution to extinction risk estimates. Underestimations in niche size could lead to understate species geographically suitable areas and such errors could be then also propagated into management plans derived (i.e. selection of favorable areas for protecting species or assisted migrations). Most importantly, these possible niche underestimations could vary depending on species distribution ranges. In addition to the error derived from the non-inclusion of climatic variability, using systematically 30-years averaged climatic periods could be specially pernicious when characterizing the climatic niche of short-lived species, as in plagues (Jaime et al. 2019) since they emerge explosively as a consequence of specific climatic conditions that appear in particular years of the period.

Estimates of invasion risk or extinction rate could be also affected by niche characterization errors. In this case, niche size underestimation could lead to understate invasion risk or to overestimate extinction debt as populations and species could be

able to survive under changing climates or extreme events more than expected with average-based niches. In addition to temporal climatic variability there are others sources of climatic variability not included in the prevalent climatic datasets (Worldclim, CHELSA), such as the climatic heterogeneity held within geographic units due to a coarse spatial resolution (Geiger et al. 1995, Lenoir et al. 2013, De Frenne et al. 2013, Lembrechts et al. 2019). This lack of resolution, which could be particularly important for plants living in particularly favorable microhabitats, and for small-stature plants which actually experience temperatures at ground-surface level (Lembrechts et al. 2019), may hinder to accurately portray species requirements (Guisan et al. 2019) and can neglect the important buffer capacity of microclimates on the ecosystem response to climate change (Ackerly et al. 2010). Nevertheless, high resolution climatic datasets - even at daily resolution - are increasingly becoming available (Wan 2008, Bramer et al. 2018) and they suppose a promising option to deal with these spatial and temporal limitations.

4

Niche distance in the environmental space as a predictor of species responses to extreme climatic events.

Pérez-Navarro M.A., Esteve M.A., Lloret F.

4.1 Abstract

From niche theory it could be assumed that population performance decreases from niche optimum toward the edge of the species niche. Species Distribution Models (SDMs) outputs have been often used to assess the relationship between demographical trends and niche space, but empirical studies has proven weak or inconclusive. Among other limitations that could impede the emergence of this relationship (species interactions, local favorable environmental conditions not included in the models), SDMs could exhibit a limited capacity to predict suitability under highly shifting environmental conditions. Here we propose the use of distances in the environmental space between niche and population environmental conditions to predict species performance under climates exceptionally distant from species optimum. For this purpose, we took advantage of an extreme drought event occurring in the SE of the Iberian Peninsula that highly affected rich semiarid shrubland communities located in three different bedrock sites implying a gradient of water availability. Then, we comparatively analyzed the relationship between (1) population decay (mortality and remaining green canopy) and distances between populations and species niche limit and centroid in the environmental space, and (2) species decay and climatic suitability estimated from SDMs (MaxEnt). We found that distances to the niche centroid and limit better explained population decay than SDMs-derived suitability, highlighting that population located farther from species' niche during the extreme episode showed higher vulnerability to drought. In addition, we found significant differences between bedrock sites suggesting a relevant buffering role of soils on species decay responses to extreme drought events. We conclude that distances between populations in the environmental space are consistent with demographic responses to extreme drought. This approach reveals to be more efficient than the use of climate suitability indices derived from SDMs, particularly when dealing with extreme climate events that correspond to situations outside the species environmental niche.

4.2 Introduction

In his concluding remarks Hutchinson (1957) defined the niche as the n-dymensional hypervolume -an abstract range of multiple ecological conditions- which allow species to persist indefinitely. In spite of the contemporary limitations of niche formalization and representation at that time, Hutchison also suggested that within this hypervolume, all points would not have equal probability for species' persistence, considering that there would be "an optimal part of the niche with markedly suboptimal conditions near the boundaries". This expectation could be considered as inspiration for a largely known paradigms in biogeography: the Centre-Periphery Hypothesis (CPH) (Pironon et al. 2017). This hypothesis predicts that species' abundance and fitness progressively declines from the geographic distribution center towards the distribution edges, by assuming an exact concordance between environmental and geographic spaces, given that population performance would decline from the niche optimum towards the limits (Maguire and Jr. 1973, Brown 1984, Pironon et al. 2016). Nevertheless, the correlation between species niche estimates and population abundance or performance is not consistently supported by literature (Sexton et al. 2009, Pironon et al. 2016, Dallas et al. 2017), particularly when considering growth or recruitment rates. These poor correlations could be due to the influence of density-dependence processes (Thuiller et al. 2014), the non-consideration of some relevant local mircrohabitat conditions (such as soils or biotic interactions) in niche estimation (Csergő et al. 2017, Lembrechts et al. 2019), or the existence of non-equilibrium dynamics (such as high population growth in recently colonized areas even though these locations are scarcely envrionmentally suitable, Thuiller et al. 2014, Osorio-Olvera et al. 2019). The existence of these decoupling factors, however, do not invalidate the potential role of niche estimates explaining population performance (Csergő et al. 2017), particularly when this could be strongly influenced by climate, as in the case of plant decay and mortality associated to extreme climatic events (Sapes et al. 2017, Lloret and Kitzberger 2018, Pérez Navarro et al. 2018).

Species Distribution Models (SDMs) provides niche statistics estimates which could be interpreted as species probability of occurrence, or environmental suitability, usually ranging between 0 –non suitable environment- to 1 –optimal environmental conditions- (Franklin 2010). They frequently consist on correlative models which

relates species occurrences with the environmental conditions of these sites without attending to the functional causality of this relationship, although there also exist other mechanistic modelling approaches which do attend to functional relationships Guisan and Zimmermann 2000, Franklin 2010, Guisan et al. 2017). SDMs are reasonably accurate for characterizing current natural distributions of species (Elith and Leathwick 2009, Guisan et al. 2013), although they are also increasingly used to predict changes in species distribution under shifting environmental conditions, as in case of climate change scenarios or potential novel areas for alien species invasion (Thomas et al. 2004, Thuiller et al. 2005, Broennimann and Guisan 2008, Araújo et al. 2019). However, when projecting SDMs under environmental conditions highly dissimilar from those used to calibrate the models, these models could lead to non-reliable suitability estimates (Dormann 2007, Elith et al. 2010), for instance, by systematically producing 0 value outputs, and therefore hindering the correlation with demographic parameters (Pérez Navarro et al. 2018).

According to the niche theoretical frame, species probability of occurrence would be null outside of the niche space, but there are several circumstances that may allow populations to persist outside of fundamental niche boundaries. For instance, they could persist under unfavorable conditions (sink habitats, with a negative population growth) if they are sustained by immigration from source habitats (Pulliam 2000). Plant longevity may also delay climate-induced changes in species distribution (Svenning and Sandel 2013). Finally, pulses of abrupt climatic changes can temporarily displace populations outside of the species niche (Pérez Navarro et al. 2018). Under these situations of populations living outside the niche space, negative population growth rates (i.e. decay) are, in fact, related to the lack of suitability of environmental conditions. So, it could be expected to find more negative growth rates in populations located far away from the niche limit compared to populations located outside but closer to the niche. This implies that, in the same way as points within species niche would not show equal capacity for hosting species presence (Hutchinson 1957, Maguire and Jr. 1973, Brown 1984), points outside of species niche would not have the same potential for hindering species occurrence.

Accordingly, niche parameters which allow to estimate niche environmental accuracy even if population are located outside of species niche (when niche suitability

estimates can attain zero values) can be useful to explain demographic responses, particularly in sink populations, population suffering extreme climatic events or alien species expansion. Here we propose the use of Euclidean distances between population locations in the environmental niche space and species niche centroid or limits as measures to obtain continuous niche estimates even outside of niche boundaries (Figure 4.1). While niche centroid represents the optimal conditions for species performance, niche limit represent the threshold separating species persistence from extinction, that is, positive from negative growth rates. So, higher distances to niche centroid are expected to result in a more decrease in populations' fitness and abundance(possibly with a particular decrease after trespassing he niche boundaries), while distances to niche limit will imply positive or negative responses depending on population position within or outside of the niche.

In this study, we took advantage of an extreme drought year occurring in the SE of the Iberian Peninsula which largely affected vegetation communities to analyze the relationship between niche estimates and demographic responses in shrubland communities located in three different bedrocks inducing different water deficit. Specifically, we (1) tested whether populations located farther from the species niche during the extreme event show higher population decay, measured as remaining green canopy (RGC) and mortality; (2) compared the predictive capacity of distances to climatic niche centroid and distances to climatic niche limit when explaining populations decay of different species; (3) compared niche-based distances and SDM outputs as predictors of populations decay; (4) compared the relationship between niche estimates and demographic responses on three different bedrock with distinct soil water retention capacity.

4.3 Material and methods

Study area

The study was carried out in three semiarid shrubland areas in the southeast of the Iberian Peninsula (Figure 4.2: Cuatro Calas (1.63°W, 37.38°N), Moreras' mountain (1.32°W, 37.56° N) and Calblanque Natural Park (0.74° W, 37.61° N), each of them sited in a different dominant lithology: sandstone, limestone and metamorphic, re-

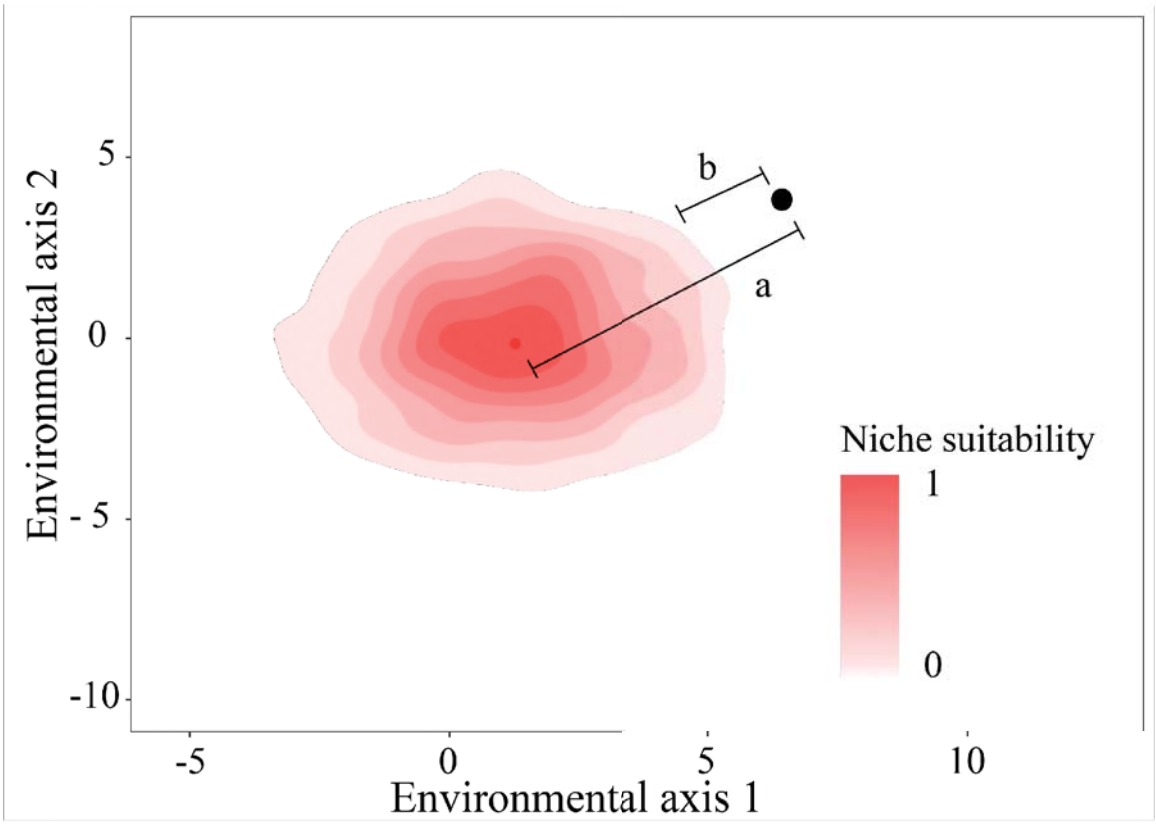

Figure 4.1: Example of species niche in an environmental space defined by two environmental axis. White to red color gradient represents species climatic suitability, where 1 correspond to niche optimum and 0 to the environmental space outside of the niche. The black dot represents a population located outside of species niche boundaries, and "a" and "b" are distances to the niche centroid and to the closest point of the niche boundary, respectively.

spectively. These areas share similar vegetation communities, dominated by semiarid shrubland species – genus *Genista* spp. (Fabaceae), *Helianthemum* spp. (Cistaceae), *Teucrium* spp. (Lamiaceae) or *Thymus* spp. (Lamiaceae)- mixed with some big-size grasses such as *Macrochloa tenacissima* (L.) (Poaceae). Study sites also show relatively low anthropization symptoms, since they are encompassed within Natura 2000 network or Natural Parks.

The study sites are included within the Mediterranean xeric bioclimate (Rivas Martínez et al. 2017), which is characterized by mean annual temperatures of 17° C, and annual rainfall of 245-280 mm (reference period 1971-2000, AEMET and IP 2011). During the hydrological year 2013-2014 the Iberian southeast suffered its driest year on record, leading to extensive plant communities' die-off. Particularly, Cuatro Calas

and Moreras Mountain accumulated less than 30% of the average precipitation for the reference period 1971-2000 and Calblanque Natural Park less than 70 % (Appendix C Figure C.1, AEMET 2014).

Regarding to site soils, Cuatro Calas and the Moreras Mountain are Lithic Leptosols (around 10 cm in depth)(IUSS Working Group WRB 2015), while in Calblanque they are Skeletic Regosol (i.e., around 1m in depth)(IUSS Working Group WRB 2015). In addition, soils in Moreras' Mountain (limestone bedrock) showed the highest water retention capacity in relation to soil volume, while Cuatro Calas soils (sandstone bedrock) showed the lowest water retention capacity (Figure 4.2). However, it is worth noting that the absolute water retention capacity was higher in Calblanque than in the other localities, due to its considerably higher soil depth. Soil water retention capacity was obtained for each bedrock as the difference between moisture content at the field capacity and wilting point. Both these values were obtained following Cassel and Nielsen (1986), from three soil samples per bedrock type, where each sample consisted on two replicates of the upper 10cm. In addition, organic carbon content (Anne 1945, Duchaufour 1970) and particle size composition (Gee and Bauder 1986) were also estimated (see Appendix C Figure C.2 and Table C.1).

Die-off data

During January-March 2016, 30 replicated plots of 5x5m were established within each area, being separated from each other by at least 25 linear meters. All plots shared similar topographic characteristics with moderate to slight slope and south or south-east orientation. Within each plot we recorded the total number of individual per woody species (total of 38 species) and visually estimated the proportion of remaining green canopy (RGC) per individual (as a proxy of species die-off, Sapes et al. 2017, Pérez Navarro et al. 2018). In order to ensure that the green cover loss resulted from the recent drought, we avoided individuals with signs of older decay (e.g., stumps, decomposed stems, branches with no thin tips). Each individual was also categorized as alive (RGC $> 0\%$) or dead (RGC $= 0\%$).

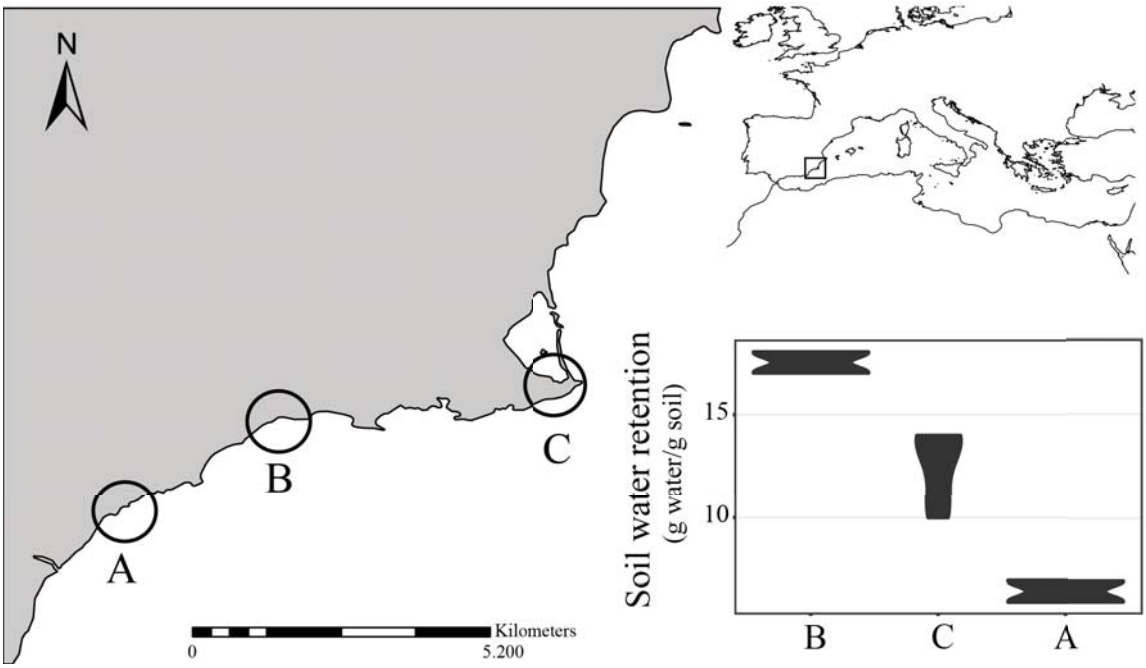

Figure 4.2: Top right panel shows the location of the study region in the Mediterranean basin. Left panel shows the expanded map of the study area, indicating the study sites: A) Cuatro Calas (sandstone bedrock), B) Moreras' mountain (limestone bedrock) and C) Calblanque Natural Park (schist metamorphic bedrock). Bottom right panel shows the soil water content available for the top 15 cm of each study site estimated following (Cassel and Nielsen 1986).

Niche characterization and distances extraction

We compiled the geographical distribution data of the 38 sampled species from the Global Biodiversity Information Facility (GBIF) (GBIF 2019, `http://www.gbif.org`) and the herbarium of the Institut Botànic de Barcelona. Species occurrence records were then filtered in order to remove taxonomic and geographic inconsistencies and to reduce possible sampling bias by randomly thinning species' records to one observation per Km^2 (in concordance with the spatial resolution of the climatic dataset) for those datasets with more than 100 occurrences. Species occurrences datasets finally ranged from 60 to 7,000 observations.

We used 12 bioclimatic variables for every year of the period 1979-2013 (34 years): annual mean temperature (bio 1), temperature seasonality (standard deviation $\times 100$) (bio 4), maximum temperature of warmest month (bio 5), minimum temperature of coldest month (bio 6), mean temperature of warmest quarter (bio

10), mean temperature of coldest quarter (bio 11), annual precipitation (bio 12), precipitation of wettest month (bio 13), precipitation of driest month (bio 14), precipitation seasonality (coefficient of variation) (bio 15), precipitation of wettest quarter (bio 16), and precipitation of driest quarter (bio 17); all of them with 1 Km^2 resolution. These variables were obtained after translating monthly temperature and precipitation variables from Chelsa database (Karger et al. 2017) by applying the biovars function (dismo package Hijmans et al. 2016). The remaining bioclimatic variables were discarded in order to facilitate the interpretation of environmental axis, removing variables that potentially correlate differently for different species or different time periods (i.e. temperature of hottest quarter with precipitation of hottest quarter, since during the average period these variables correlates negatively due to summer drought, while during the extreme year rainfall was higher precisely during summer months).

Then, we used a Principal Component Analysis (PCA) to convert the environmental space of the 12 bioclimatic variables for the 1979-2012 period into a two-dimensional surface defined by the first and second principal components (Broennimann et al. 2012). The PCA was calibrated using every year-climate from all the occurrences sites of all the 38 analysed species (Appendix C Table C.2). These first and second axes explained together the 60.8% of the 12 variables' variability (see Appendix C Figure C.2). This explicit consideration of between-year climatic variability allows for a more accurate niche characterization, while considering a time scale (yearly) comparable to the extreme event.

We characterized species climatic niches by translating species' geographical occurrences into the environmental climatic space and applying kernel density functions (Broennimann et al. 2012) (ks package version 1.11.3, Duong 2018), which allow to determine density values for each cell of the species environmental space. Particularly, we applied Gaussian kernel functions and selected optimal bandwidth by cross-validation (Duong and Hazelton 2005). Then, we estimated the species niche centroid as the gravity center of species' niche (i.e. mean of environmental axis values weighted by species' density), and species niche limit as the perimeter of species' niche space after discarding densities below the 0.05 lowest percentile.

We then translated the climatic conditions of each studied population (i.e., occurring in plots) during the reference average period 1979-2012 and during the

extreme year 2013-2014 into the two-dimension environmental space (population climate, hereafter). Mean climatic conditions of the reference period 1979-2013 period were obtained by averaging yearly climate of each population site for the previously selected variables. Climatic variables of the extreme year 2013–2014 were obtained in 1 Km^2 resolution from monthly precipitation and maximum, minimum, and mean temperature records from between 68 and 114 weather stations of the Spanish Meteorological Agency (AEMET), by applying Ninyerola et al. (2000) procedure (Pérez Navarro 2018) and the "biovars" function (dismo package; Hijmans et al. 2016). Then, we selected the same 12 bioclimatic variables used for niche characterization. Since the climate databases had 1 Km^2 resolution, almost all the plots within the same study area had the same observed climate value.

Finally, we estimated Euclidean distances in the environmental space between (1) population climate and species climatic niche centroid, and (2) between population climate and the closest point of the niche limit, for both the reference 1979-2012 period and during the extreme 2013-2014 year. In addition, we also classified species' population according to whether they were "inside" or "outside" of species niche perimeter.

Species niche modelling

From these described species occurrence and climatic average datasets, we built Species Distribution Models (SDMs) for every sampled species in order to estimate populations' climatic suitability both during the average 1979-2012 and the extreme drought episode 2013-2014. We specifically used MaxEnt algorithm throughout R (dismo package Hijmans et al. 2011), with 5 biologically relevant and uncorrelated variables from the 12 variables used in niche characterization: bio 4, bio 10, bio 12, bio 15 and bio 17. We also compared PCA axis built with all the 12 variables and with this 5, in order to discard differences between the two approaches (SDMs and niche distances) due to the use of different climatic variables (Appendix C Figure C.2 and C.3). Each species model was built with 20,000 background points in the biogeographic study region (i.e., Mediterranean basin), five-fold cross-validation, regularization multiplier of 3, and threshold feature unselect to produce smoother response curves. Then models accuracy was evaluated using the area under of the Receiver Operating Characteristic curve (ROC) curve (AUC; Hanley and McNeil

1982), where values higher to 0.75 indicates high model performance (Elith et al. 2002). Each species' model was finally projected over the average reference climate (1979-2012), and also over the extreme climatic conditions (2013-2014), in order to obtain populations' climatic suitability during the reference and the extreme period.

Statistical analyses

We applied generalized linear mixed models (GLMM) (lmerTest R package, version 3.1.0., Kuznetsova et al. 2017) with species decay (RGC or mortality) as response variable, and population distances to species niche and bedrock type as explanatory variables, with species and plot as crossed random effects. In order to reduce noise in model residuals we aggregated the original database with 12,124 individuals and added the number of individuals as a weighting factor of mix models. Due to the high affectation of species during the extreme drought year, RGC variable showed a zero-inflated distribution, so we decided to separately model RGC > 0 as response variable (with Gaussian error distribution) and mortality percentage (with binomial error distribution) as response variables. We finally built four models for each subset of population distances to niche for both reference (1979-2017) and extreme (2013-2014) period: (1) RGC as a function of niche centroid distance, bedrock type and their interaction (2) RGC as a function of niche limit distance bedrock type and their interaction, (3) mortality as a function of niche centroid distance, bedrock and their interaction; and (4) mortality as a function of limit distance, bedrock type and their interaction (Appendix C Table C.3). In order to know whether population distance to the niche limit was inwards or outwards the niche, we additionally included a niche location variable ("inside" or "outside") interacting with limit distance. The interactions between bedrock and population distance to centroid or limit were discarded from models in those cases where models showed convergence limitation.

Then, we replicated RGC generalized mix models but replacing distance to niche by climatic suitability derived from SDMs as explanatory variable. Therefore, RGC was the response variable and lithology and climatic suitability during the reference period or during the extreme period as explanatory variables. We therefore built two alternative models for climatic suitability: RGC as response variable with lithology and suitability during the average period and their interaction as explanatory variables, and RGC as response variable with lithology and suitability during

the extreme episode and their interaction as explanatory variables (Appendix C Table C.3). In both cases we used Gaussian error distribution and plot and species as crossed random effects.

4.4 Results

Both distances to niche in the environmental space and climatic suitability estimated for the reference period significantly explained the observed remaining green canopy (RGC) after the extreme events (Figure 4.3 A-B and Appendix C figure C.5 A-B), supporting that species farther from their climatic niche or with lower climatic suitability during the reference period were more vulnerable during extreme drought episodes in terms of green cover. Particularly, in the case of niche estimates, distance to centroid was marginally significant while distance to the niche limit for population located within the niche (meaning population located closer to centroid) was significant related to higher RGC (Appendix C Figure C.5 A-B, and Tables C.5 and C.6). Also, distance to niche limit for population located out of the niche related significantly with more RGC, probably due to the low number of population located outside of the niche.

However when considering climatic conditions of the extreme episode, only distances in the environmental space significantly explained species decay in terms of green canopy (Figure 4.3 A-B, Figure 4.4 A), indicating that those population located farther from species niche during the extreme period suffered higher losses in species green canopy. In this case both distance to niche centroid and distance to niche limit when species where located outside of the niche were significant (Tables 4.1 and 4.2). Contrastingly, climatic suitability during the extreme event did not correlate with RGC presumably due to the extremely low suitability values obtained for almost every populations, as a consequence of the high difference between calibration and projection conditions (Appendix C Figure C.6, and Table C.9).

On the other hand, when analyzing the relationship between mortality and distances in the environmental space we obtained that distance to species niche limit interacting with population position significantly related to species mortality whereas population distance to niche centroid didn't show to be significant (Figure 4.3 C-D, Tables 4.3 and 4.4, and Appendix C Figure C.5 C-D and Tables C.6 and C.7).

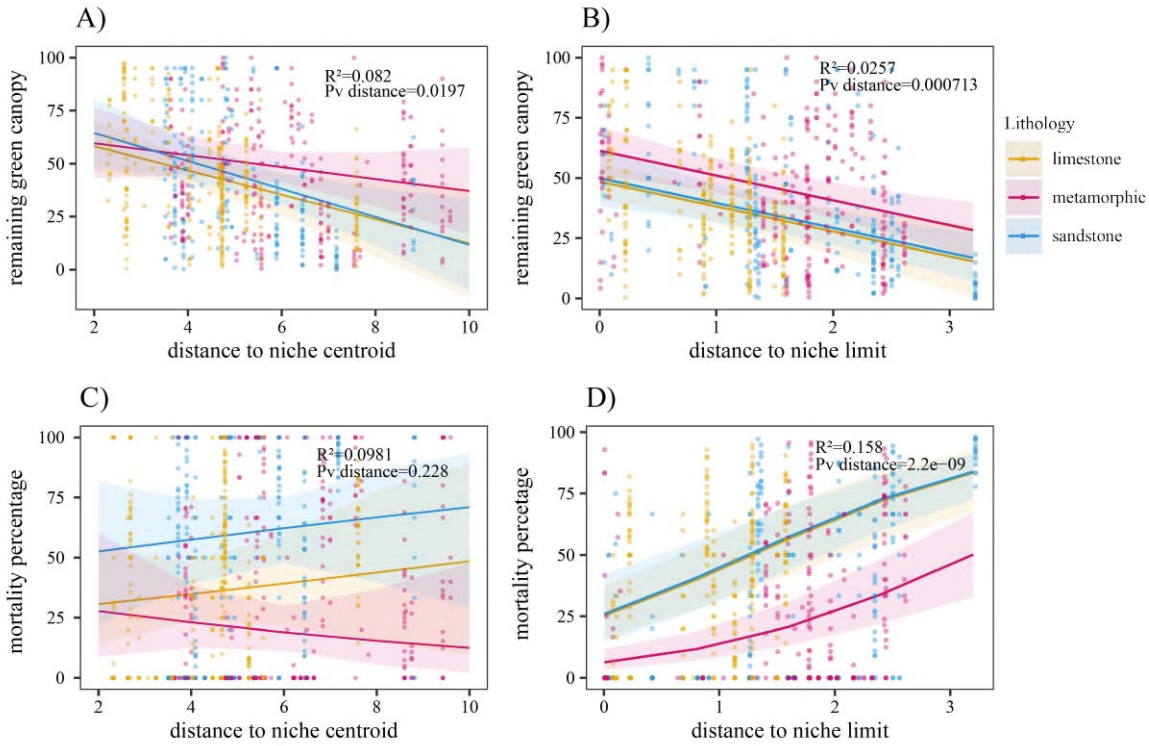

Figure 4.3: Remaining Green Canopy (RGC) in relation to population distances during the extreme drought event to their respective species niche centroid (A) and to the closest point of the niche limit (B); and mortality percentage in relation to population distances during the extreme drought event to their respective species niche centroid (C) and to the closest point of the niche limit (D). In all four cases, only the subset of populations located outside the niche were considered. Yellow dots shows distances of populations located in Moreras' Mountain (limestone bedrock), magenta dots shows distances of plots located in Calblanque Natural Parck (metamorphic bedrock) and blue dots show distances of populations located in Cuatro Calas (sandstone bedrock). Yellow line, magenta and blue lines represent the regression lines of each model for each bedrock type (limestone, metamorphic, and sandstone, respectively). Each panel also shows R^2 model values and ANOVA P-values (Pv) for testing significance of niche distances.

Finally, site bedrock also showed to be significant, where Metamorphic exhibited the higher RGC and lower mortality percentage while limestone and sandstone did not show difference between them in most models explaining decay as a response of distances during extreme event and bedrock type (Appendix C Table C.11).

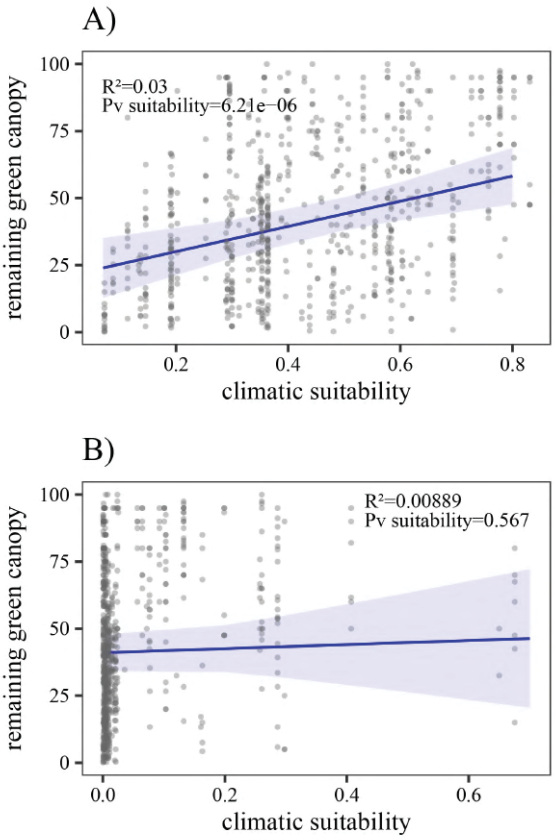

Figure 4.4: Relationship between Remaining Green Canopy (RGC) and climatic suitability estimated for each plot for (A) the reference period 2079-2012, and (B) the extreme drought year 2013-2014; in both cases climatic suitability was estimated with MaxEnt. Although both models included bedrock as explanatory variable this is not represented in order to better visualize the lack of significance of climatic suitability estimated during the extreme year. Complete model results are included in Appendix C Table C.6 and C.7. Each panel also shows R^2 model values and ANOVA P-value (Pv) for testing the significance of climatic suitability.

Table 4.1: Results of Generalized Mixed Models explaining Remaining Green Canopy (RGC) as a function of soil bedrock and populations' distances to the species niche centroid during the extreme drought episode (2013-2014) and the interaction between these two variables, with plot and species as crossed random effects.

	Estimate	Std. Error	df	t value	Pr(>|t|)	
(Intercept)	69.813	10.056	41.689	6.942	0.000	***
Metamorphic	-4.462	7.846	554.030	-0.569	0.570	
Sandstone	7.942	8.224	628.866	0.966	0.335	
centroid_distance	-5.751	2.212	40.492	-2.600	0.013	*
Metamorphic:centroid_distance	2.923	1.342	634.558	2.178	0.030	*
Sandstone:centroid_distance	-0.864	1.517	667.956	-0.570	0.569	

Statistical significant levels: "." p<0.1 ; "*" p<0.05 ; "**" p<0.01 ; "***" p<0.001

Table 4.2: Results of Generalized Mixed Models explaining Remaining Green Canopy (RGC) as a function of soil bedrock and populations distances to the closest point of species niche limit during the extreme drought episode (2013-2014), and the interaction with population position inside (in) or outside (out) the niche during the extreme event, with plot and species as crossed random effects.

	Estimate	Std. Error	df	t value	Pr(>|t|)	
(Intercept)	48.507	3.809	61.546	12.735	0.000	***
Metamorphic	12.890	3.235	204.888	3.984	0.000	***
Sandstone	1.438	4.105	213.173	0.350	0.726	
limit_distance:in	16.321	16.292	616.216	1.002	0.317	
limit_distance:out	-10.334	2.689	143.419	-3.843	0.000	***

Statistical significant levels: "." p<0.1 ; "*" p<0.05 ; "**" p<0.01 ; "***" p<0.001

Table 4.3: Results of Generalized Mixed Models explaining mortality percentage as a function of soil bedrock and populations' distances to species niche centroid during the extreme drought episode (2013-2014) and the interaction between these two variables, with plot and species as crossed random effects.

	Estimate	Std. Error	Z value	Pr(>|z|)	
(Intercept)	-1.006	0.844	-1.192	0.233	
Metamorphic	0.294	0.336	0.875	0.382	
Sandstone	0.913	0.438	2.083	0.037	*
centroid_distance	0.095	0.189	0.501	0.616	
Metamorphic:centroid_distance	-0.218	0.034	-6.369	0.000	***
Sandstone:centroid_distance	0.005	0.063	0.073	0.942	

Statistical significant levels: "." p<0.1 ; "*" p<0.05 ; "**" p<0.01 ; "***" p<0.001

Table 4.4: Results of Generalized Mixed Models explaining mortality as a function of soil bedrock and populations' distances to the closest point of species niche limit during the extreme drought episode (2013-2014), and the interaction with population position inside (in) or outside (out) the niche during the extreme event (2013-2014), with plot and species as crossed random effects.

	Estimate	Std. Error	z value	Pr(>|z|)	
(Intercept)	-1.087	0.286	-3.794	0.000	***
Metamorphic	-1.608	0.200	-8.042	0.000	***
Sandstone	0.035	0.235	0.150	0.881	
limit_distance:in	-3.240	1.425	-2.274	0.023	*
limit_distance:out	0.844	0.138	6.117	0.000	***

Statistical significant levels: "." p<0.1 ; "*" p<0.05 ; "**" p<0.01 ; "***" p<0.001

4.5 Discussion

Niche estimates and demographic responses under extreme events

In this study we show that population distances in the environmental space to species' niche limit and centroid both during the extreme event and during the reference climatic period explained species different green canopy and mortality during an extreme drought episode (Figure 4.3 and Appendix C Figure C.5). In spite of the weak literature support to the correlation between species performance and niche parameters (Sexton et al. 2009, Dallas et al. 2017), several studies have shown populations higher performance or abundance at species niche core compared to the species range margins (Jump and Woodward 2003, VanDerWal et al. 2009, Martinez-Meyer et al. 2013, Sangüesa-Barreda et al. 2018), especially under extreme climatic conditions (Sapes et al. 2017, Lloret and Kitzberger 2018, Pérez Navarro et al. 2018). These last studies evidenced the correlation between climatic suitability under historical reference conditions and population decay during extreme drought, pointing that populations historically located farther from species' climatic optimums showed higher sensitivity to extreme climatic events. Nevertheless, by using distances in environmental space we have also demonstrated that those populations more displaced from the species niche during the extreme climatic episode are also more prone to decay, indepen-

dently from the population location within the species niche during the reference period. Actually, population distances to niche limit and centroid during the extreme episode even explained a slightly higher percentage of variability in decay models than distances during the reference period, particularly when analyzing mortality (see models R^2, Figure 4.3 and Appendix C Figure C.5). The relationship between populations' performance and niche distances could emerge more evidently during extreme climatic episodes in relation to normal years, because demographic responses under exceptionally extreme climates are likely more influenced by climate than by other environmental forces such as unmeasured microhabitat conditions, species interactions or favorable community structure (Dallas et al. 2017).

Looking closely at decay models during the extreme event, we observe that the models analyzing green canopy loss showed lower explained variability than mortality models. These results are consistent with other studies in which green cover losses were seen to be influenced by a wider range of contributors beyond the purely climatic ones comparing to mortality responses (Galiano et al. 2010). Interestingly, distances to niche limit or centroid seemed not to be completely interchangeable when explaining continuous physiological responses or binary states (dead-alive). Whereas distances to niche centroid resulted slightly better explicative than distances to niche limit to explain population differences in green canopy (Figure 4.3 A-B and Tables 4.1 and 4.2), distances to niche limit and population position (within or outside of the niche), better explained population mortality observed patterns (Figure 4.3 C-D, Tables 4.3 and 4.4). These findings are consistent with general biogeographic paradigms assuming a gradient of population fitness within the niche, from niche centroid to niche boundaries (Maguire and Jr. 1973, Pironon et al. 2016), with mortality being particularly relevant outside of species niche, where environmental conditions do not fulfill species' requirements (Hutchinson 1957, Maguire and Jr. 1973).

Distances in the environmental space vs climatic suitability

Our finding supports the use of niche estimates other than climatic suitability under climatic conditions that are highly dissimilar from species tolerance. While population distances to niche limit and centroid during an extreme drought event significantly explain population observed decay responses (both mortality and green cover losses), the near-zero suitability values obtained from SDM (MaxEnt) for the majority of

species during the extreme event presumably prevented from obtaining a significant correlation between decay and suitability. These extremely low climatic suitability values probably emerge as a consequence of the exceptionality of the extreme year that actually displaced most populations outside of the species niche, even for those species with more arid distribution, in addition to the limited ability of models to predict suitability under climatic scenarios highly dissimilar from calibration climatic conditions (Elith et al. 2010). Although MaxEnt does not lead to response curves particularly unrealistic outwards training data (since it makes "clamped" predictions, which constantly keep the same prediction of the most extreme environmental value) (Elith and Graham 2009, Elith et al. 2010), it implicitly assumes that modelled parameters and variables interaction obtained for calibration dataset will be maintained in shifting environmental scenarios (Phillips and Dudík 2008, Merow et al. 2013), which could potentially lead to extrapolation errors. Conversely, other simpler methods that do not include variables interaction or complex parametrization, can provide output values beyond niche limits. They can be particularly useful to explain demographic responses under highly dissimilar environmental conditions by predicting decay under extreme climatic events, determining negative growth rates for populations located outside of species niche (sink populations) (Pulliam 2000), or assessing niche shift risk (Guisan et al. 2014) for invasive species in novel conditions. Particularly euclidean distances in the environmental space and Mahalanobis distances have been proposed as good proxies of climatic suitability when aiming to relate population performance and species niche (Martinez-Meyer 2013, Osorio-Olvera 2019). These approaches correct for variables correlation and do not include variables interaction, not making interaction assumptions under changing conditions. In addition, they provide continuous values, not constrained between 0 and 1, obtaining values even if environmental conditions do not fulfill species requirements.

Nonetheless, it worth noting some considerations concerning both approaches. Niche-related variables and suitability indices do not necessarily depict real species physiological optimums and limits, as far as they do not represent the species fundamental niche. They are derived from geographical species occurrences, which only account for the regions of the fundamental niche which correspond to the current climate and implicitly include species interactions and dispersal limitations (Colwell and Rangel 2009). In addition, the impossibility of distinguishing between source and

sink populations in most occurrence databases (Osorio-Olvera et al. 2019), as well as the possible bias in record sampling makes it difficult to exactly portray species' realized niche. Here we tried to overcome this last limitation by randomly thinning species records to 1 occurrence per km^2 and by visually checking every species' niches and SDMs response curves. In addition, our niche estimations did not account for environmental conditions actually experienced at plant or population level (Lenoir et al. 2013, Lembrechts et al. 2019a), since global environmental databases frequently present a relatively coarse spatial resolution (i.e., 1 Km^2). Finally, both niche distances and SDMs outputs were highly sensitive to the selected climatic variables defining niche dimensions, since different climatic variables subsets are differently related among them - both temporal and spatially (Elith et al. 2010)- leading to different environmental hyperspaces. We tried to overcame this constraint in niche characterization by avoiding variables that temporally correlates in different way within the study area (ie. precipitation of hottest quarter negatively correlated with temperature of hottest quarter during the average period, but positively during the extreme drought year since most precipitation were recorded precisely in summer), and we also discarded highly correlated variables in SDM analyses.

Soils' relevance on species decay

Even using the most accurate niche estimates, the correlation between population performance and niche position could be total or partially masked by the influence of other factors and processes, such as species interaction (Svenning and Sandel 2013, Dallas and Hastings 2018), local adaptation (Benito Garzón et al. 2011), or microhabitat variables which usually are not included in niche characterization (Lenoir et al. 2013, De Frenne et al. 2013, Csergő et al. 2017). In our case, we included soil bedrock as explanatory variable in the decay models, obtaining that this variable was always significantly relevant explaining RGC and mortality (Tables 4.1 to 4.4 and Appendix C Tables C.4 to C.9). Although our study design had a block-site structure, where population living in the same bedrock type are also located in the same area, soils are the main candidates among local environmental factors to determine site differences in RGC and mortality since study plots share similar topography, slope, orientation and distance to coast line. Specifically, we found that populations located over metamorphic bedrock type was less affected during the extreme drought

event (Figure 4.3 and Appendix C Figure C.5), being also significantly different from populations located in the other two bedrocks types (Appendix C Table C.10). These differences could be due to metamorphic bedrock soils having the lowest C:N ratio (Appendix C Table C.1) therefore higher available N, and higher total water holding capacity. These results are consistent with the generally acknowledged role of soils on species performance, particularly under drought conditions (Shantz 1927, Ashraf et al. 2011, Lévesque et al. 2016, Davis et al. 2019).

Conclusion

Our study empirically supports the use of niche distances in the environmental space in relation to climatic suitability as a proxy of environmental accuracy to explain population responses under conditions that do not fulfill species requirements. Our results specifically highlight that species located farther from niche centroid and limit during extreme drought episode were more prone in terms of defoliation and mortality. Similarly, populations historically located farther from the niche were more vulnerable. Nevertheless local environmental conditions such as soils characteristics could buffer the impact of this adverse macroclimatic events.

5

Extreme drought events and soil water balance reduce climatic disequilibrium in dryland communities

Pérez-Navarro M.A., Serra-Diaz J.M., Svenning J.-C, Esteve M.A., Hernández-Bastida J., Lloret F.

5.1 Abstract

The high velocity of contemporary climate change is exceeding plant species' capacity to track the climate, leading to an ecological context in which climatic conditions do not reflect the climatic preferences of the species present in a community. This disequilibrium between climate and community composition could diminish, however, when critical climate thresholds are exceeded, due to widespread reductions in less suitable species. Here, we assessed the effect of an extreme drought episode which led to compositional changes in rich semiarid shrubland communities in the SE Iberian Peninsula. Using a community climate framework, we compared the community climatic disequilibrium before and after the drought episode along a gradient of water availability in three bedrock types. Disequilibrium was computed as the difference between observed climate and community-inferred climate, which was calculated as the mean of species' climatic optimum weighted by species abundance collected in field surveys. We found that extreme drought nested within a decadal trend of increasingly aridity led to a reduction in community climatic disequilibrium, particularly when combined with low water-retention bedrocks. In addition, community climatic disequilibrium also varied before the extreme event across bedrock types, according to soils water-retention capacity. Our study highlights the fact that extreme drought events pushing communities in the same direction as climate change trends may decrease community climatic mismatch, thus acting as environmental filters that reduce the abundance of species with lower drought tolerance limits. Nevertheless, local environmental conditions, such as soils in different types of bedrock, may constraint such direct climatic effects by buffering or enhancing water limitation via water retention capacity. Therefore, the forecasting of community dynamics under climate change would benefit from integrating local and macro-scale environmental drivers on community composition, particularly under the increasingly extreme climatic events expected with climate change.

5.2 Introduction

It has been recognized that climatic gradients influence species distribution and affect community composition. Accordingly, changes in climate are expected to modify many species distribution; however, populations and communities do not always respond properly or instantly to climatic modifications (Blonder et al. 2015). As a consequence, community composition may not accurately match the climatic conditions observed at local scale (Davis 1986, Svenning and Sandel 2013, Blonder et al. 2015). This mismatch between the observed climatic conditions and those inferred from the community composition (hereafter community-inferred climate, Lenoir et al. 2013, Blonder et al. 2015) is generally known as climatic disequilibrium or climatic lag (Davis 1986, Svenning and Sandel 2013, Blonder et al. 2015, Bertrand et al. 2016). This lag depends on a species' capacity to keep up with climate, across a spectrum ranging from equilibrium state, in which all the species have niche optimums close to the climate observed at a given occurrence locality and occur in all such suitable localities, to different disequilibrium states, in which species lack the niches best suited to the observed climate or those species with climatically appropriate niches are, nevertheless, absent from the community (Blonder et al. 2017). Nevertheless, certain amount of species absences could be expected at equilibrium at fine spatial grains under some population dynamics (Holt et al. 2005).

Several processes underlie the climatic disequilibrium of vegetation. Some are connected to the establishment of species in the community: the failure of more climatically appropriate species to immigrate because their low dispersal capacity (Svenning and Skov 2007), a slow rate of establishment and growth (Svenning and Sandel 2013) or absence from the regional pool (Blonder et al. 2015). Other causes are related to the durability of established species: persistence in the community of largely unsuitable species, mainly due to their longevity (Kuussaari et al. 2009, Jackson and Sax 2010, Bertrand et al. 2016), delayed loss of ecosystem structures modifying microclimates (e.g. arboreal strata)(Davis et al. 2019), existence of remaining appropriate conditions at a microscale (De Frenne et al. 2013), positive interactions between species (Webb 1986, Svenning and Sandel 2013), or adaptation to local conditions (Benito Garzón et al. 2011). Thus, this climatic mismatch constitutes a climatic debt (Bertrand et al. 2016), in which species are expected to

eventually disappear from the community, but how or when these losses may happen is still unknown.

Community climatic disequilibrium could, however, be reduced due to changes in relative species abundance (Lenoir and Svenning 2015), by abundance increases or immigration of better climatically adapted species, or by abundance decreases or extinction of less climate suitable ones (Blonder et al. 2015). Eventually, rapid reductions in community climatic disequilibrium would represent a sudden payment of the community climatic debt, such as after extreme climatic events or as a consequence of long-term accumulated changes in climatic conditions, when these exceed a critical threshold (van Mantgem et al. 2009, Carnicer et al. 2011, Lenoir and Svenning 2015).

Extreme climatic events may act as environmental filters by removing less well-adapted species, thereby triggering community re-assembly and abruptly reducing the lag between community-inferred climate and observed climate (Lenoir and Svenning 2015). Significantly, this reduction is mainly likely to occur as long as extreme climatic events push communities in the same direction as the trends in climate change (Allen and Breshears 1998, Miriti et al. 2007, De Frenne et al. 2013, Grant et al. 2016). In contrast, other aspects such as microhabitat, mutualistic species interactions and species plasticity could buffer the impact of extreme climatic events, preventing any major changes in species composition (Ackerly et al. 2010, Lloret and Granzow-de la Cerda 2013, De Frenne et al. 2013, Valladares et al. 2014, Graae et al. 2018). Particularly in arid environments, some microhabitat characteristics, such as bedrock and soil properties, emerge as key determinants of plant community composition (Maestre and Cortina 2002, Ulrich et al. 2014), reflecting the role of soils as a major regulator of water availability through their water-holding capacity (Cornwell and Ackerly 2009, Piedallu et al. 2013). Thus, soils and bedrocks could buffer or exacerbate the impact of extreme drought events on vegetation, depending on the belowground water uptake that they provide (McDowell et al. 2019).

In this study, we aim to quantify and compare the effect of extreme climate episodes on community climatic disequilibrium, using a recent extreme drought event which largely affected shrubland communities in the southeast Iberian Peninsula (AEMET, 2014) as the study case. Using a community climate framework (Blonder et al. 2015), we estimated the community climatic disequilibrium before and

after the drought event along a gradient of soil water-holding capacity determined by three different types of bedrock. Climatic disequilibrium was calculated as the difference between community-inferred climate and observed climate, considering inferred climate as the centroid of species climatic optimums weighted by species' relative abundance before and after the drought. This consideration of species abundance is particularly relevant since studies on community climatic disequilibrium usually obviate it (Gotelli et al. 2010, Blonder et al. 2015) and only consider species extinction and colonization. Indeed, local changes in abundance could be considered as intermediate states of ongoing shifting composition (Maggini et al. 2011, Lenoir and Svenning 2015) and they may be detectable anywhere within species range (Bowler and Böhning-Gaese 2017). Specifically, we hypothesized that: (1) Extreme drought episodes would act as environmental filters by pushing communities in the same direction as recent trends in climate change, (in this case, increasing aridity (IPCC, 2014), leading to a reduction in the climatic disequilibrium. (2) Furthermore, the interaction between drought and bedrock types with a low capacity for water retention will exacerbate the disequilibrium reduction, while the interaction between drought and those bedrock types with higher water-retention capacities will buffer against climatic disequilibrium reduction. (3) According to its water retention capacity, site bedrock will, by itself, influence variations in climatic disequilibrium, even under non-extreme climatic conditions, reflecting buffer effects also towards non-extreme climate variation.

5.3 Material and methods

We integrated local climatic data, species composition and abundance in local communities and species climate niches to build community climate diagrams which served as the basis for estimating both the community-inferred climate and climatic disequilibrium before and after the drought following Blonder et al. (2015).

Study area and field analyses

The study was carried out in three semiarid shrubland areas close to each other in the southeast of the Iberian Peninsula, each with a different type of bedrock (Figure 5.1): Cuatro Calas (1.63°W, 37.38°N) on sandstone, Moreras Mountain (1.32°W, 37.56°

N) on limestone, and Calblanque Natural Park (0.74° W, 37.61° N) on metamorphic bedrock of schist and slate. Moreover, these areas show relatively low human influence as they are all located within protected areas (Natura 2000 network and Natural Park).

All the sites fall under the Mediterranean xeric bioclimate (Rivas-Martínez et al. 2017) and they share the same potential vegetation, with a great number of medium-size and small shrubs such as *Anthillys spp.*, *Chamaerops humilis L.*, *Genista spp.*, *Helianthemum spp.*, *Periploca angustifolia Labill.*, *Salsola spp.*, *Sideritis spp.* and *Teucrium spp.*, as well as some abundant long-lived grasses such as Macrochloa tenacissima (L.) Kunth. The average climate (historical reference period 1970-2000) is similar across the three sites, with a mean annual temperature of 18° C and annual rainfall ranging between 245 and 275 mm (Worldclim version 2.0, Fick and Hijmans 2017) (Figure 5.1), with no significant differences in inter-annual precipitation variability (Appendix D Figure D.1). During the hydrological year 2013-2014 the Iberian southeast suffered the most intense drought on record (since 1941, AEMET 2014), causing extensive die-off and plant mortality in several forests and scrublands (Esteve-Selma et al. 2015). During that year, in Cuatro Calas and the Moreras Mountain (on sandstone and limestone bedrock, respectively), the accumulated rainfall was less than 30% of the average precipitation for the reference period 1970-2000, while in Calblanque (metamorphic bedrock) it amounted to around 65% of the average (Figure 5.1).

Soils in Cuatro Calas and the Moreras Mountain are Lithic Leptosols (around 10 cm in depth) (IUSS Working Group WRB 2015), while in Calblanque they are Skeletic Regosol (i.e., around 1m in depth) (IUSS Working Group WRB 2015). In each case, we estimated soil properties using three soil samples per bedrock type, each one consisting of two replicates of the upper 10 cm. In each sample, we measured the moisture content at field capacity (-0.5 MPa) and wilting point (-1.5 MPa) (Richards and Weaver 1943, Richards 1954, Cassel and Nielsen 1986), as well as the organic carbon content (Anne 1945, Duchaufour 1970) and particle size composition (Gee and Bauder 1986) (see Appendix D Figure D.4 and Table D.1). Finally, we estimated the annual water deficit of each plot during the extreme period, as the sum of the deficit months, by considering the monthly precipitation of each plot, extractable water (field

capacity – wilting point) and the monthly potential evapotranspiration (Thornthwaite and Mather 1957). The soil in the Moreras Mountain (limestone bedrock) presented the highest water retention capacity per soil volume unit, followed by the Calblanque and Cuatro Calas soils (metamorphic and sandstone bedrock, respectively) (Figure 5.1 and Appendix D Figure D.5); nevertheless, the absolute extractable water was

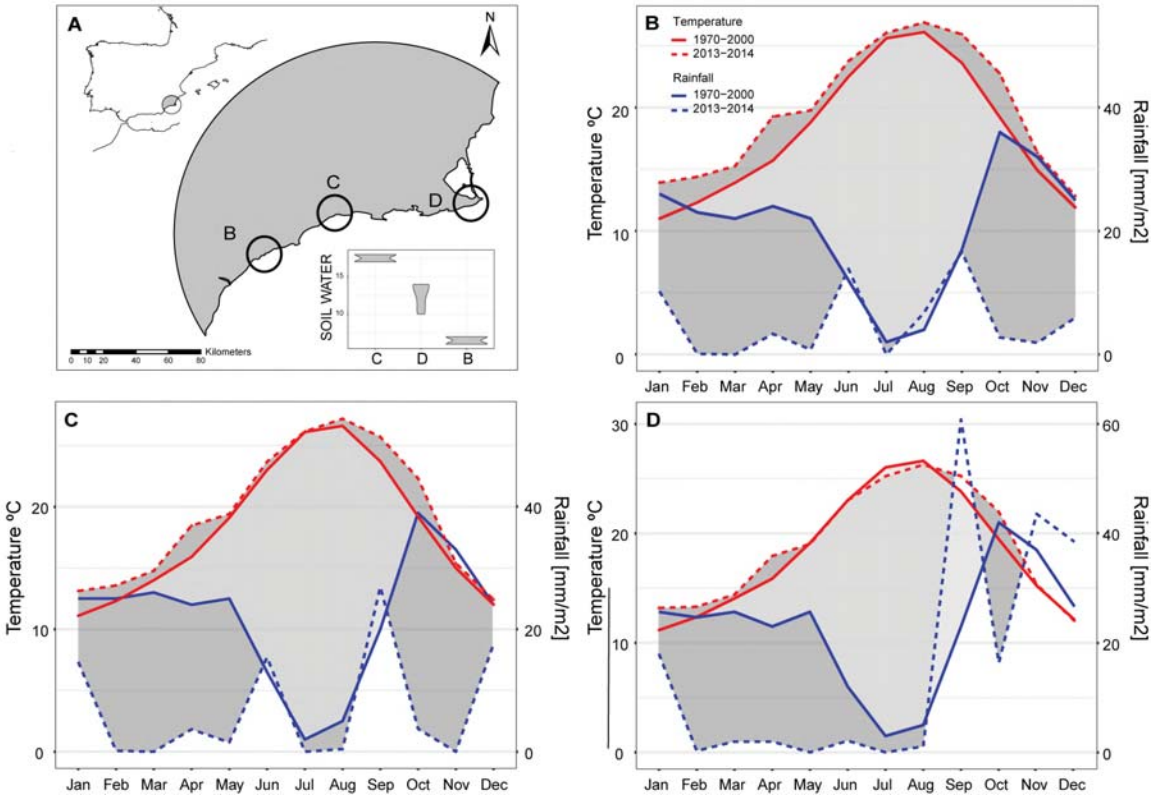

Figure 5.1: A) Study region within the Iberian Peninsula (SE region: grey shading in the inset, upper left map) and studied localities within the SE region, indicating study sites: (B) indicates Cuatro Calas locality (sandstone bedrock), (C) Moreras Mountain (limestone bedrock) and (D) Calblanque Natural Park (metamorphic bedrock). Soil water content available for the top 15cm is shown in the bottom-left inset. B), C) and D) represent the ombrothermic diagrams for Cuatro Calas, Moreras Mountain and Calblanque Natural Park, respectively. Red lines correspond to temperatures while blue lines correspond to precipitation. Solid lines correspond to average climatic period (1970-2000, Worldclim v.2.0, Fick and Hijmans, 2017); dotted lines correspond to data from the extreme climatic year (from Spanish Weather Agency, AEMET). Light grey area represents average water deficit for the average period and dark grey area represents extra water deficit for the extreme year

Community data

During January-March 2016, 30 replicated plots of 5×5m were established within each area (total number of plots: 90), separated from each other by at least 25 m. All plots presented a gentle low slope and a south or southeast orientation. On each plot, we recorded the number of dead and living individuals from each woody species (38 species in total). The dead individuals were identified according to the following two criteria: (1) lack of green leaves and (2) presence of thin branches (to ensure that they had not died long before the drought episode) (Sapes et al. 2017, Pérez Navarro et al. 2018). In addition, we intentionally dismissed small and low-lignified individuals with less than three whorls (indicating stem yearly elongation) in order to avoid individuals established after the drought period. From these records, we calculated the species' relative abundance before and after the drought. Species' relative abundance before drought was measured as the sum of surviving and dead individuals per species/total of dead and surviving individuals, so considering that each dead individual was alive before the extreme event). Very small individuals could have died and disintegrated beyond recognition, but we assume that this eventuality would occurred similarly in the different species and affected to a reduced number of individuals. Species' relative abundance after drought was measured as the sum of surviving individuals from each species/total surviving individuals. We chose this relative species abundances approach in our study since it is widely assumed that the number of individuals is a good proxy for estimating species requirements (Sexton et al. 2009, Thuiller et al. 2014).

Species occurrence data

The geographical distribution data from the 38 sampled species were collected from the Global Biodiversity Information Facility (GBIF) database (GBIF 2019, `http://www.gbif.org`) and the herbarium of the Institut Botànic de Barcelona. The species occurrence records were then scrubbed for taxonomic name (to remove any non-accurate synonyms) and location (to remove taxonomic and geographic inconsistencies). In order to deal with possible sampling bias, we also reduced the occurrence density, for those datasets with more than 100 occurrences, by randomly thinning species' records to one observation per sq. km – equivalent to the grid resolution of

climate dataset. The final datasets ranged from 60 to 7,000 observations per species.

Climate data

We used 12 bioclimatic variables for the reference period 1970-2000 (Worldclim version 2.0, Fick and Hijmans 2017). These correspond to the observed climate, and all were obtained with a 1 sq. km resolution: annual mean temperature, temperature seasonality (standard deviation $\times 100$), maximum temperature of warmest month, minimum temperature of coldest month, mean temperature of warmest quarter, mean temperature of coldest quarter, annual precipitation, precipitation of wettest month, precipitation of driest month, precipitation seasonality (coefficient of variation), precipitation of wettest quarter and precipitation of driest quarter. We selected these 12 bioclimatic variables instead of the total 19 biovariables available in the Worldclim database in order to facilitate subsequent interpretation, avoiding highly correlated variables which correspond to those integrating temperature and precipitation information (i.e. maximum temperature of driest quarter).

Community climate framework

To build the community climate diagram, we first used a Principal Component Analysis (PCA) to convert the environmental space of the 12 bioclimatic variables for the 1970-2000 period (observed climate) into a two-dimensional surface defined by the first and second principal components (Broennimann et al. 2012). The PCA was built using climate data from all the occurrences sites of all the 38 analysed species (Appendix D Table D.2) and it explained 78.5% of the 12 variables' variability (see Appendix D Figure D.2). We chose this multivariate climatic approach to integrate all climate variables, weighting equally independent climate gradients and to determine the overall displacement of the community-inferred climate after drought. Furthermore, we explored the associated univariate relations to assist interpretation of results.

We next characterized each species climatic niche by translating the geographical species occurrences into the environmental space and using kernel density functions (Broennimann et al. 2012) (ks package version 1.11.3, Duong 2018) that allow determining density values for each cell of the environmental space. We applied Gaussian

kernel, selected optimal bandwidth by cross-validation (Duong and Hazelton 2005), and removed values under 0.05 percentile. In addition, we established the species niche centroid as the gravity centre of the niche (i.e. mean of environmental values weighted by species' density). From that, we estimated the community-inferred climate for each of the 90 study plots, before and after the drought episode as the centre of species realized niches by weighting each species' climatic niche centroid by its relative observed abundance in the plot.

We also translated the observed climate of each of the plots during the average period 1970-2000 (Worldclim version 2.0, Fick and Hijmans 2017) into the same two-dimensional environmental space. Since the climate database has a 1000 m resolution, almost all the plots within the same study area had the same observed climate value. Both the observed climate, the species composition of a community and the community-inferred climate can be seen on a community climate diagram (Figure 5.2). This approach follows that of Blonder et al. (2015) while also accounts for species abundance, which is a relevant factor for describing community composition. Finally, we also estimated a plot's climatic disequilibrium as the Euclidean distance (i.e., difference) in the PCA space between community-inferred climate and observed climate, where values of 0 in climatic disequilibrium should be interpreted as the complete equilibrium of community composition-inferred climate with the observed climate period.

Statistical analyses

Following this approach, we obtained 30 disequilibrium values per bedrock type before drought and 30 disequilibrium values per bedrock type after drought (one climatic disequilibrium estimate per plot and period time). In order to evaluate the effects of the extreme event and bedrock type on climatic disequilibrium, we built a linear mixed model (lmerTest R package, version 3.0-1, Kuznetsova et al. 2017) with climatic disequilibrium as the response variable and period (before and after drought), bedrock type, and their interaction as explanatory ones. Plot was included as a random effect. We then used least-square means (lsmeans R package, version 2.27-62, Lenth 2016) to perform comparisons between bedrock types within period and differences between periods within bedrock types. We used t-test within each bedrock type before the extreme event to elucidate whether climatic disequilibrium values were significantly

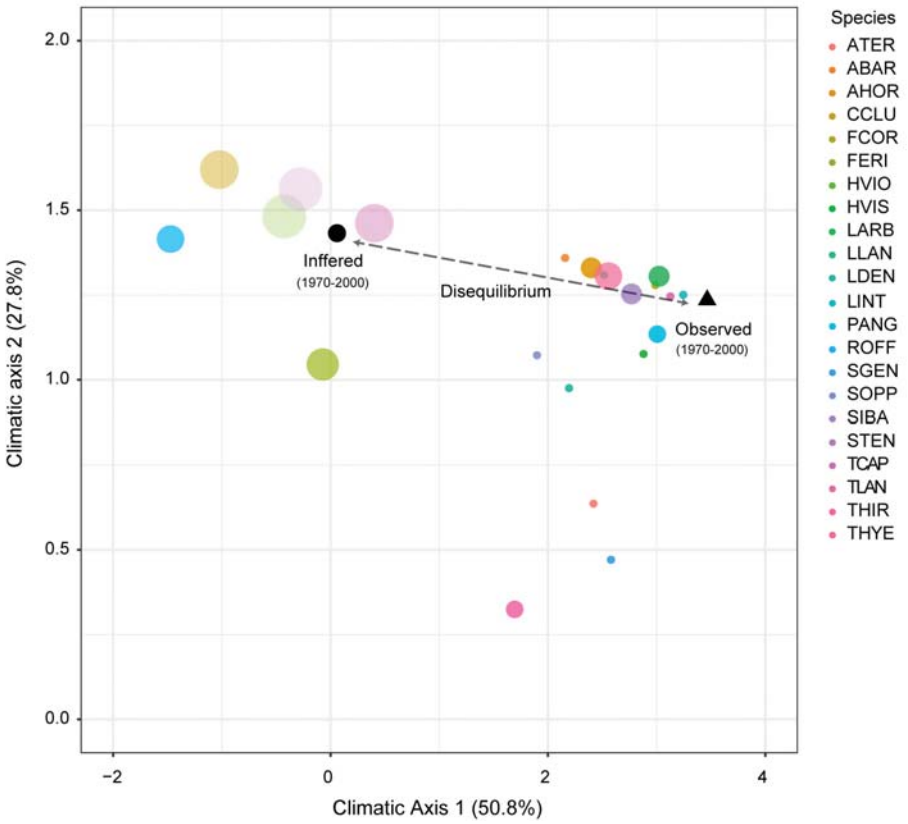

Figure 5.2: Example of community climate diagram (plot 29 of sandstone before drought). The panel shows a twodimensional projection of the climatic space obtained from the PCA analysis with the twelve selected climatic variables (see Figure D.2 in Appendix D). Each colour dot represents a different species niche centroid for those species present within the plot, sized by observed species abundance. Species acronyms are listed in Table D.2 in Appendix D. Black dot shows the community-inferred climate while black triangle represents the observed plot climate (1970-2000, Worldclim v.2.0, Fick and Hijmans, 2017), translated into this two-dimensional climatic surface. Grey arrow represents the climatic disequilibrium between observed and inferred climate.

different than 0 and community inferred climate were not in equilibrium before the extreme drought. Finally, using the abovementioned methods, we also ran univariate analyses of changes in disequilibrium per each climatic variable within each bedrock type, by using similar mixed models with disequilibrium values per each variable separately as a response variable, period as an explanatory variable and plot as a random effect.

5.4 Results

Community climatic disequilibrium showed considerable variations between communities before and after drought, and between communities located in different bedrock types. In general, disequilibrium was higher before the drought (Table 5.1, Table 5.2) and considerably reduced after drought, with important differences of magnitude between bedrock types (Table 5.2, Figure 5.3). Sandstone communities showed the highest change, with a significant decrease in community climatic disequilibrium of 11.34% (from 2.47 mean disequilibrium before drought to 2.19 after drought) (Table 5.1). Climatic disequilibrium in the limestone plots also showed a significant decrease, of 3.81% from 2.89 mean disequilibrium before drought to 2.78 after drought (Table 5.1). In contrast, plots located in the area with metamorphic bedrock did not show significant changes in climatic disequilibrium (2.97 mean disequilibrium before and 2.98 mean disequilibrium after the drought).

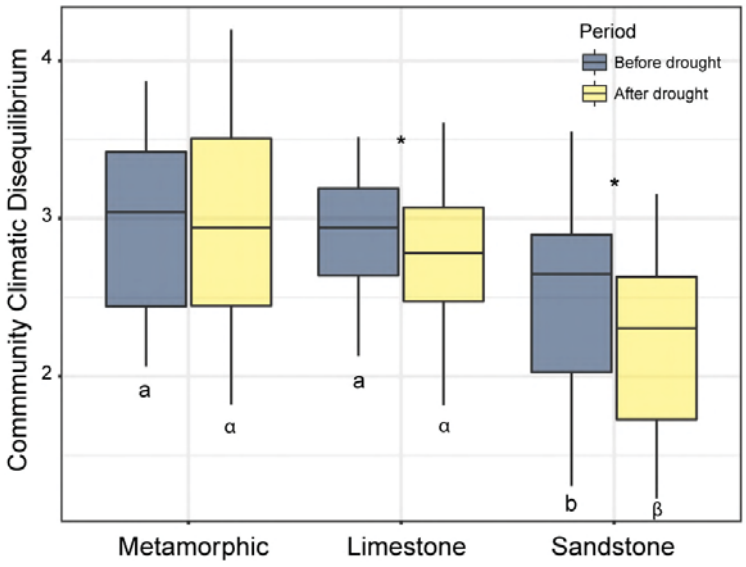

Figure 5.3: Community climatic disequilibrium (distance between inferred and observed climate in the community climate diagram) before and after the extreme drought event in the three studied bedrock types. Asterisks indicate significant decrease in climatic disequilibrium after drought in the respective bedrock type; different letters (a,b) indicate significant differences in climatic disequilibrium between bedrock type (lsmeans pairwise test) before drought; the various symbols (α, β) indicate significant differences in climatic disequilibrium between bedrock type (lsmeans pairwise test) after drought

Table 5.1: Mean and standard deviation of Climatic Disequilibrium (CD) before and after drought in each bedrock type; asterisks indicate significant difference from 0.

bedrock	mean CD before	sd CD before	mean CD after	sd CD after
sandstone	2.474	0.645	2.197	0.598
limestone	2.891	0.367	2.777	0.431
metamorphic	2.965	0.550	2.978	0.650

Statistical significant levels: "." p<0.1 ; "*" p<0.05 ; "**" p<0.01 ; "***" p<0.001

As regards the individual climatic variables, the highest significant reduction in climatic disequilibrium was observed in the precipitation of driest month and the driest quarter in all three bedrocks (Appendix D Figure D.3). While plots in the sandstone bedrock showed significant changes in climatic disequilibrium in almost all the climatic variables, plots in the metamorphic and limestone bedrocks showed significant changes in only a few variables, mostly related to precipitation (Appendix D Figure D.3).

We also found that climatic disequilibrium values differed between bedrock types both before and after the drought and always showed distributions with mean values significantly different from 0 (Table 5.1). Particularly, sandstone had significantly lower disequilibrium than the other two bedrock types before and after the drought (Figure 5.3 and Appendix D Table D.3). In addition, these disequilibrium differences between sandstone plots with its metamorphic and limestone counterparts were even higher after the extreme drought (Figure 5.3 and Appendix D Table D.3).

Table 5.2: Results of mix models explaining community climatic disequilibrium as a function of bedrock type (sandstone, limestone, metamorphic), time period (before or after the extreme event) and their interaction (bedrock type: time period) with plot as random effect variable.

	Estimate	Std. Error	df	t value	Pr(>|t|)	
(Intercept)	2.778	0.100	99.335	27.642	0.000	***
bedrock metamorphic	0.200	0.142	99.335	1.410	0.162	
bedrock sandstone	-0.580	0.142	99.335	-4.084	0.000	***
time before	0.113	0.052	87	2.186	0.032	*
bedrock metamorphic : time before	-0.126	0.073	87	-1.720	0.089	.
bedrocks andstone : time before	0.164	0.073	87	2.236	0.028	*

Statistical significant levels: "." p<0.1 ; "*" p<0.05 ; "**" p<0.01 ; "***" p<0.001

5.5 Discussion

Impact of extreme drought on climatic disequilibrium

We found that those communities living on areas subject to more severe water limitations during the extreme drought year significantly reduced their climatic mismatch with respect to the average contemporary climate (Figure 5.3), endorsing the role of extreme climatic events as drivers of community assembly (Jentsch et al. 2007, Lenoir and Svenning 2015). Hence, our results support that extreme climatic events would act as environmental filters that remove species with niches conferring low performance (here, species associated to relatively moist climate) in favour of those more adapted to the new climatic circumstances (here, associated to relatively dry climate) (Keddy 1992, Diaz et al. 1998, Grant et al. 2016).

We note that this effect of extreme events, like the drought in our study case, likely only caused a reduction in community climatic disequilibrium because it acted as a pressure in the same direction as the prevailing climatic trends (in this case, increasingly arid conditions, Guiot and Cramer 2016), instead of producing random or stochastic changes in community composition (Kreyling et al. 2011). Therefore, the drought episode pushed communities to faster track the changing climate (Easterling

et al. 2000). Actually, this directional pressure in favour of more arid-adapted species is further supported by the fact that climate variables related with precipitation showed the highest reductions in community disequilibrium in the univariate analyses (Appendix D Figure D.3).

This explicit influence of the extreme drought on community composition is also consistent with the prevalence of environmental filtering as the main carver of community structure under harsh environmental conditions (Valladares et al. 2008, de la Riva et al. 2017, Li and Shipley 2018). It is supposed that extreme climatic events lead to fast ecological shifts and dramatic changes in local abundance in comparison with gradual changes in climatic trends (Svenning and Sandel 2013). However, the impact of extreme climatic events on community composition may remain unnoticed in the long term, being confounded with gradual changes, as extreme climatic events occur in pulses as part of larger climate trends (Easterling et al. 2000).

Bedrock and soil modulate vegetation response to climate

Despite the potential impact of extreme events on communities, they do not always imply changes in community climatic mismatch. Community compositional changes could be buffered by the intrinsic characteristics of plant communities, such as species longevity, biotic interactions (facilitation), as well as species' phenotypic plasticity and adaptation (Benito Garzón et al. 2011, Svenning and Sandel 2013, Blonder et al. 2017). In addition, local-scale environmental factors, such as ecosystem structure, topoclimatic variability and edaphic characteristics likely play an important role (Lenoir et al. 2013, Svenning and Sandel 2013, De Frenne et al. 2013).

Since our study system is dominated by species with relatively short lifespans, climatic mismatch cannot be attributed to plant longevity, which is often the main cause of communities' climatic mismatch on the trailing edge (Svenning and Sandel 2013). In contrast, our study highlights the importance of local-scale environmental factors such as bedrock and associated soil properties. Although our study design (with all same bedrock plots blocked within the same site) prevent us to separate the effect of soil and bedrock from other local circumstances, soils could be one of the main reasons explaining differences in climatic disequilibrium, particularly because the analysed plots were particularly homogeneous in terms of topography and

vegetation structure. The sandstone area had the lowest climatic mismatch during the reference period, although this was still significantly higher than 0 (Table 5.1), among other possible reasons because its soil structure and low water retention capacity exacerbates arid climatic conditions (Figure 5.3). In contrast, metamorphic bedrock, which has a high water retention capacity and deep soil, showed the highest historical climatic disequilibrium (Figure 5.3). The relevance of soil properties, largely due to bedrock characteristics, on community composition has been widely recognized, (Prentice et al. 1992, Kruckeberg 2002, Fridley et al. 2011); actually, the interaction between climate and soils can contribute to decouple the species-climate relationship (Fridley et al. 2011, Ulrich et al. 2014, Simpson et al. 2016, Pérez-Ramos et al. 2017, Davis et al. 2019).

In addition to site differences before drought, our results also revealed differences in the magnitude of disequilibrium change between sites during the extreme event. While differences in disequilibrium change between metamorphic and the other two bedrocks could also be due to the higher precipitation in the metamorphic site during the extreme event (Figure 5.1), differences in disequilibrium changes between limestone and sandstone could not be linked to different water deficits during the drought (limestone and sandstone, Figure 5.4). Although not significant, the quantitative differences between sandstone and limestone plots could be related to soil properties. For example it could be due to lower nutrient content and higher C:N ratio of sandstone plots (Appendix D Table D.2). This low soil nutrient content has often been related to low plant resistance to drought (Ashraf et al. 2011, Lévesque et al. 2016). So, including soil properties in biogeographical analyses would improve our understanding of species distribution, community structure and vegetation's responses to climate change (Bertrand et al. 2012, Piedallu et al. 2013, Lévesque et al. 2016).

Considerations about community climate (disequilibrium) characterization

There are, however, some methodological limitations to plant community analysis based on species' bioclimatic characterization. Firstly, the climatic niches represented here are equivalent to species realized niches as far as they derive from contemporary observational species occurrences (which implicitly include biotic interactions and anthropogenic impacts) (Kearney 2006), and therefore, they do not necessarily portray species' physiological optimums (Murphy et al. 2006, Blonder et al. 2015). Currently,

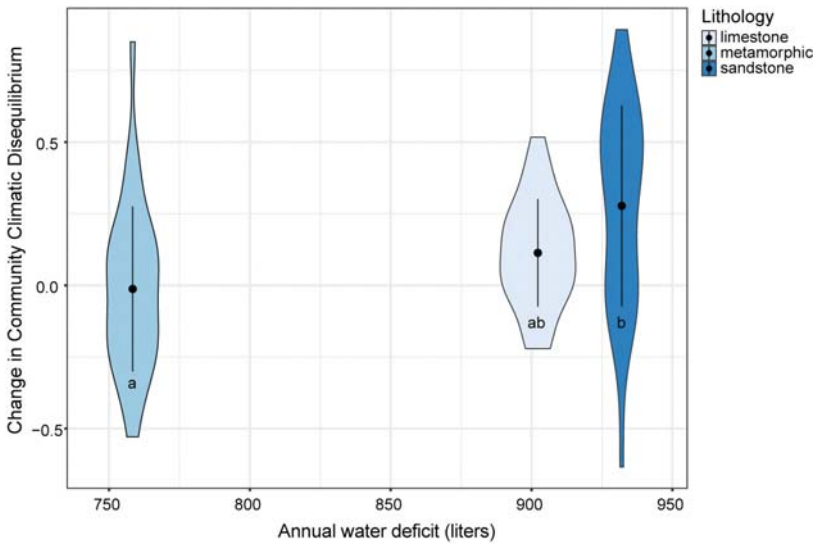

Figure 5.4: Change in climatic disequilibrium respect to annual water deficit of the three different bedrock types during the extreme drought event. Annual water deficit was calculated as the sum of monthly deficits. Change in climatic disequilibrium was calculated as disequilibrium before drought minus disequilibrium after drought. Different letters (a,b) indicate significant differences in changes in climatic disequilibrium between bedrock types.

this limitation could only be overcome for few species with available experimentally-derived response curves (Araújo et al. 2013). Secondly, since species are considered uniform entities constant over time, this approach neglects local or temporal adaptation, that could endow a population with different environmental requirements from the mean niche requirements of its species (Benito Garzón et al. 2011, Svenning and Sandel 2013). This assumption could be particularly important in our analyses since most of the species were located on the margins of their geographical range, where populations are particularly prone to show deviant local adaptations (Hampe and Petit 2005, Valladares et al. 2014, Solarik et al. 2018). Finally, special caution should be taken as regards occurrence and climate databases. Since community-inferred climate relies on every single species' climatic niche, any bias in the estimation of individual species' niches will be also propagated to community-scale statistics (Blonder et al. 2017). In order to reduce possible bias, we standardized the bandwidth selection for all the species (Blonder et al. 2014) and visually checked every species' niche to rule out any overfitting. With respect to climate databases, both community-inferred climate and observed climate are frequently computed on the basis of a relatively coarse spatial resolution (i.e., 1 sq. km) that fails to capture the local climatic conditions

(at 10- to 100-m resolution) actually experienced at population level (Fridley 2009, Randin et al. 2009, Ackerly et al. 2010, Lenoir et al. 2013).

In addition to these general limitations, we overcame another habitual constraint on bioclimatic-based community analysis, namely equal weighting of species (Gotelli et al. 2010, Blonder et al. 2015), by comparing species abundance data before and after the extreme climatic episode. This allowed us to detect more subtle impacts on species abundance relative to the total loss of a local population, which can be considered as proxies of intermediate states of ongoing range shifts, before changes in the overall range could be detected (Parmesan 2006, Maggini et al. 2011, Lenoir and Svenning 2015).

Implications for plant communities under climate change

Our results confirm a community trend to be dominated by species living in more arid environments in contexts of increasing drought, in addition to the generally expected tendency towards increases in warm-adapted species to the detriment of species adapted to cooler conditions (Barry et al. 1995, De Frenne et al. 2013). The predicted increase in the recurrence of heat waves and extreme drought events associated with climate change (IPCC, 2014) will foreseeably favour communities tracking the new climate, particularly if communities' resistance is overwhelmed by the magnitude or recurrence of extreme events. Moreover, reduced resilience would be especially dangerous in arid environments, as it could trigger desertification processes (Vicente-Serrano et al. 2013).

However, large uncertainty is still present in predictions of community responses to climate change, notably since they are frequently based on species distribution approaches, which commonly disregard lags between species ranges and climate (Blonder et al. 2017, Gaüzère et al. 2018), as well as rarely incorporate biotic effects and their interaction with abiotic processes. Actually, changes in the species abundance of plant communities induced by extreme events would also alter the strength and direction of biotic interaction and coexistence dynamics (Thibault and Brown 2008, Grant et al. 2016), which may lead to more stochastic community trajectories (Kreyling et al. 2011, Alexander et al. 2016, Cadotte and Tucker 2017). Disregarding community

climatic disequilibrium and coexistence dynamics could lead to misleading conclusions on diversity dynamics under climate change. Our results highlight the impact of extreme climatic events, such as strong droughts, on community assembly. Our case study illustrates how such events may act as catalyst of species filtering driven by climate change, accelerating species tracking of climate and associated community change. At the same time, community responses to these events are modulated by local environmental conditions such as soil characteristics, particularly as regards water availability. Therefore, the improvement of community predictability under climate change will require better understanding of the interactions between local environmental drivers and species requirements and interactions, particularly when large perturbations affect the dynamics of species coexistence. Our approach is based on the bioclimatic characterization of the community by scaling-up species' niches using a biogeographic perspective. This approach has proved valuable for assessing the effect of climate change on plant communities in the short and medium term, particularly when extreme episodes occur.

General conclusions

- Historical climatic suitability derived from Species Distribution Models (SDMs) showed to be a useful proxy to explain drought-induced population decay, independently of the SDM algorithm applied. In the studied semiarid communities of SE Spain, species with lower historical climatic suitability, i.e., historically located further from species climatic optimum, showed to be more vulnerable to decay.

- Populations' climatic suitability during the extreme episode failed to explain species green canopy losses in the studied community. Presumably, the exceptional climatic conditions during the extreme episode lead to extremely low climatic suitability values indistinctly for all species, hindering to obtain contrasted values between species and preventing any possible significant correlation with decay.

- Extremely low climatic suitability values could derive, in part, as a consequence of the non-inclusion of temporal climatic variability in species niche characterization. Climatic suitability derived from species niche which accounted for inter-annual climatic variability better explained observed patterns of monospecific (*Pinus halepensis*) forest mortality than climatic suitability derived from climate averaged-based niches.

- Populations living in the environmental space located between the niches derived from inter-annual climate and from average climate, are likely wrongfully estimated to be out of the niche space when using average climatic variables, so, not showing correlation between demographic processes associated to decay and niche suitability.

- Differences between climatic inter-annual based and average based niches were relatively higher in species with restricted distribution ranges, in comparison with widely distributed species, suggesting that, in the Mediterranean context, spatial variability may compensate for temporal variability. So, when characterizing species niches with climatic averages, these species are expected to exhibit overestimated extinction inferred risk and smaller potential distribution range.

- In contrast to SDMs-derived climatic suitability, population distances in the environmental space to species' niche limit and centroid properly explained population performance responses when population climatic conditions exceed niche range boundaries, such as during extreme climatic events. In particular, those populations further displaced during the extreme climatic episode from species niche limit and centroid showed to be more prone to decay.

- Extreme climatic events pushing communities in the same direction as the prevailing climatic trends led community composition to be re-sorted in favor of those species with climatic niche optimum closer to the current climate, as evidenced by the reduction of climatic disequilibrium between Community Inferred Climate and contemporary observed climate during an extreme drought episode nested within a decadal trend of increasing aridity.

- Soils in different types of bedrock, mainly via water holding capacity, can modulate population responses under extreme drought climatic events, therefore exacerbating or buffering the effect of extreme drought events on community assembly. Those soils with higher water retention capacity buffered extreme drought impact on less drought adapted species and hindered for considerable reductions in community climatic disequilibrium.

A

Appendix Chapter 2

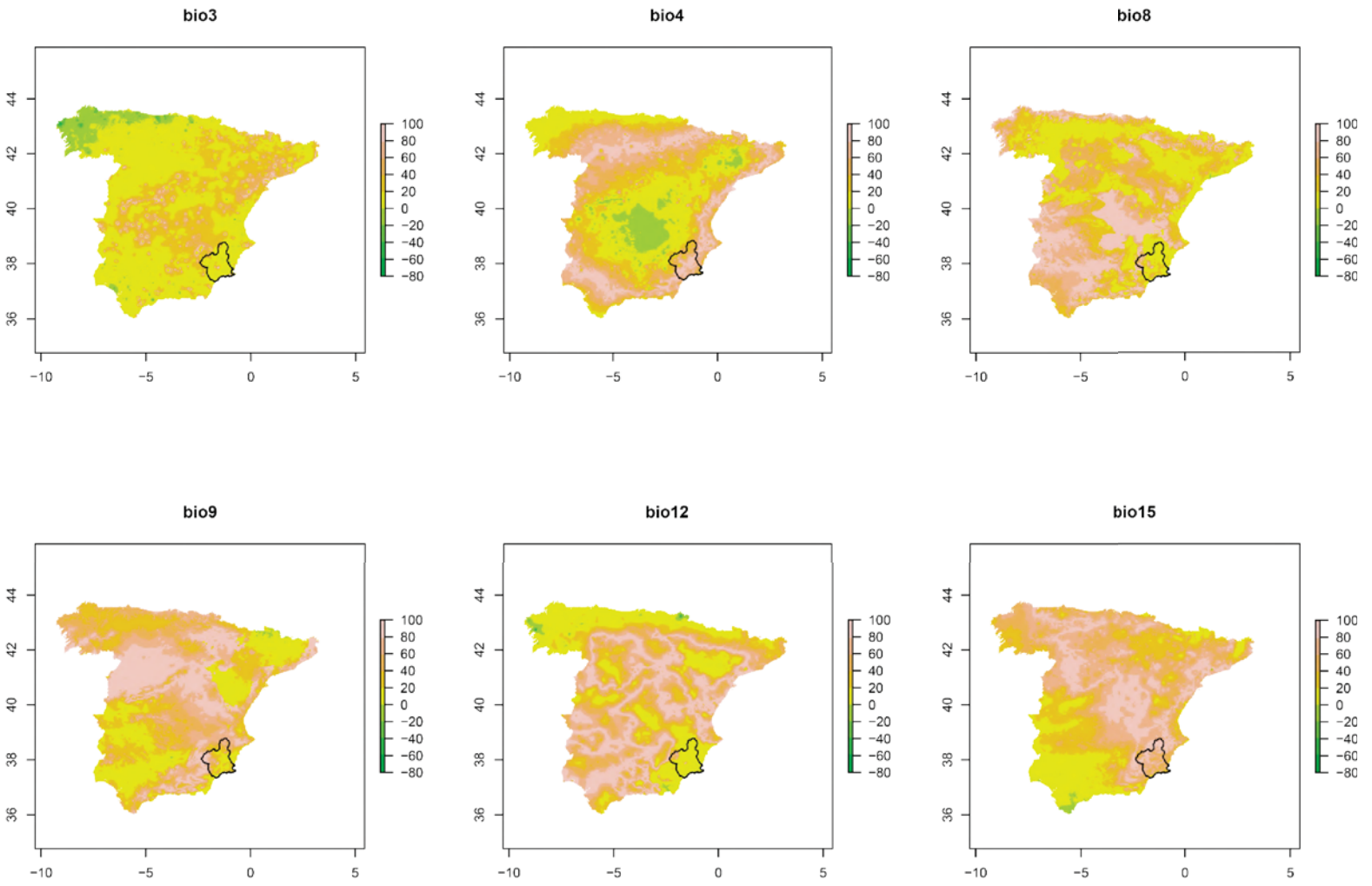

Figure A.1: Multivariate Environmental Similarity Surface (MESS) analysis between Worldclim data base and Spanish climatic data base following Ninyerola and others 2000 and climatic data from iberian climatic atlas for 1950-2000 period. Negative values mean dissimilarities between the two data bases. BIO3= Isothermality, BIO4= Temperature Seasonality, BIO8= Mean Temperature of Wettest Quarter, BIO9= Mean Temperature of Driest Quarter, BIO12= Annual Precipitation and BIO15= Precipitation Seasonality.

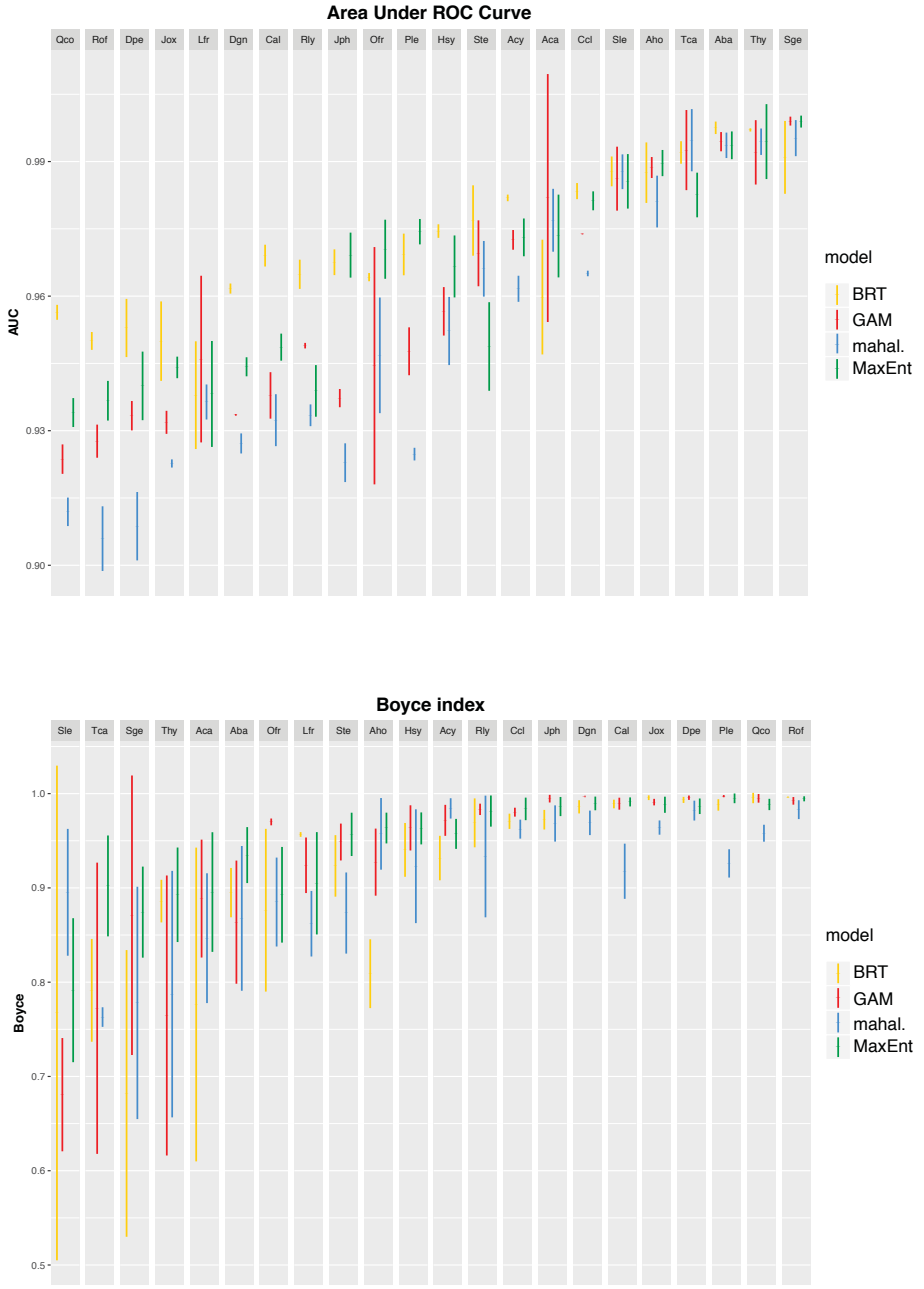

Figure A.2: Above: Area Under ROC Curve (AUC) by specie and models. Vertical lines represent AUC standard deviation interval of each model while horizontal lines show AUC mean values. Below: Boyce index values by specie and models. Vertical lines represent standard deviation for Boyce values while horizontal lines show Boyce mean values. Notice that the species order is different for each plot.

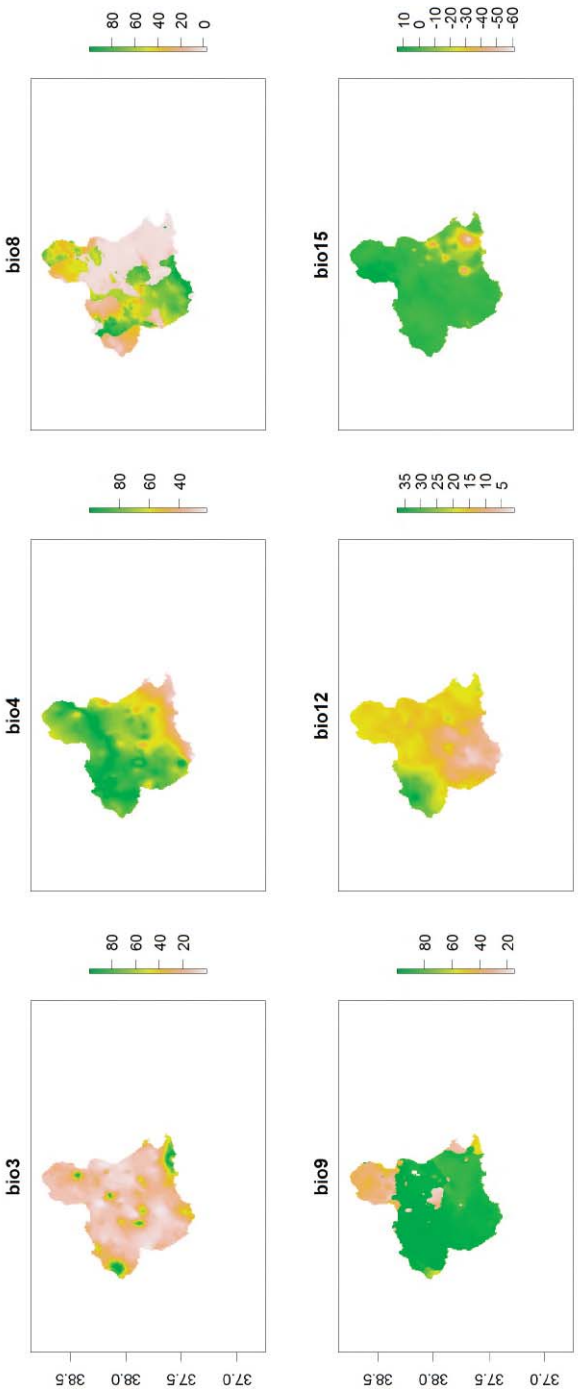

Figure A.3: Multivariate Environmental Similarity Surface (MESS) analysis for the Region of Murcia. Bio3 to Bio15 shows the similarity between the new environment (extreme episode 2013-2014) and the environments use to calibrate the model (historic period 1950-2000) for each different variables implemented in the models. BIO3= Isothermality, BIO4= Temperature Seasonality, BIO8= Mean Temperature of Wettest Quarter, BIO9= Mean Temperature of Driest Quarter, BIO12= Annual Precipitation and BIO15= Precipitation Seasonality. Negative values are indicative of environmental dissimilarities between variables. Note that bio15 (precipitation seasonality) is the main contributor to final MESS. Black square represents the study site location.

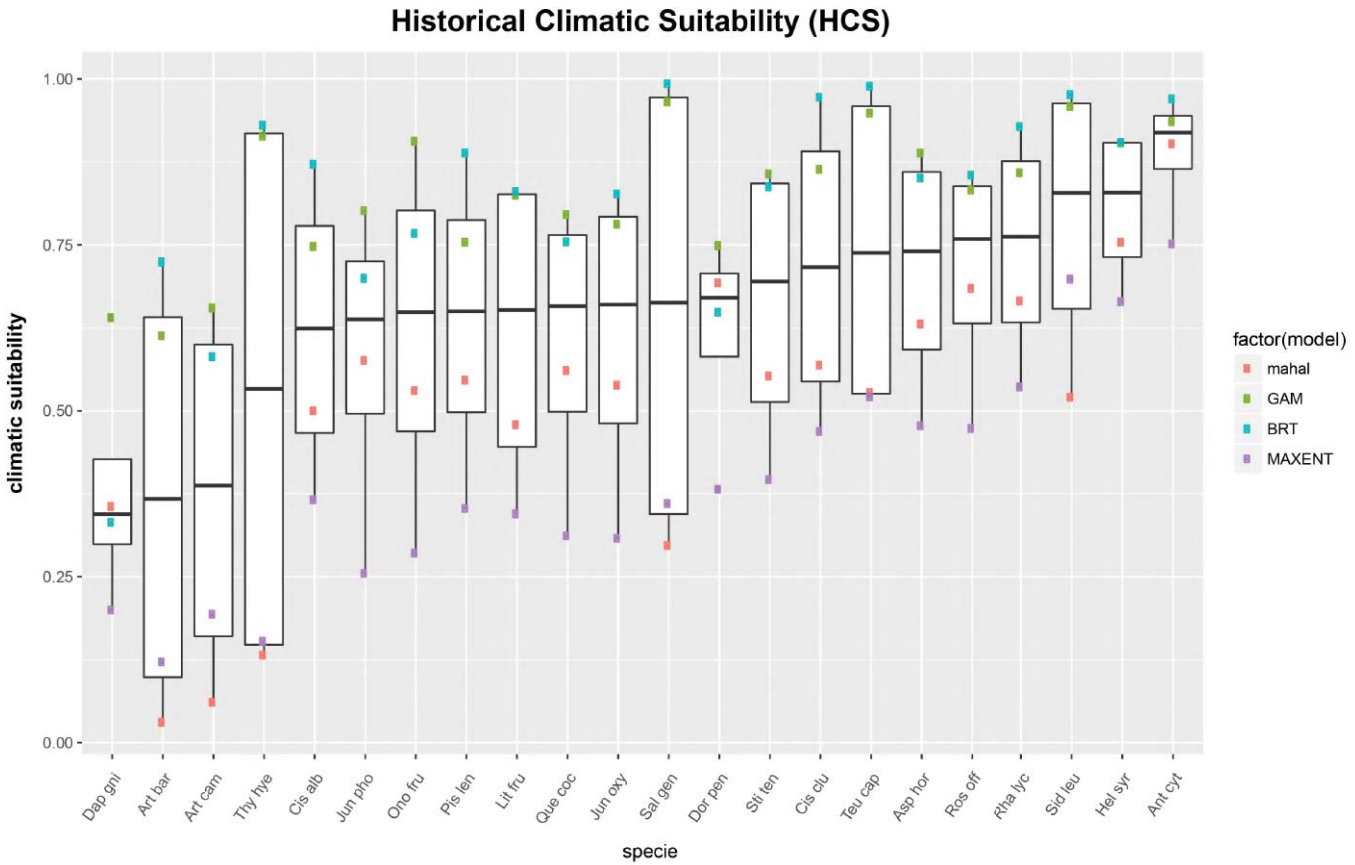

Figure A.4: HCS averaged values of the sample plots by species for each implemented model.

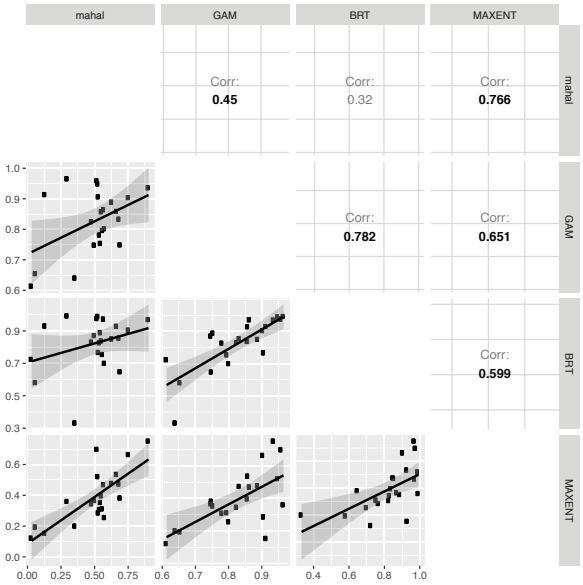

Figure A.5: Pearson correlation values among different implemented models for HCS. Significant values are highlighted in bold. Correlation plots are also shown

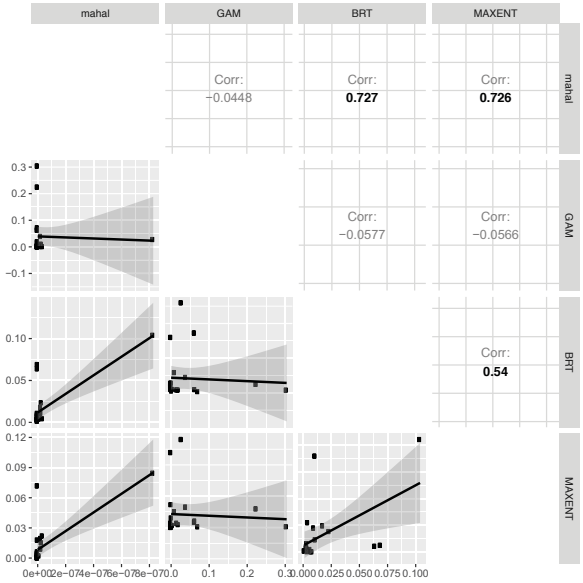

Figure A.6: Pearson correlation values among different implemented models for ECS. Significant values are highlighted in bold. Correlation plots are also shown.

Anthyllis cytisoides

Artemisia barrelieri

Artemisia campestris sub. glutinosa

Asparagus horridus

Cistus albidus

Cistus clusii

Daphne gnidium

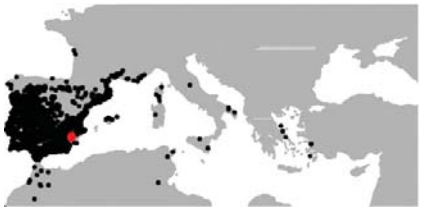

Dorycnium pentaphyllum

Helianthemum syriacum

Juniperus oxycedrus

Juniperus phoenicea

Lithodora fruticosa

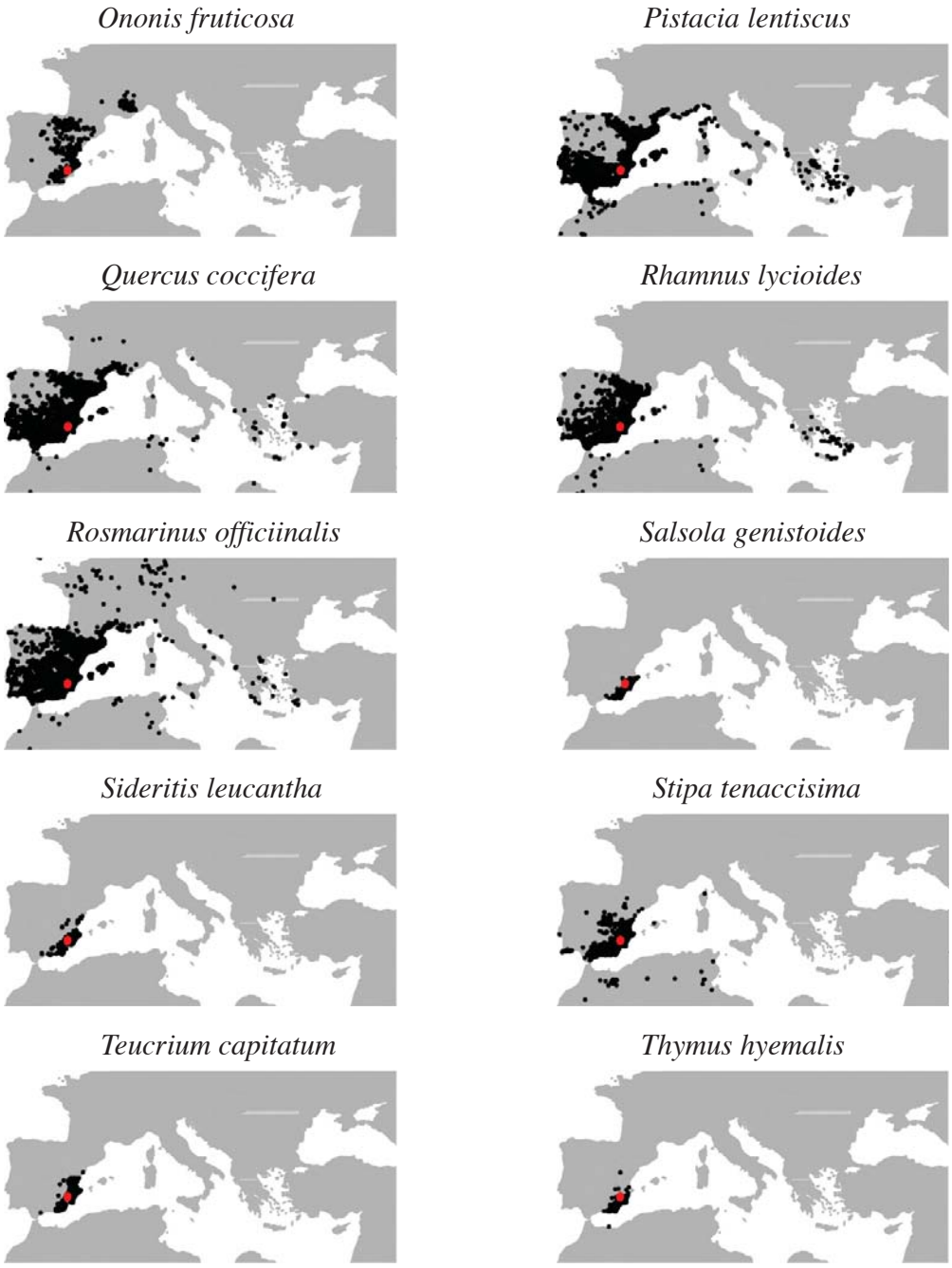

Figure A.7: Filtered occurences of every analized species.

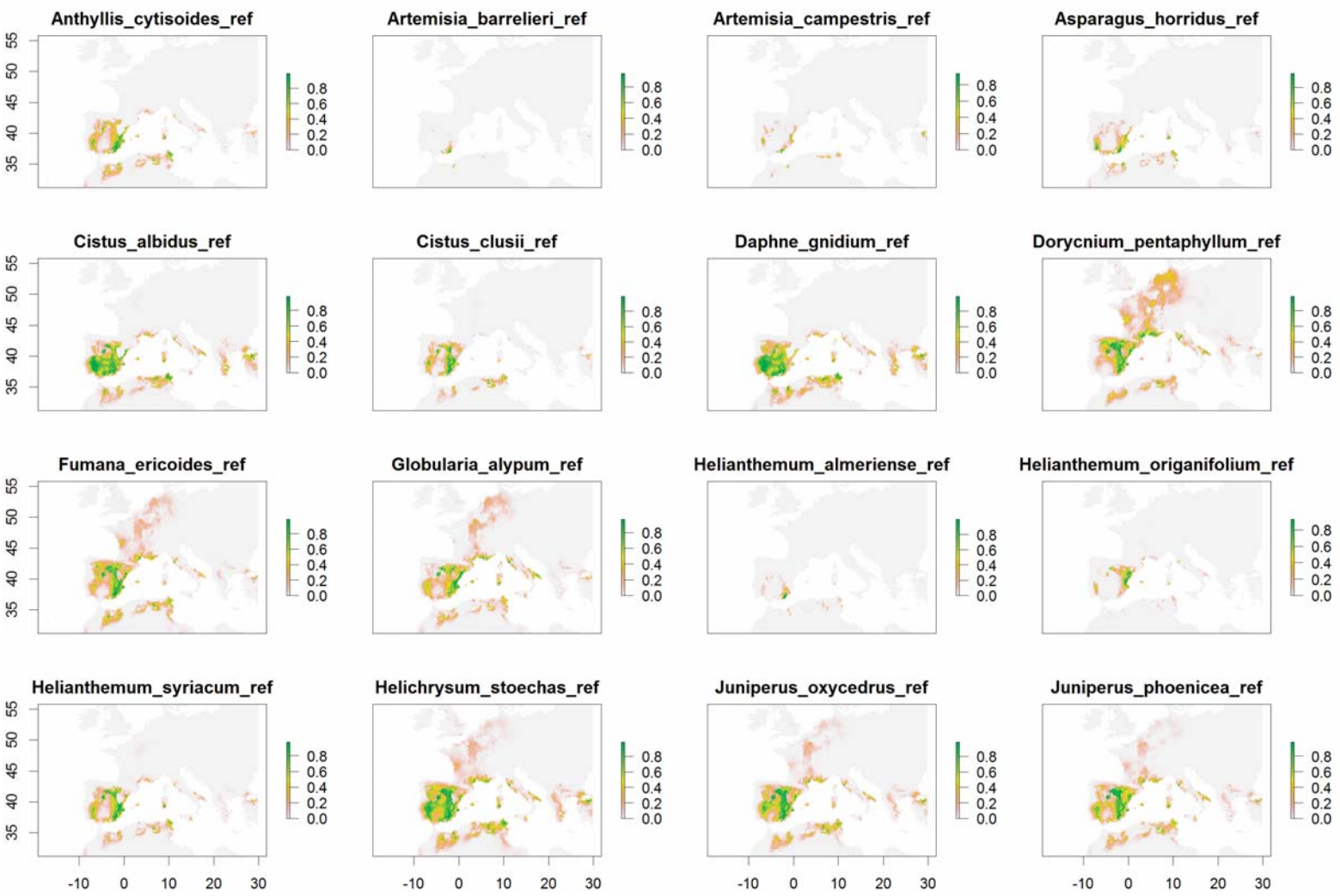
Anthyllis_cytisoides_ref
Artemisia_barrelieri_ref
Artemisia_campestris_ref
Asparagus_horridus_ref
Cistus_albidus_ref
Cistus_clusii_ref
Daphne_gnidium_ref
Dorycnium_pentaphyllum_ref
Fumana_ericoides_ref
Globularia_alypum_ref
Helianthemum_almeriense_ref
Helianthemum_origanifolium_ref
Helianthemum_syriacum_ref
Helichrysum_stoechas_ref
Juniperus_oxycedrus_ref
Juniperus_phoenicea_ref
35
40
45
50
55
-10
0
10
20
30
0.0
0.2
0.4
0.6
0.8

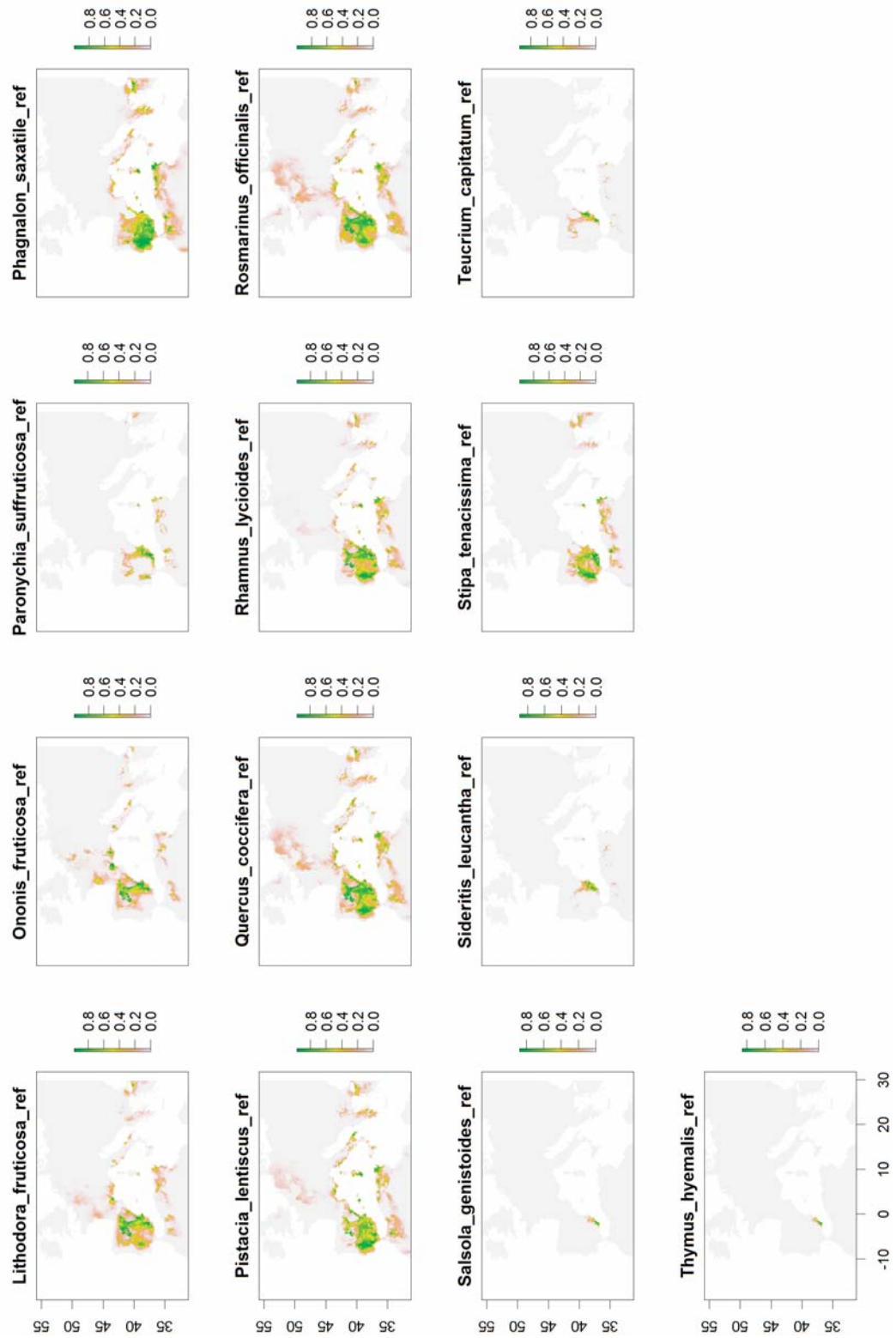
Phagnalon_saxatile_ref
Paronychia_suffruticosa_ref
Rosmarinus_officinalis_ref
Rhamnus_lycioides_ref
Teucrium_capitatum_ref
Stipa_tenacissima_ref
Ononis_fruticosa_ref
Quercus_coccifera_ref
Sideritis_leucantha_ref
Lithodora_fruticosa_ref
Pistacia_lentiscus_ref
Salsola_genistoides_ref
Thymus_hyemalis_ref
0.8
0.6
0.4
0.2
0.0
35 40 45 50 55
-10 0 10 20 30


Anthyllis_cytisoides_sequia
Artemisia_barrelieri_sequia
Artemisia_campestris_sequia
Asparagus_horridus_sequia
Cistus_albidus_sequia
Cistus_clusii_sequia
Daphne_gnidium_sequia
Dorycnium_pentaphyllum_sequia
Fumana_ericoides_sequia
Globularia_alypum_sequia
Helianthemum_almeriense_sequia
Helianthemum_origanifolium_sequia
Helianthemum_syriacum_sequia
Helichrysum_stoechas_sequia
Juniperus_oxycedrus_sequia
Juniperus_phoenicea_sequia
37.4
37.8
38.2
38.6
-2.5
-2.0
-1.5
-1.0
-0.5

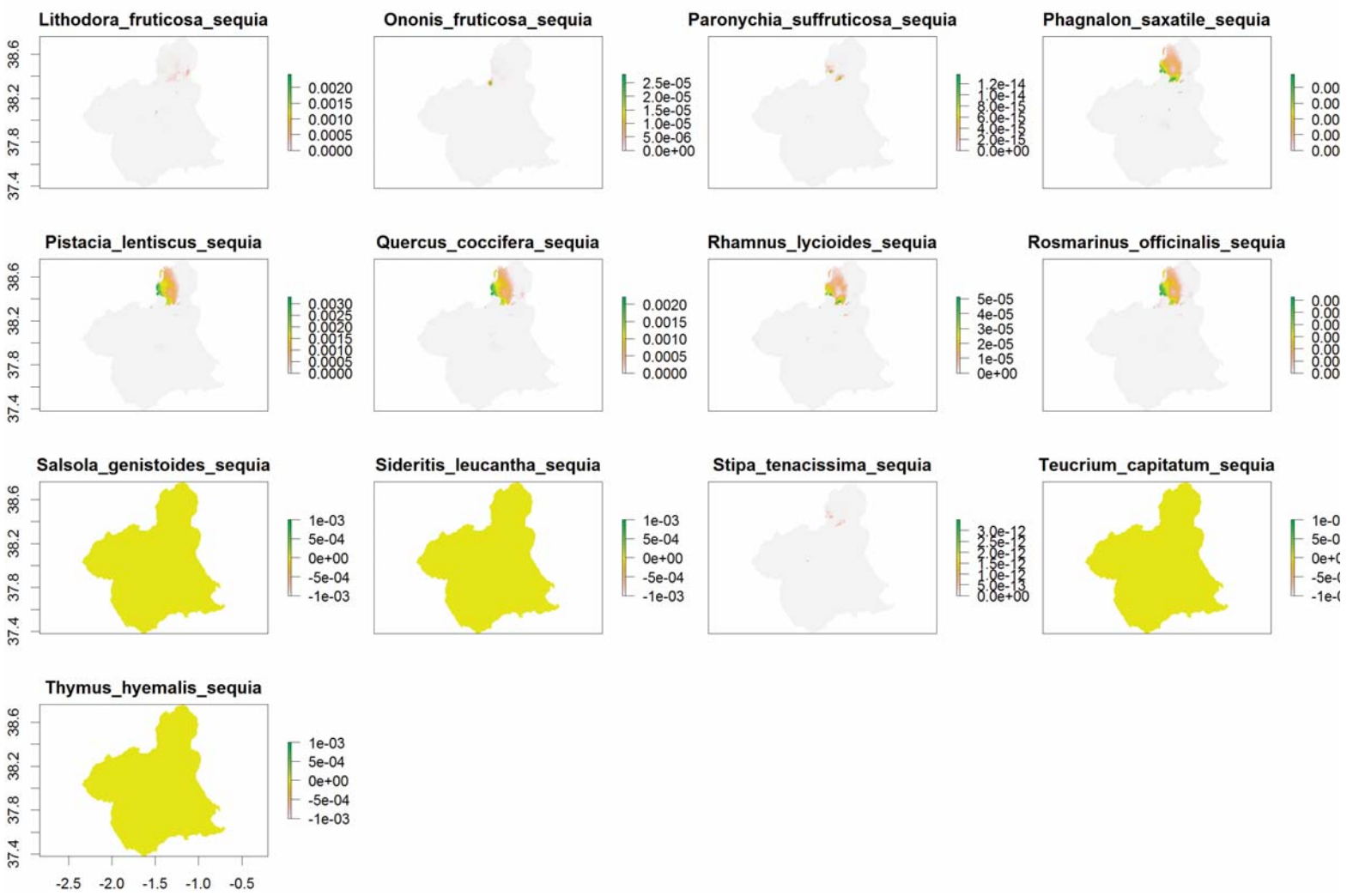

Figure A.8: Suitability maps obtained from Mahalanobis distance. Note that Mediterranean basin maps were used to project the models under 1950-2000 average conditions, while Region of Murcia maps were used to project the models under extreme hydrological year 2013-2014.

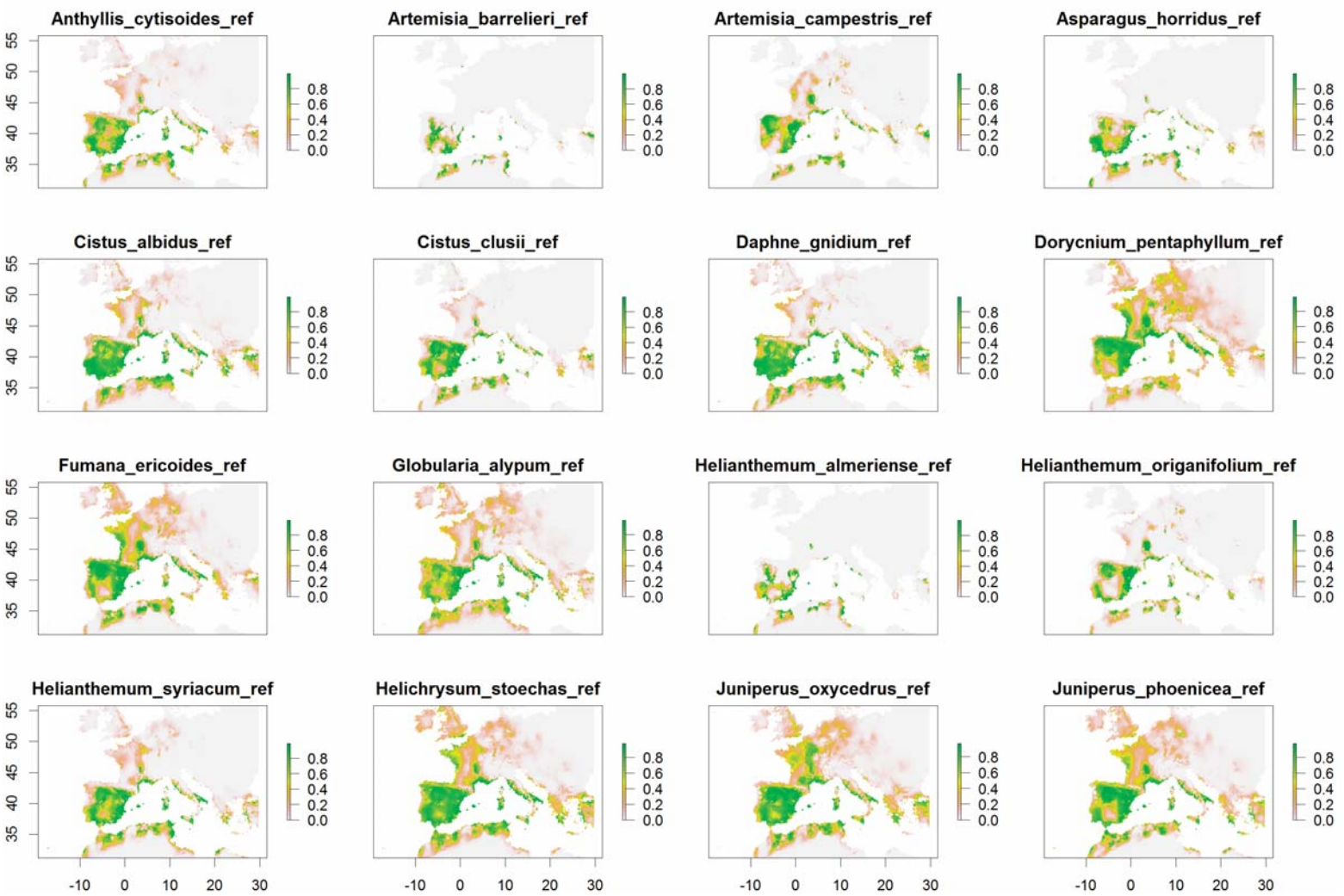
Anthyllis_cytisoides_ref
Artemisia_barrelieri_ref
Artemisia_campestris_ref
Asparagus_horridus_ref
Cistus_albidus_ref
Cistus_clusii_ref
Daphne_gnidium_ref
Dorycnium_pentaphyllum_ref
Fumana_ericoides_ref
Globularia_alypum_ref
Helianthemum_almeriense_ref
Helianthemum_origanifolium_ref
Helianthemum_syriacum_ref
Helichrysum_stoechas_ref
Juniperus_oxycedrus_ref
Juniperus_phoenicea_ref
35
40
45
50
55
-10
0
10
20
30
0.0
0.2
0.4
0.6
0.8

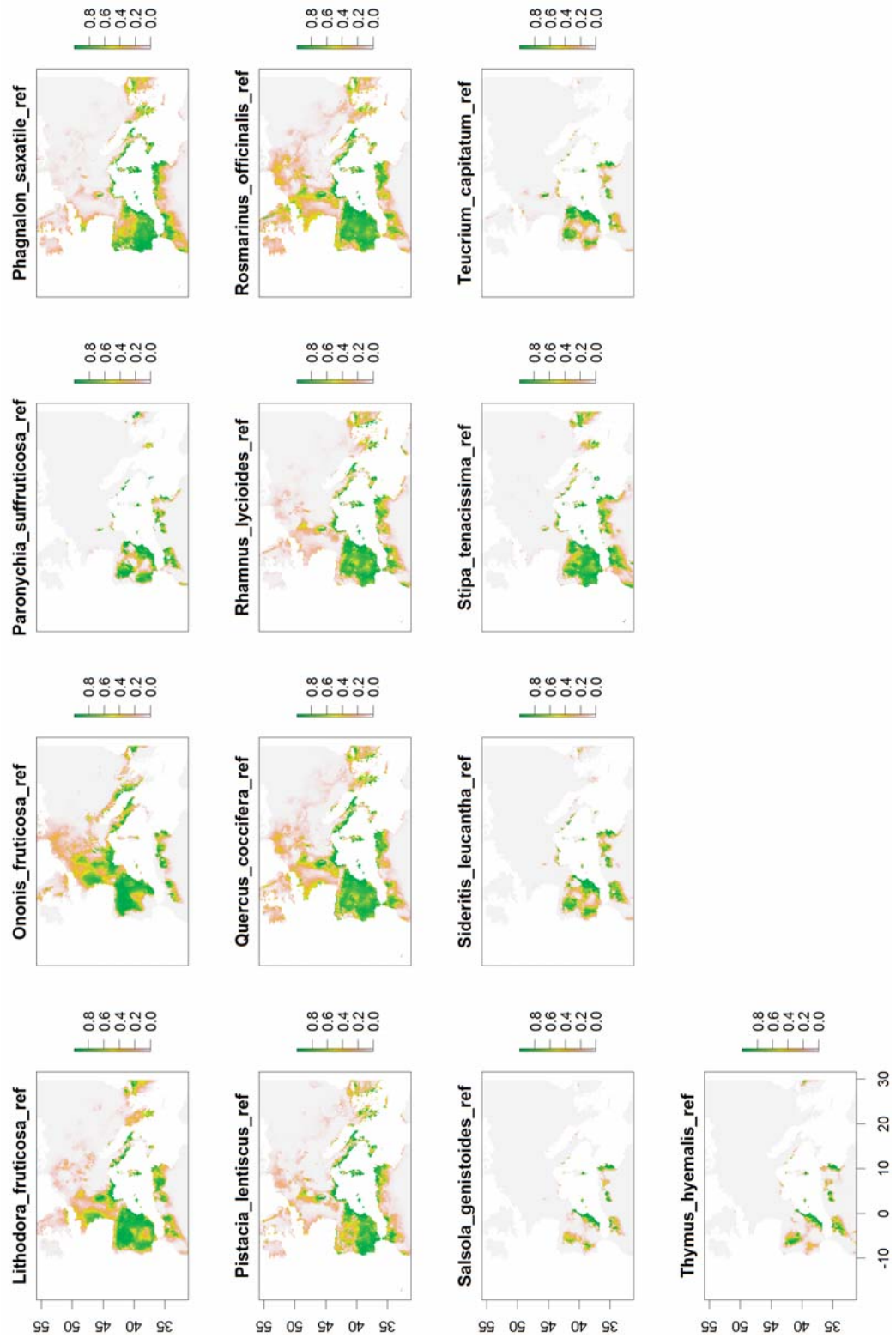
Phagnalon_saxatile_ref
Paronychia_suffruticosa_ref
Rosmarinus_officinalis_ref
Rhamnus_lycioides_ref
Teucrium_capitatum_ref
Stipa_tenacissima_ref
Ononis_fruticosa_ref
Quercus_coccifera_ref
Sideritis_leucantha_ref
Lithodora_fruticosa_ref
Pistacia_lentiscus_ref
Salsola_genistoides_ref
Thymus_hyemalis_ref
0.8
0.6
0.4
0.2
0.0
35 40 45 50 55
-10 0 10 20 30

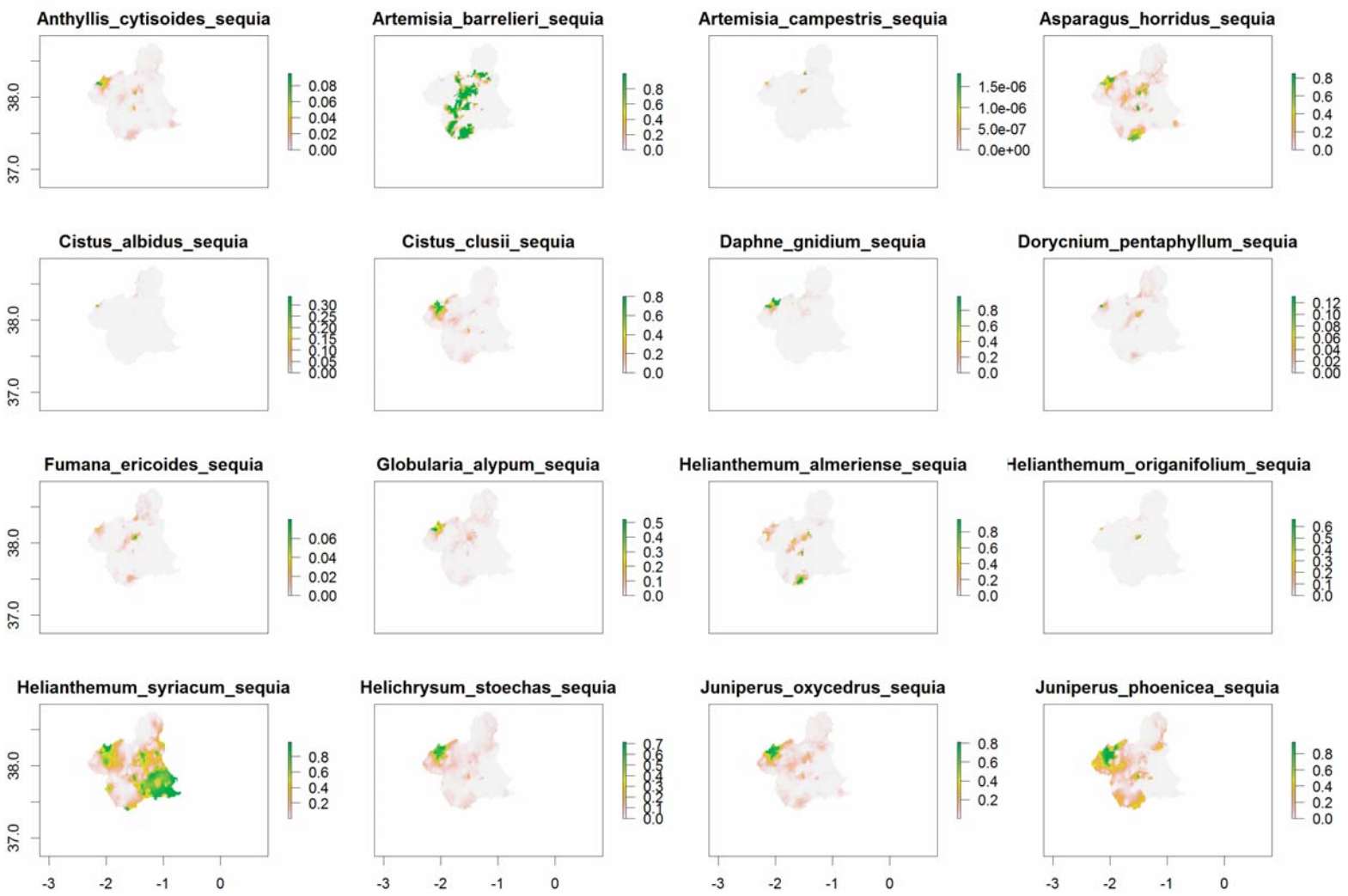
Anthyllis_cytisoides_sequia
Artemisia_barrelieri_sequia
Artemisia_campestris_sequia
Asparagus_horridus_sequia
Cistus_albidus_sequia
Cistus_clusii_sequia
Daphne_gnidium_sequia
Dorycnium_pentaphyllum_sequia
Fumana_ericoides_sequia
Globularia_alypum_sequia
Helianthemum_almeriense_sequia
Helianthemum_origanifolium_sequia
Helianthemum_syriacum_sequia
Helichrysum_stoechas_sequia
Juniperus_oxycedrus_sequia
Juniperus_phoenicea_sequia
38.0
37.0
-3
-2
-1
0

Figure A.9: Suitability maps obtained from Generalize Additive Models (GAM). Note that Mediterranean basin maps were used to project the models under 1950-2000 average conditions, while Region of Murcia maps were used to project the models under extreme hydrological year 2013-2014.

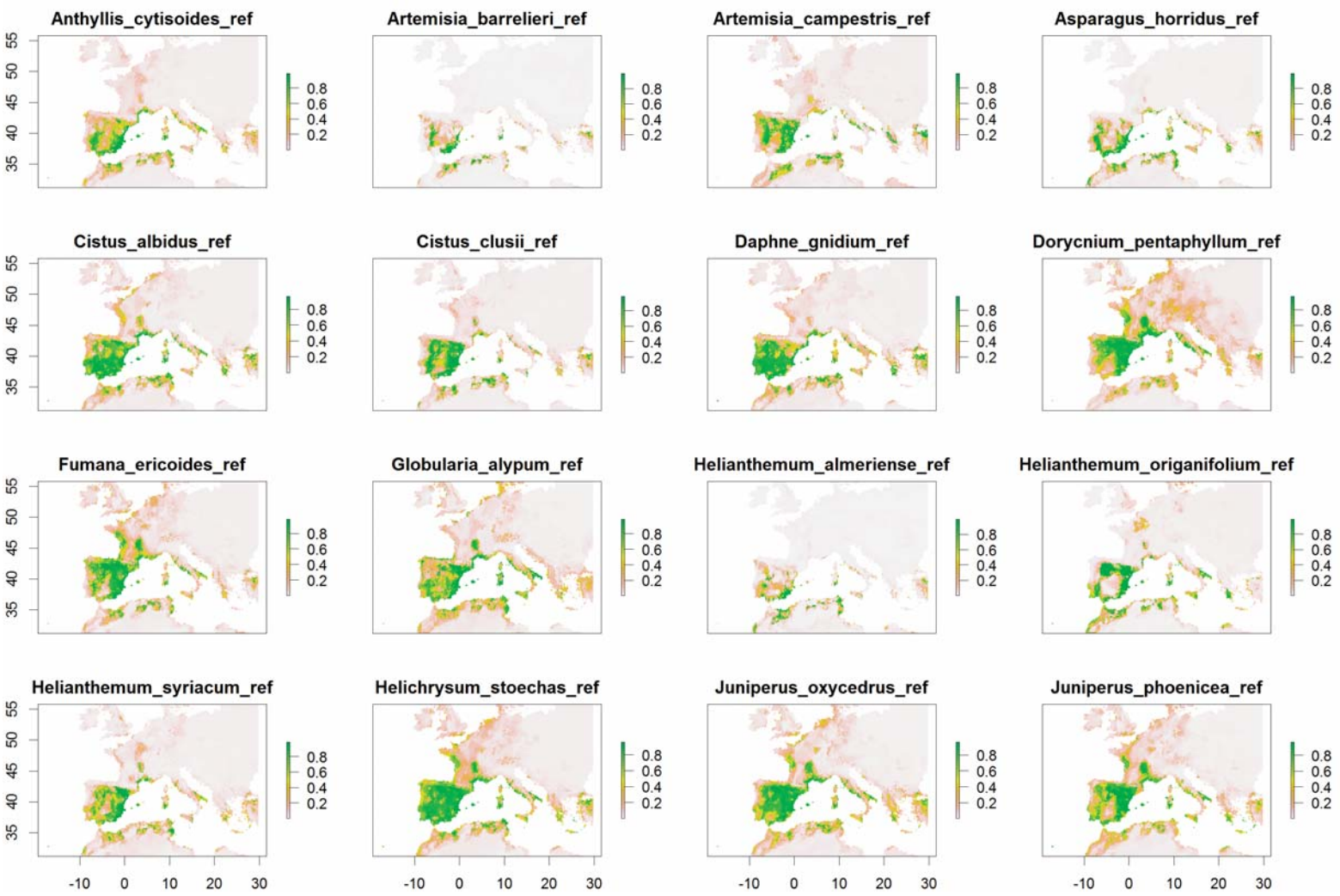
Anthyllis_cytisoides_ref
Artemisia_barrelieri_ref
Artemisia_campestris_ref
Asparagus_horridus_ref
Cistus_albidus_ref
Cistus_clusii_ref
Daphne_gnidium_ref
Dorycnium_pentaphyllum_ref
Fumana_ericoides_ref
Globularia_alypum_ref
Helianthemum_almeriense_ref
Helianthemum_origanifolium_ref
Helianthemum_syriacum_ref
Helichrysum_stoechas_ref
Juniperus_oxycedrus_ref
Juniperus_phoenicea_ref
35
40
45
50
55
-10
0
10
20
30
0.2
0.4
0.6
0.8

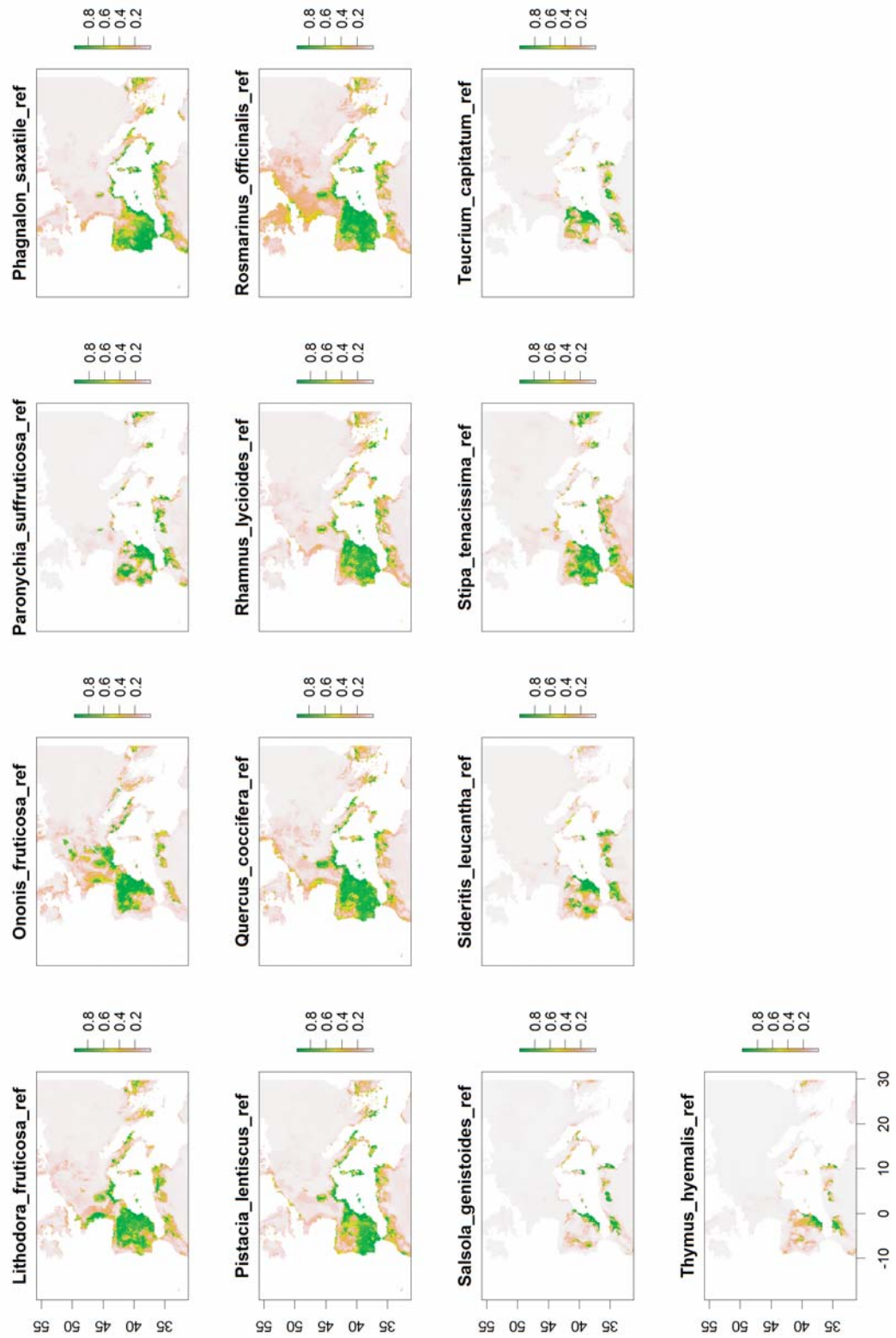
Phagnalon_saxatile_ref
Rosmarinus_officinalis_ref
Teucrium_capitatum_ref
Paronychia_suffruticosa_ref
Rhamnus_lycioides_ref
Stipa_tenacissima_ref
Ononis_fruticosa_ref
Quercus_coccifera_ref
Sideritis_leucantha_ref
Lithodora_fruticosa_ref
Pistacia_lentiscus_ref
Salsola_genistoides_ref
Thymus_hyemalis_ref
0.8
0.6
0.4
0.2
35 40 45 50 55
-10 0 10 20 30


Anthyllis_cytisoides_sequia
Artemisia_barrelieri_sequia
Artemisia_campestris_sequia
Asparagus_horridus_sequia
Cistus_albidus_sequia
Cistus_clusii_sequia
Daphne_gnidium_sequia
Dorycnium_pentaphyllum_sequia
Fumana_ericoides_sequia
Globularia_alypum_sequia
Helianthemum_almeriense_sequia
Helianthemum_origanifolium_sequia
Helianthemum_syriacum_sequia
Helichrysum_stoechas_sequia
Juniperus_oxycedrus_sequia
Juniperus_phoenicea_sequia
38.0
37.0
-3
-2
-1
0

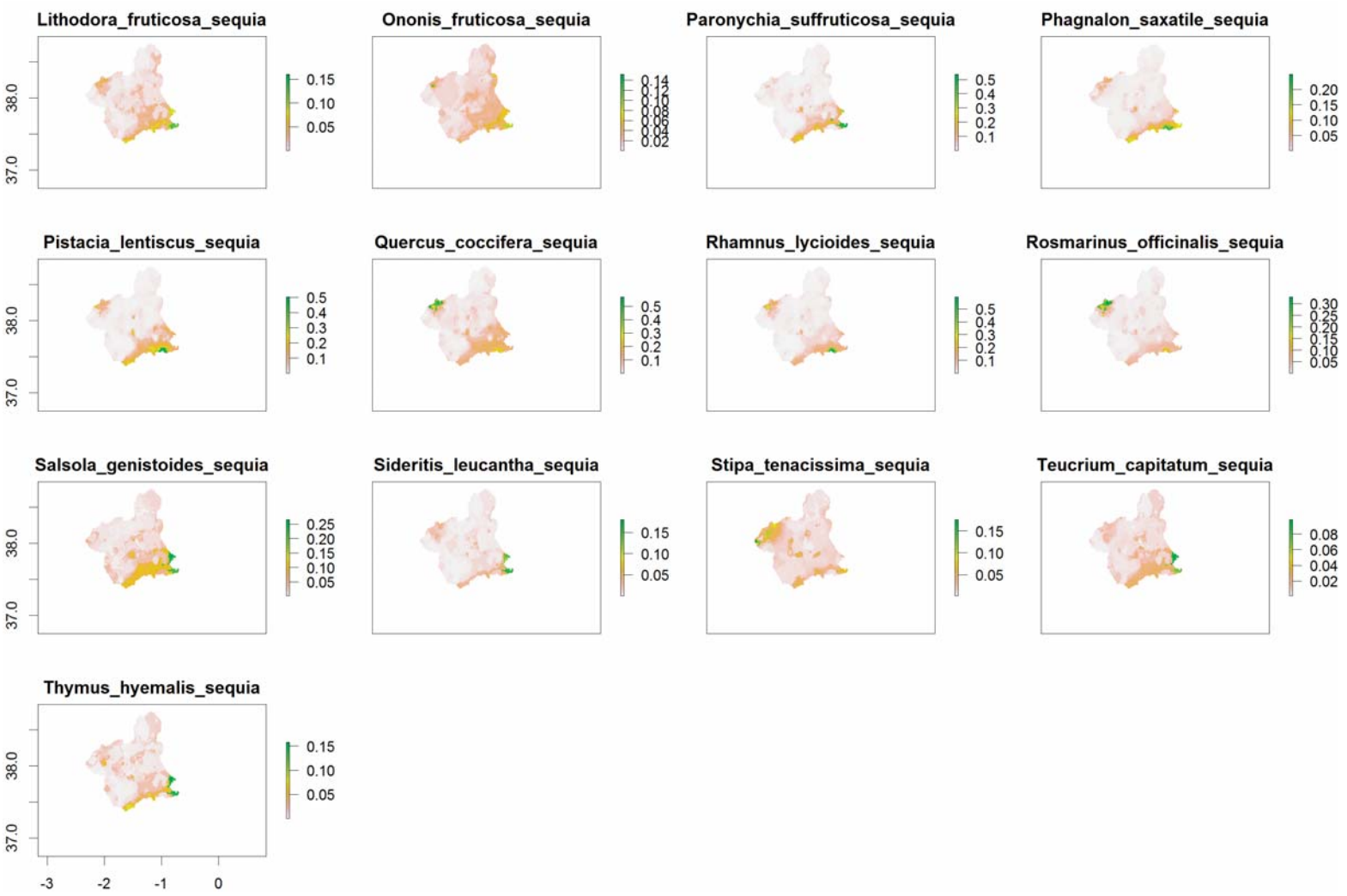

Figure A.10: Suitability maps obtained from Boosted Regression Trees (BRT). Note that Mediterranean basin maps were used to project the models under 1950-2000 average conditions, while Region of Murcia maps were used to project the models under extreme hydrological year 2013-2014.

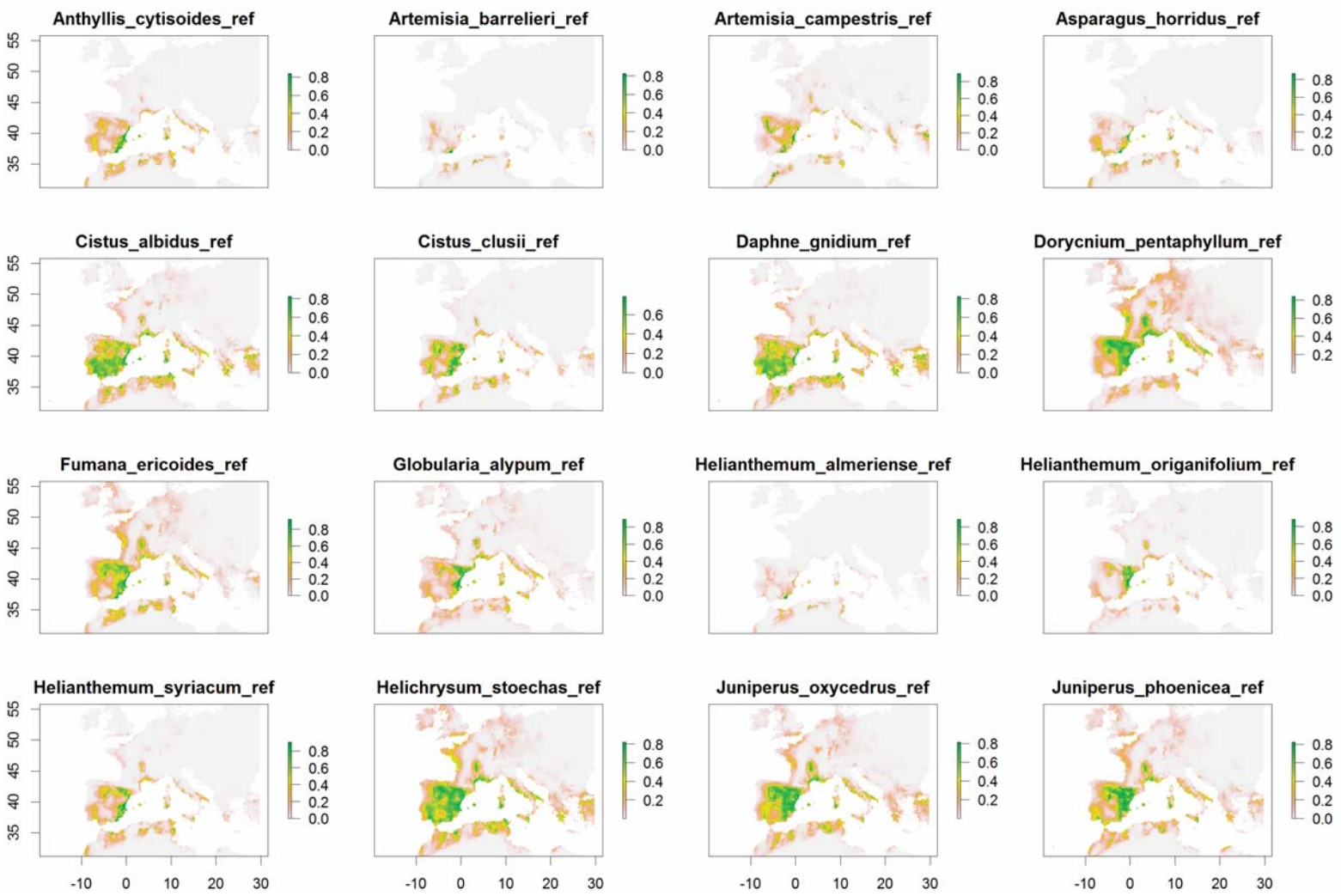
Anthyllis_cytisoides_ref
Artemisia_barrelieri_ref
Artemisia_campestris_ref
Asparagus_horridus_ref
Cistus_albidus_ref
Cistus_clusii_ref
Daphne_gnidium_ref
Dorycnium_pentaphyllum_ref
Fumana_ericoides_ref
Globularia_alypum_ref
Helianthemum_almeriense_ref
Helianthemum_origanifolium_ref
Helianthemum_syriacum_ref
Helichrysum_stoechas_ref
Juniperus_oxycedrus_ref
Juniperus_phoenicea_ref
35
40
45
50
55
-10
0
10
20
30
0.0
0.2
0.4
0.6
0.8

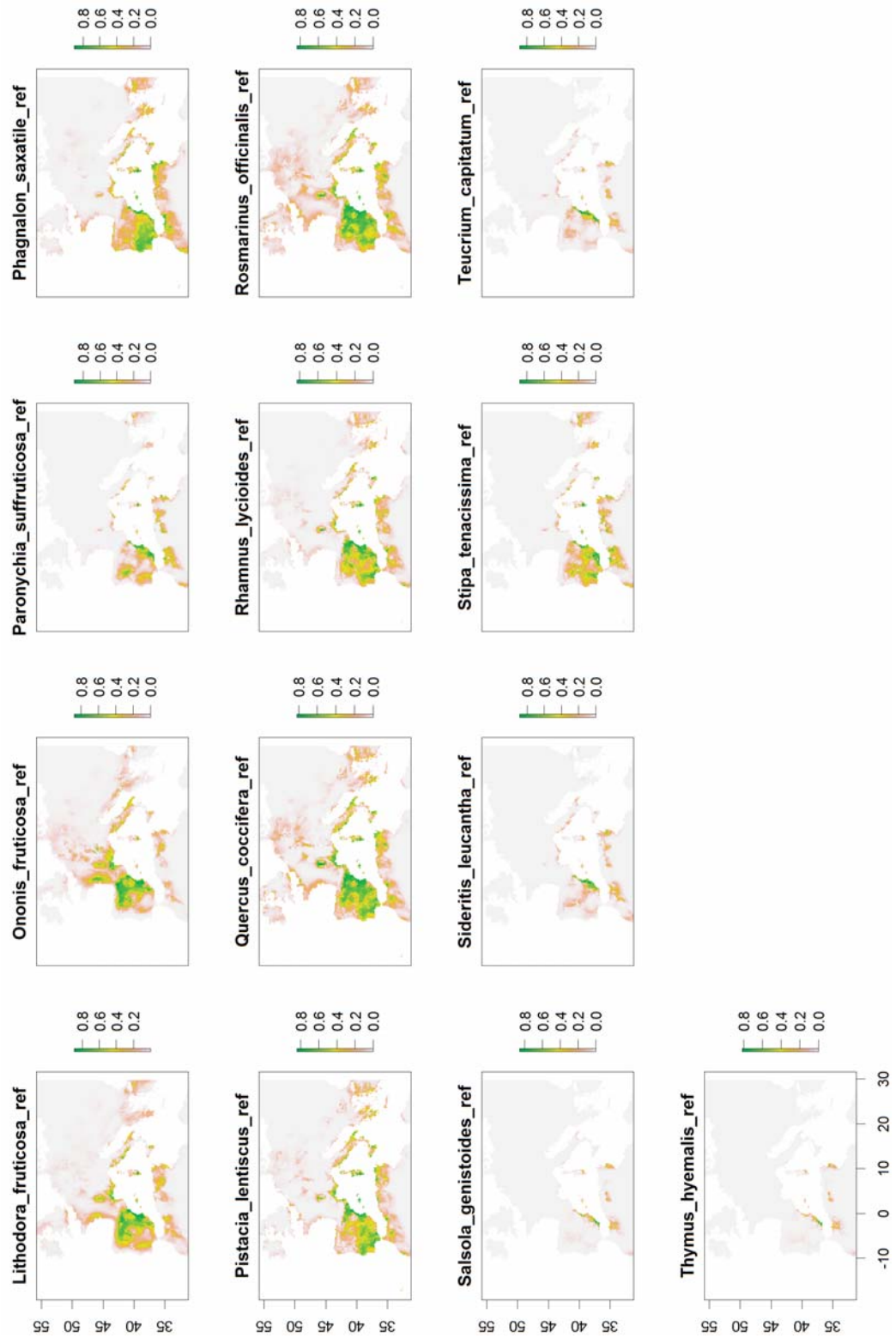
Phagnalon_saxatile_ref
Paronychia_suffruticosa_ref
Ononis_fruticosa_ref
Lithodora_fruticosa_ref
Rosmarinus_officinalis_ref
Rhamnus_lycioides_ref
Quercus_coccifera_ref
Pistacia_lentiscus_ref
Teucrium_capitatum_ref
Stipa_tenacissima_ref
Sideritis_leucantha_ref
Salsola_genistoides_ref
Thymus_hyemalis_ref
0.8
0.6
0.4
0.2
0.0
35
40
45
50
55
-10
0
10
20
30

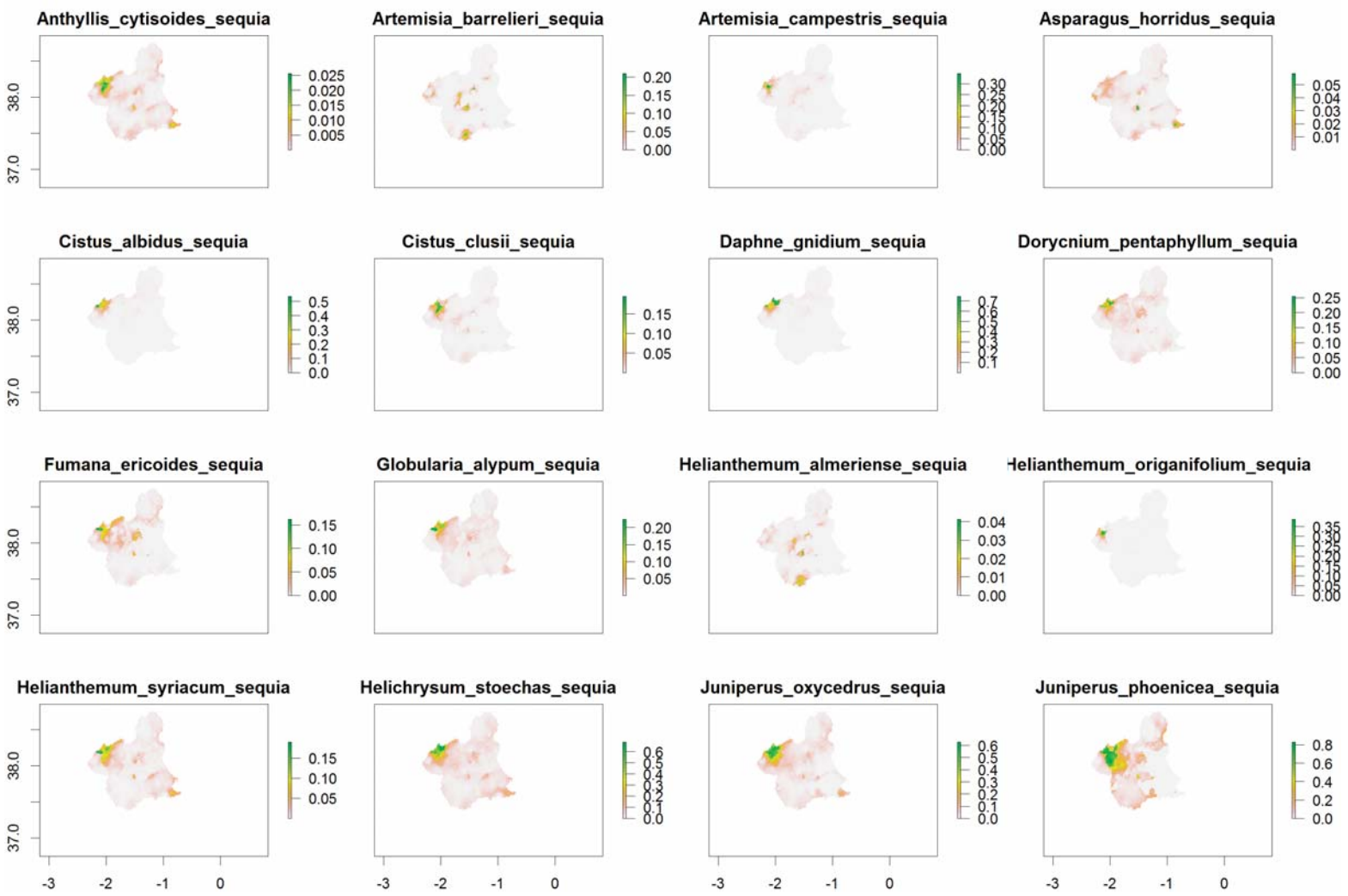
Anthyllis_cytisoides_sequia
Artemisia_barrelieri_sequia
Artemisia_campestris_sequia
Asparagus_horridus_sequia
Cistus_albidus_sequia
Cistus_clusii_sequia
Daphne_gnidium_sequia
Dorycnium_pentaphyllum_sequia
Fumana_ericoides_sequia
Globularia_alypum_sequia
Helianthemum_almeriense_sequia
Helianthemum_origanifolium_sequia
Helianthemum_syriacum_sequia
Helichrysum_stoechas_sequia
Juniperus_oxycedrus_sequia
Juniperus_phoenicea_sequia
38.0
37.0
-3
-2
-1
0

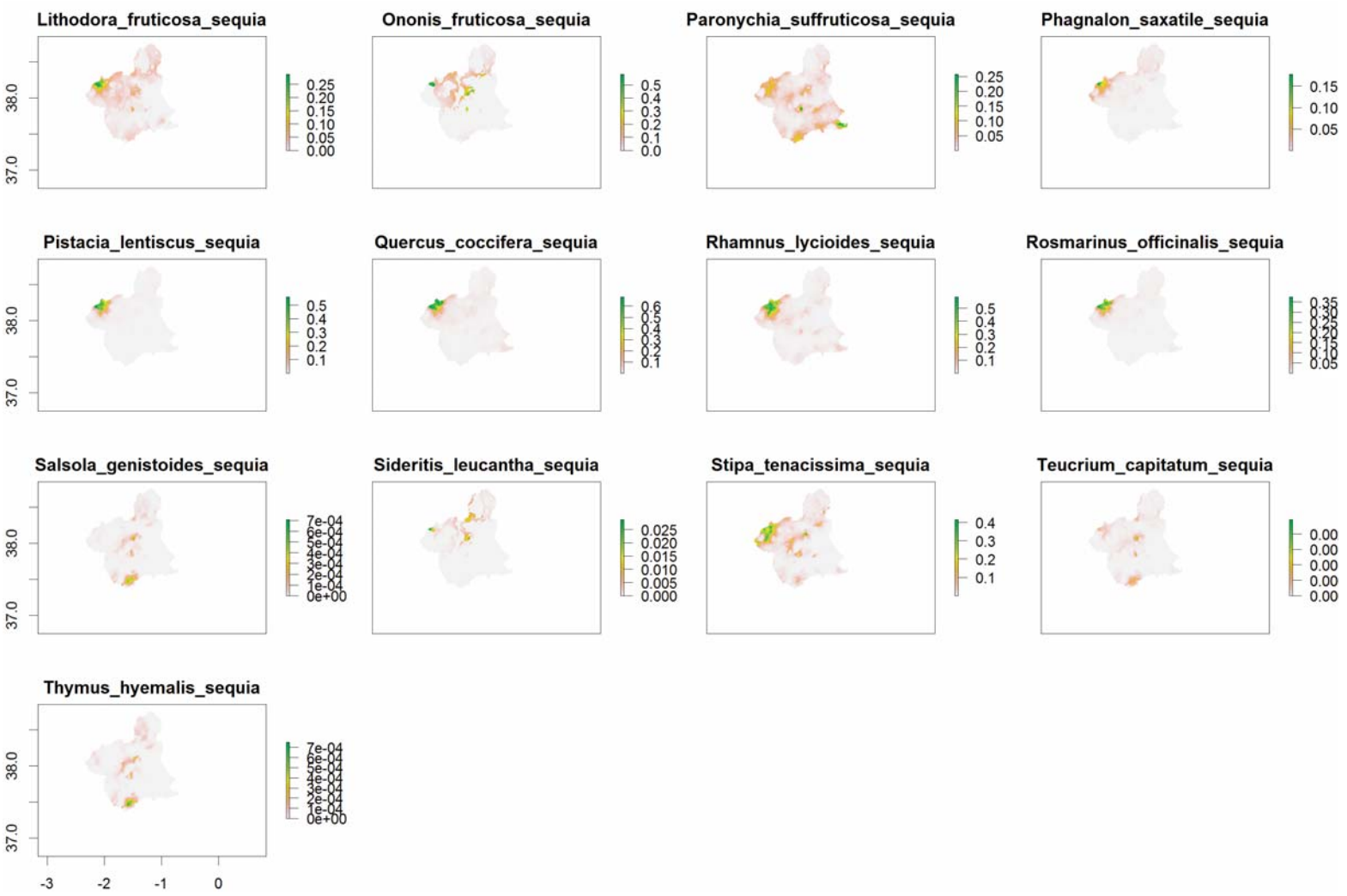

Figure A.11: Suitability maps obtained from MaxEnt. Note that Mediterranean basin maps were used to project the models under 1950-2000 average conditions, while Region of Murcia maps were used to project the models under extreme hydrological year 2013-2014.

Table A.1: Pearson correlation values comparing visual drought estimate and defoliation directly measure by centimeters, for each measured species. N is the number of measured individual for all study site.

Species	N	Pearson corr
Anthyllis cytisoides	60	0.919
Artemisia barrelieri	90	0.938
Artemisia campestris	10	0.966
Asparagus horridus	10	0.935
Cistus albidus	10	0.701
Cistus clusii	86	0.978
Daphne gnidium	20	0.720
Dorycnium pentaphyllum	50	0.935
Fumana ericoides	90	0.984
Helianthemum syriacum	30	0.935
Juniperus oxycedrus	44	0.899
Juniperus phoenicea	10	0.901
Lithodora fruticosa	10	0.882
Ononis fruticosa	40	0.851
Pistacia lentiscus	50	0.889
Quercus coccifera	70	0.961
Rhamnus lycioides	25	0.890
Rosmarinus officinalis	100	0.860
Salsola genistoides	15	0.821
Sideritis leucantha	13	0.880
Stippa tenacissima	100	0.952
Teucrium capitatum gracillimum	44	0.873
Thymus hyemalis	100	0.946

Table A.2: Median and range values for Historical Climatic Suitability (HCS) and Episode Climatic Suitability (ECS) of different SDM applied for the co-occurring species in the studied community.

X1	mahal	GAM	BRT	MaxEnt
HCS range	0.902 - 0.031	0.965 - 0.613	0.992 - 0.332	0.751 - 0.121
HCS median	0.5423	0.845	0.8527	0.3632
ECS range	8.267x10-7 - 0	0.303 - 2.22x10-16	0.104 - 1.26x10-3	0.084 - 1.51x10-5
ECS median	4.83x10-16	0.0032	0.0053	0.0034

B

Appendix Chapter 3

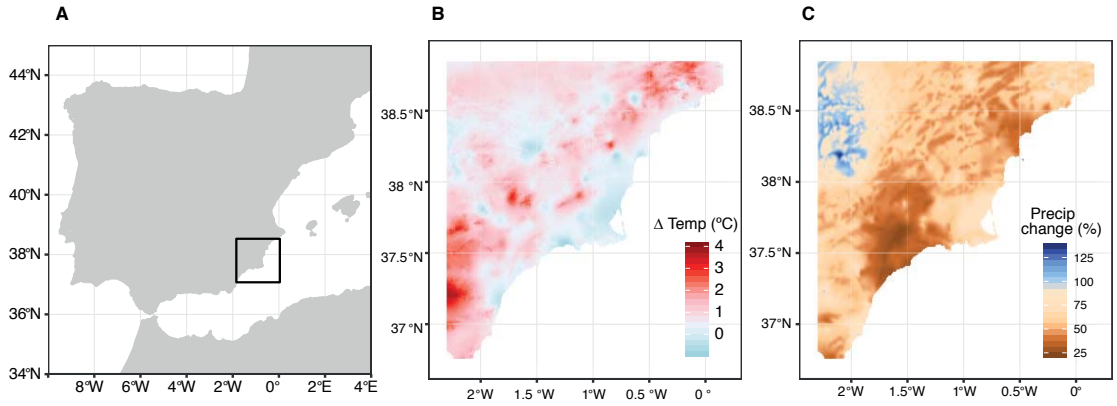

Figure B.1: Climatic anomaly of the extreme climatic year 2013-2014 in the Spanish SE. Temperature anomaly is measured as degrees change respect to the average for the period 1970-2000, while precipitation anomaly is estimated as relative change (%) respect to the average period 1970-2000.

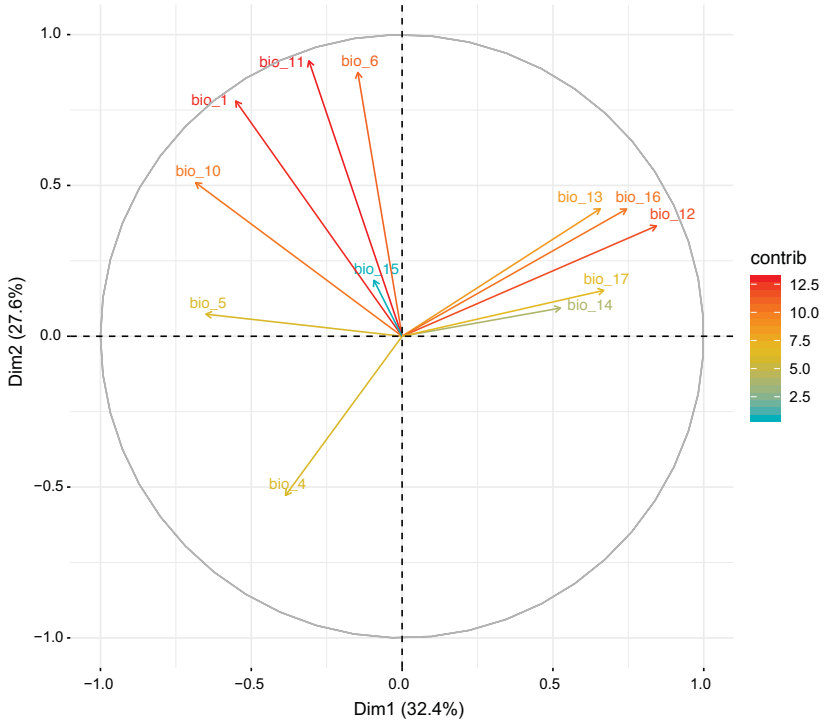

Figure B.2: Correlation circle obtained from PCA from the twelve selected climatic variables. Where BIO1= Annual Mean Temperature, BIO4= Temperature Seasonality (standard deviation×100), BIO5= Max Temperature of Warmest Month, BIO6= Min Temperature of Coldest Month, BIO10= Mean Temperature of Warmest Quarter, BIO11= Mean Temperature of Coldest Quarter, BIO12= Annual Precipitation, BIO13= Precipitation of Wettest Month, BIO14= Precipitation of Driest Month, BIO15= Precipitation Seasonality (Coefficient of Variation), BIO16= Precipitation of Wettest Quarter, BIO17= Precipitation of Driest Quarter. The PCA was calibrated using climatic data from the total filtered 9,959 occurrences of *Pinus halepensis* occurrences from the Spanish National Forest Inventory (IFN). First and second axes contained 60% of explained variability. The variables' color represents the percentage of each variable' contribution to the PCA.

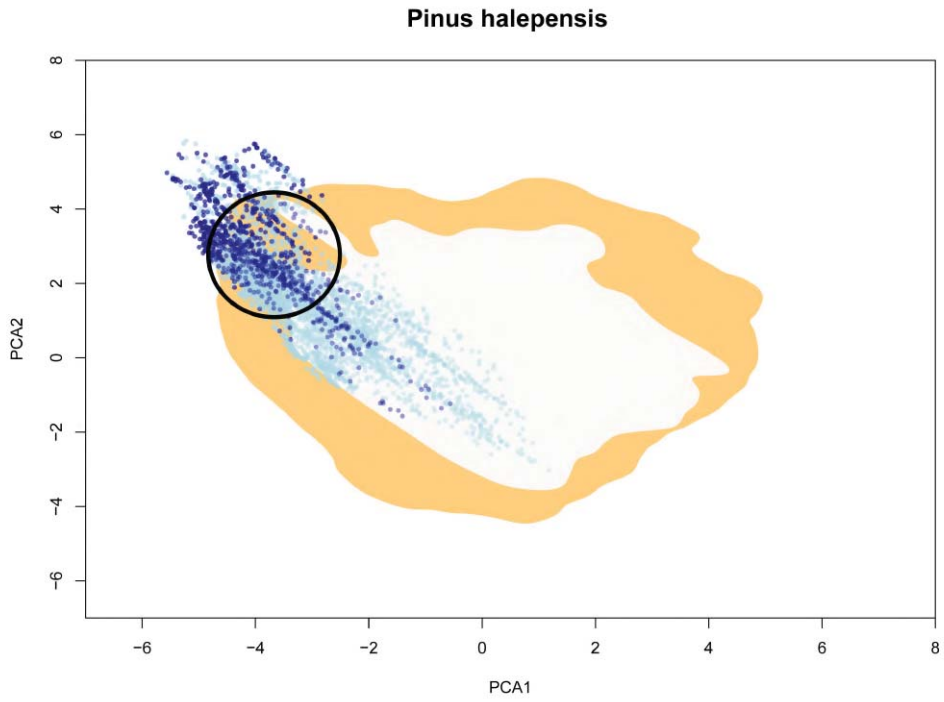

Figure B.3: Populations located in the niche space that is not shared by the average-based and the inter-annual variability-based niches. Orange region represents the area of the variability-based niche that is not included within the average-based niche area.

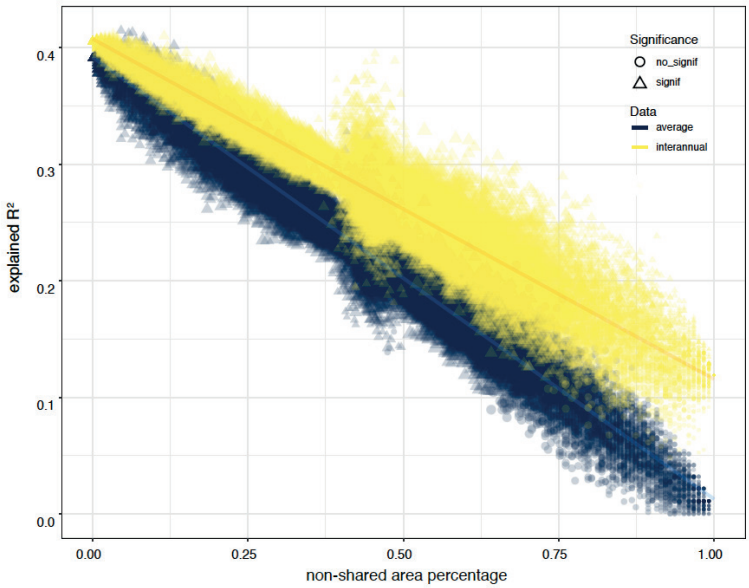

Figure B.4: Model explained R^2 depending on population subset, where response variable was plot mortality percentage and explanatory variables was plot climatic suitability. X axis ranged from 0 percentage of population located in the non-shared niche space by inter-annual and average-based niches to 100. Blue color represent R^2 values obtained with climatic suitability derived from the average-based niche while yellow color represent R^2 values obtained with climatic suitability derived from the inter-annual variability-based niche.

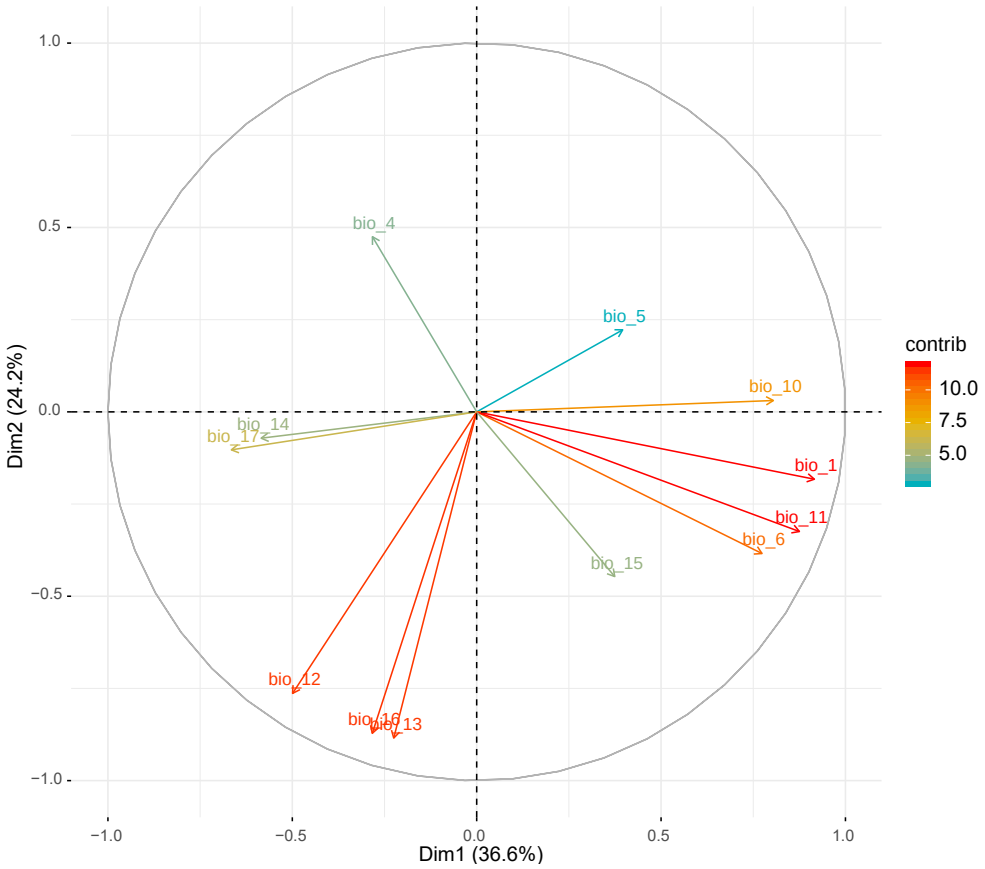

Figure B.5: Correlation circle obtained from PCA from the twelve selected climatic variables. Where BIO1= Annual Mean Temperature, BIO4= Temperature Seasonality (standard deviation×100), BIO5 = Max Temperature of Warmest Month, BIO6= Min Temperature of Coldest Month, BIO10 = Mean Temperature of Warmest Quarter, BIO11= Mean Temperature of Coldest Quarter, BIO12= Annual Precipitation, BIO13= Precipitation of Wettest Month, BIO14 = Precipitation of Driest Month, BIO15= Precipitation Seasonality (Coefficient of Variation), BIO16= Precipitation of Wettest Quarter, BIO17 = Precipitation of Driest Quarter. The PCA was calibrated using climatic data from the total filtered 116,835 occurrences from the Spanish National Forest Inventory (IFN) and gbif.org for all the 42 selected species. First and second axes contained 60.8% of explained variability. The variables' color represents the percentage of each variable' contribution to the PCA.

Table B.1: Species used for analyses of changes in niche space depending on species climatic range. Table shows area of average based-niche (niche area av), inter-annual based-niche (niche area in), niche rate (area of average based-niche/area of inter-annual variability based-niche) and species' distribution range, where endemic SE means species endemic from the Spanish south east and mediterraneean occ means species mostly distributed in the west of the Mediterranean basin.

Species	Niche area av	Niche area in	Niche rate	Distr range
Anthyllis terniflora	8.185	21.856	2.670	endemic SE
Artemisia barrelieri	12.619	34.393	2.725	endemic SE
Asparagus horridus	37.065	59.544	1.606	mediterranean
Chamaerops humilis	19.124	39.579	2.070	iberoafrican
Cistus clusii	15.010	35.679	2.377	mediterranean occ
Cistus monspeliensis	35.642	64.681	1.815	mediterranean
Coronilla juncea	19.049	39.719	2.085	mediterranean occ
Dorycnium pentaphyllum	33.890	61.624	1.818	mediterranean occ
Frankenia corymbosa	8.917	26.437	2.965	iberoafrican
Fumana ericoides	35.136	65.437	1.862	mediterranean occ
Fumana laevipes	19.356	39.366	2.034	mediterranean occ
Fumana thymifolia	35.459	62.157	1.753	mediterranean
Genista valentina	8.635	30.559	3.539	endemic SE
Globularia alypum	22.391	46.018	2.055	mediterranean
Helianthemum syriacum	18.758	39.410	2.101	mediterranean
Helianthemum violaceum	18.513	40.585	2.192	iberoafrican
Helianthemum viscarium	6.997	21.046	3.008	iberoafrican
Helichrysum stoechas	31.154	56.958	1.828	mediterranean
Hyparrhenia hirta	31.256	58.032	1.857	iberoafrican
Launaea arborescens	22.925	46.767	2.040	iberoafrican
Launaea lanifera	9.986	25.835	2.587	iberoafrican
Lavandula dentata	26.418	47.171	1.786	iberoafrican
Lycium intricatum	13.456	33.463	2.487	iberoafrican
Lygeum spartum	16.895	35.325	2.091	iberoafrican
Paronychia suffruticosa	23.259	50.011	2.150	endemic SE
Periploca angustifolia	6.763	25.751	3.808	iberoafrican
Phagnalon rupestre	43.312	70.418	1.626	mediterranean
Phagnalon saxatile	37.291	62.075	1.665	mediterranean
Pinus halepensis	20.781	41.029	1.974	mediterranean occ
Rhamnus lycioides	34.148	60.770	1.780	mediterranean
Rosmarinus officinalis	35.674	62.756	1.759	mediterranean
Salsola genistoides	6.980	20.683	2.963	endemic SE
Salsola oppositifolia	10.617	24.630	2.320	iberoafrican
Salsola papillosa	4.144	14.237	3.435	endemic SE
Satureja obovata	17.471	40.550	2.321	mediterranean occ
Sideritis ibanyezii	3.161	12.455	3.940	endemic SE
Stipa tenacissima	18.355	37.528	2.045	iberoafrican
Teucrium capitatum	14.707	31.387	2.134	mediterranean occ
Teucrium freynii	5.638	17.164	3.044	endemic SE
Teucrium lanigerum	3.424	13.174	3.847	endemic SE
Thymelaea hirsuta	22.451	44.471	1.981	mediterranean
Thymus hyemalis	5.540	18.523	3.344	endemic SE

Table B.2: GLM binomial model results relating species decay (as binary or continuous response) with species niche suitability obtained from average-based and from inter-annual variability-based models. Models R^2 and AIC are given in the main text (Figure 3.3).

Dataset	Response	Explanatory	Estimate	SE	Pvalue
interannual	binary	intercept	-0.58	0.05	<0.001
		suitability	-4.40	0.26	<0.001
interannual	continuous	intercept	-0.53	0.19	0.006
		suitability	-5.70	1.40	<0.001
average	binary	intercept	-1.02	0.04	<0.001
		suitability	-3.80	0.28	<0.001
average	continuous	intercept	-0.84	0.16	<0.001
		suitability	-7.02	2.08	<0.001

Table B.3: Model results relating models explanatory capacity (R^2) in relation to the percentage of populations located in the non-shared area between the two niche estimations (average-based and inter-annual variability-based niche). R^2 were obtained by models that relate decay records as continuous response with different subsets of the records, in order to simulate the different percentages of population located in the non-shared area. Explanatory variables of the model are: corona percentage (percentage of population located in the non-shared niches area), niche model (averaged-based or inter-annual variability-based and n (number of records of the model, which varies from 118 to 264).

Explanatory	Estimate	SE	Pvalue	R^2= 0.954
Intercept	0.387	0.000472	<0.001	
corona percentage	-0.379	0.000457	<0.001	
dataset interannual	0.0157	0.000331	<0.001	
n	2.18x10-5	1.5x10-6	<0.001	
Corona percentage : dataset interannual	0.0872	0.000632	<0.001	

Table B.4: Model results with ratio of niche area (inter-annual variability-based niche area/average-based area) as response variable and log(average-based niche area) and distribution range as explanatory variables.

Explanatory	Estimate	SE	Pvalue	R^2 = 0.895
Intercept (SE endemic)	4.79	0.16	<0.001	
Log(niche area average)	-0.85	0.08	<0.001	
Distrib ib af	-0.12	0.11	0.279	
Distrib med	-0.06	0.15	0.701	
Distrib med occ	-0.14	0.13	0.299	

C

Appendix Chapter 4

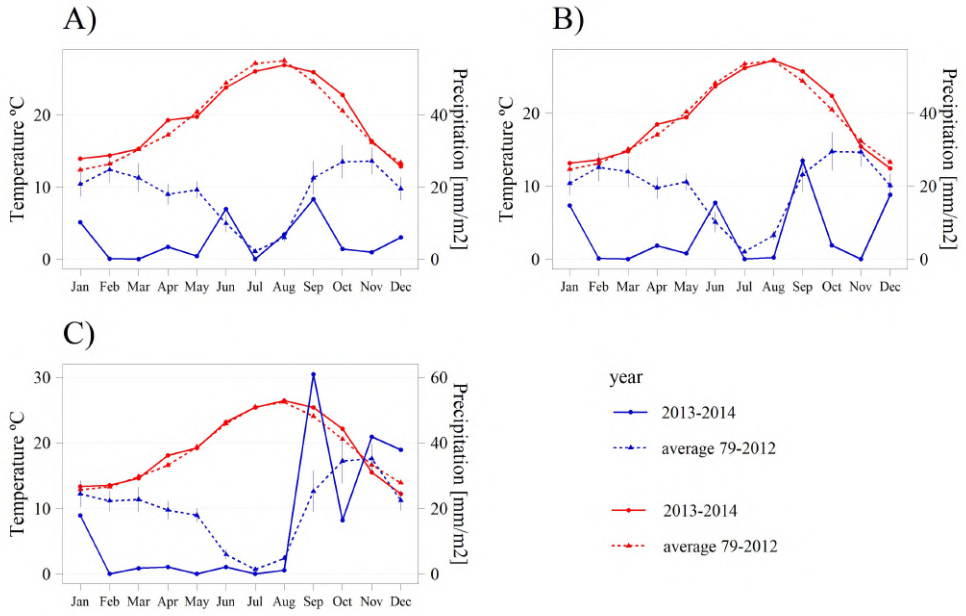

Figure C.1: Ombrothermic diagrams for A) Cuatro Calas, B) Moreras Mountain and C) Calblanque Natural Park, respectively. Red lines correspond to temperatures, and blue lines correspond to precipitation. Solid lines correspond to the reference climatic period (1979-2012, Chelsa v.1.2, Karger et al. 2017) and dotted lines correspond to extreme climatic year (2013-2014) (data from Spanish Weather Agency, AEMET). Vertical blue and red lines over the reference period lines show Standard Error estimated for each month in the period 1979-2012.

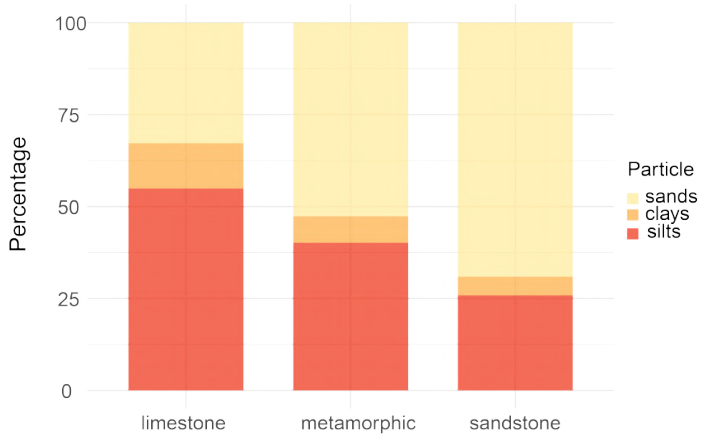

Figure C.2: Soil particle composition of the three different study sites' bedrocks (i.e., Moreras' Mountain, Calblanque Natural Parck, and Cuatro Calas, respectively to this graphic order. Yellow colour represents the proportion of sands, orange the proportion of clays and 30 dark orange the proportion of silts.

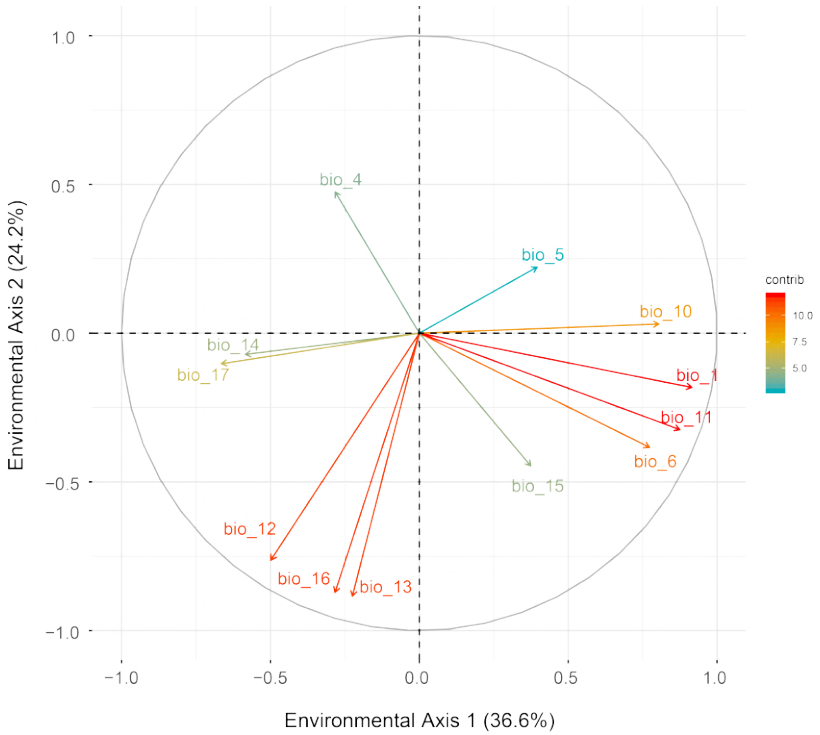

Figure C.3: Correlation circle obtained from PCA from the twelve selected climatic variables. Where BIO1 = Annual Mean Temperature, BIO4 = Temperature Seasonality (standard deviation×100), BIO5 = Max Temperature of Warmest Month, BIO6 = Min Temperature of Coldest Month, BIO10= Mean Temperature of Warmest Quarter, BIO11 = Mean Temperature of Coldest Quarter, BIO12 = Annual Precipitation, BIO13 = Precipitation of Wettest Month, BIO14 = Precipitation of Driest Month, BIO15 = Precipitation Seasonality (Coefficient of Variation), BIO16 = Precipitation of Wettest Quarter, BIO17 = Precipitation of Driest Quarter. The PCA was calibrated using climatic data from the total filtered 106,876 occurrences from gbif.org for all the 38 sampled species. The first and second axes contained 60.8% of explained variability. The variables' colour represents the percentage of each variable' contribution to the PCA.

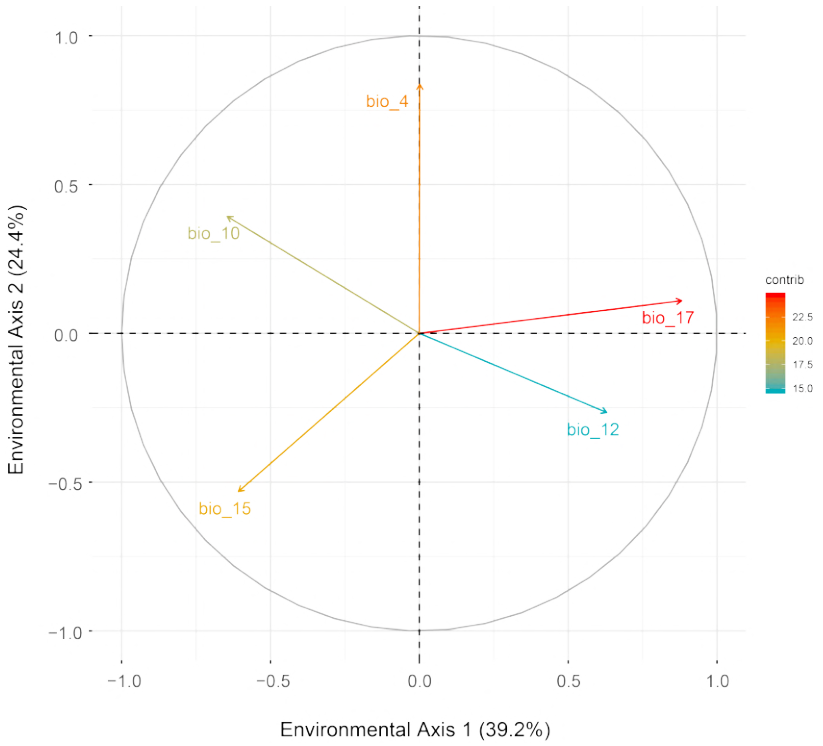

Figure C.4: Correlation circle obtained from PCA calibrated with the five climatic variables included in SDMs (MaxEnt) using climatic data from the total filtered 106,876 occurrences from gbif.org for all the 38 sampled species. In order to discard difference between environmental spaces calibrated with the first 12 variables (Figure S3) instead of this 6 variables. We calculated the pearson correlation between the contribution of these 6 variables in both calibrated pca. We obtained a correlation of -0.9425 for axis 1, and 0.9115 for axis 2. BIO1 = Annual Mean Temperature, BIO4 = Temperature Seasonality (standard deviation×100), BIO10 = Mean Temperature of Warmest Quarter, BIO12 = Annual Precipitation, BIO15 = Precipitation Seasonality (Coefficient of Variation), BIO17 = Precipitation of Driest Quarter. The PCA was calibrated using climatic data from the total filtered 106,876 occurrences from gbif.org for all the 38 sampled species. The first and second axes contained 63.6% of explained variability. The variables' colour represents the percentage of each variable' contribution to the PCA.

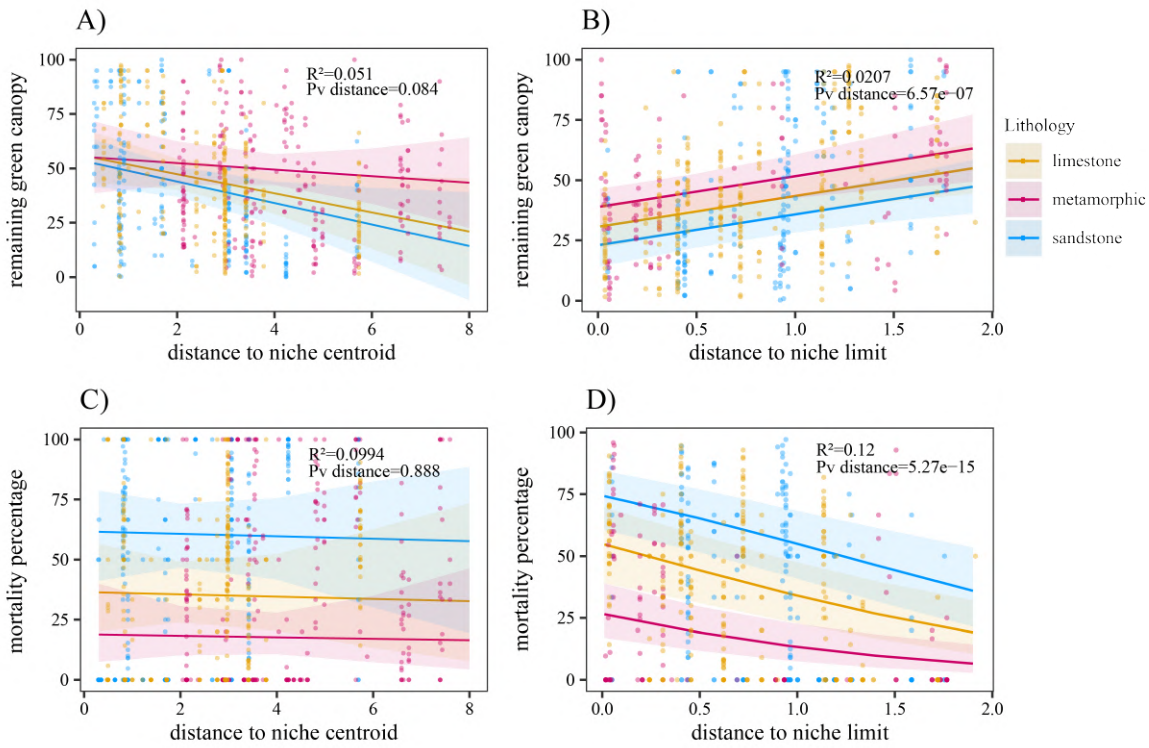

Figure C.5: Remaining Green Canopy (RGC) in relation to population distances during the reference period 1979-2012 to their respective species niche centroid (A) and to the closest point of the niche limit (B),.; Mortality percentage in relation to population distances during the reference period 1979-2012 to their respective species niche centroid (C) and to the closest point of the niche limit (D). In all four cases, only the subset of populations located within the niche were considered. Yellow dots show distances of populations located in Moreras' Mountain (limestone bedrock), magenta dots show distances of populations located in Calblanque Natural Parck (metamorphic bedrock) and blue dots show distances of populations located in Cuatro Calas (sandstone bedrock). Yellow, magenta and blue lines represent the regression lines of the model for each bedrock type. Each panel also shows R^2 model values and ANOVA P-values (Pv) for testing significance of niche distances.

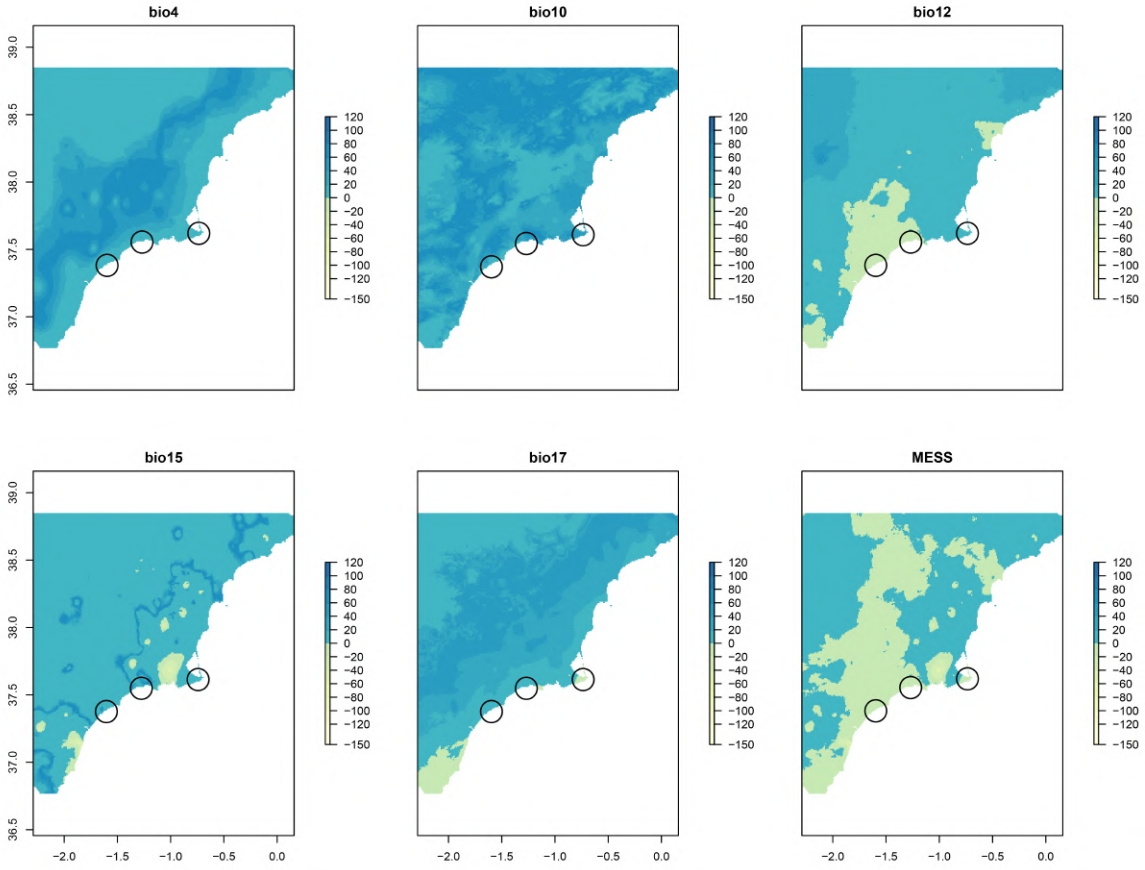

Figure C.6: Multivariate Environmental Similarity Surface (MESS) analysis for the South East of the Iberian Peninsula. We calculated the median similarity between the new environment (extreme episode 2013-2014) and the environment used to fit each species model (average reference period 1979-2012 CHELSA database) for each variable implemented in our models. Negative values are indicative of high environmental dissimilarities between variables.

Table C.1: Carbon and nitrogen content of each studied bedrock, following (Anne 1945, Duchaufour 1970) method.

Bedrock	Locality	Replicate	Organic C (g/100g)	Total N (g/100g)	C:N ratio
		C1	1.42	0.19	7.47
Metamorphic	Calblanque	C2	1.22	0.17	7.18
		C3	3.91	0.31	12.61
		H1	0.71	0.06	11.83
Sandstone	Cuatro Calas	H2	0.94	0.09	10.44
		H3	1.09	0.09	12.11
		M1	3.17	0.35	9.06
Limestone	Moreras	M2	1.83	0.22	8.32
		M3	2.52	0.23	10.96

Table C.2: Summary table of analysed species found in the different study sites. The table shows the species codes used in climatic diagrams and the species families, as well as the study area in which they were found. In the latter column, S represents Cuatro Calas area (sandstone bedrock), M Calblanque area (metamorphic bedrock) and L Moreras Mountain area (limestone bedrock).

SPECIES NAME	SPECIES CODE	FAMILY	LOCALITY
Anthyllis terniflora	ATER	Leguminosae	S
Artemisia barrelieri	ABAR	Asteraceae	S, M
Asparagus horridus	AHOR	Asparagaceae	S, L, M
Chamaerops humilis	CHUM	Arecaceae	M
Cistus Clusii	CCLU	Cistaceae	S, M
Cistus monspeliensis	CMON	Cistaceae	M
Coronilla juncea	CJUN	Leguminosae	M
Dorycnium pentaphyllum	DPEN	Leguminosae	M
Frankenia corymbosa	FCOR	Frankeniaceae	S, M
Fumana ericoides	FERI	Cistaceae	S, L, M
Fumana laevipes	FLAE	Cistaceae	L, M
Fumana thymifolia	FTHY	Cistaceae	L
Genista valentina	GVAL	Leguminosae	L
Globularia alypum	GALY	Plantaginaceae	L
Helianthemum syriacum	HSYR	Cistaceae	M
Helianthemum violaceum	HVIO	Cistaceae	S, L
Helianthemum viscarium	HVIS	Cistaceae	S
Hyparrhenia hirta	HHIR	Poaceae	L
Launaea arborescens	LARB	Asteraceae	S, L, M
Launaea lanifera	LLAN	Asteraceae	S, L
Lavandula dentata	LDEN	Lamiaceae	S
Lycium intricatum	LINT	Solanaceae	S, M
Lygeum spartum	LSPA	Poaceae	M
Paronychia suffruticosa	PSUF	Caryophillaceae	M
Periploca angustifolia	PANG	Apocynaceae	S, L
Rosmarinus officinalis	ROFF	Lamiaceae	S, L, M
Salsola genistoides	SGEN	Amaranthaceae	S, L
Salsola oppositifolia	SOPP	Amaranthaceae	S
Salsola papillosa	SPAP	Amaranthaceae	M
Satureja obovata	SOBO	Lamiaceae	L
Sideritis ibanyezii	SIBA	Lamiaceae	S, M
Stipa tenacissima	STEN	Poaceae	S, L, M
Teucrium capitatum	TCAP	Lamiaceae	S, M
Teucrium freynii	TFRE	Lamiaceae	L
Teucrium lanigerum	TLAN	Lamiaceae	S, L
Thymelaea hirsuta	THIR	Thymelaeaceae	S, L, M
Thymus hyemalis	THYE	Lamiaceae	S, L, M

Table C.3: Final generalized mix models applied for Remaining Green Canopy (RGC) and mortality respectively.

Response variable	Explanatory variables	Random effects
RGC	$centroid\,distance\,av + lithology + centroid\,distance\,av : lithology$	$species + plot$
RGC	$limit\,distance\,av : in\,out\,av + lithology$	$species + plot$
mortality	$centroid\,distance\,av + lithology$	$species + plot$
mortality	$limit\,distance\,av : in\,out\,av + lithology$	$species + plot$
RGC	$centroid\,distance\,av + lithology + centroid\,distance\,av : lithology$	$species + plot$
RGC	$limitdistance\,av : in\,out\,av + lithology$	$species + plot$
mortality	$centroid\,distance\,av + lithology$	$species + plot$
mortality	$limit\,distance\,av : in\,out\,av + lithology$	$species + plot$
RGC	$climatic\,suitability\,av + lithology + climatic\,suitability\,av : lithology$	$species + plot$
RGC	$climatic\,suitability\,ex + lithology$	$species + plot$

Table C.4: Model accuracy of each sampled species distribution model estimated with MaxEnt. AUC column shows average of 5 alternative models (5-fold cross-validation) and Sd-AUC column shows the standard deviation of AUC values per species.

species	AUC	sd AUC
Anthyllis terniflora	0.998	0.001
Artemisia barrelieri	0.992	0.001
Asparagus horridus	0.974	0.002
Chamaerops humilis	0.990	0.001
Cistus clusii	0.994	0.001
Cistus monspeliensis	0.970	0.002
Coronilla juncea	0.989	0.001
Dorycnium pentaphyllum	0.974	0.002
Frankenia corymbosa	0.993	0.002
Fumana ericoides	0.974	0.004
Fumana laevipes	0.992	0.001
Fumana thymifolia	0.971	0.002
Genista valentina	0.998	0.001
Globularia alypum	0.987	0.001
Helianthemum syriacum	0.988	0.001
Helianthemum violaceum	0.990	0.001
Helianthemum viscarium	0.991	0.005
Helichrysum stoechas	0.959	0.003
Hyparrhenia hirta	0.983	0.001
Launaea arborescens	0.985	0.004
Launaea lanifera	0.992	0.002
Lavandula dentata	0.985	0.003
Lycium intricatum	0.991	0.004
Lygeum spartum	0.978	0.002
Paronychia suffruticosa	0.993	0.001
Periploca angustifolia	0.985	0.008
Rosmarinus officinalis	0.955	0.004
Salsola genistoides	0.998	0.000
Salsola oppositifolia	0.993	0.002
Salsola papillosa	0.998	0.002
Satureja obovata	0.994	0.001
Sideritis ibanyezii	0.998	0.001
Stipa tenacissima	0.990	0.001
Teucrium capitatum	0.997	0.001
Teucrium freynii	0.996	0.002
Teucrium lanigerum	0.997	0.004
Thymelaea hirsuta	0.987	0.002
Thymus hyemalis	0.997	0.001

Table C.5: Results of Generalized Mixed Models explaining Remaining Green Canopy (RGC) as a function of soil bedrock and population distances to species niche centroid during the reference period 1979-2012 and the interaction between these two variables, with plot and species as crossed random effects.

	Estimate	Std. Error	df	t value	Pr(>|t|)	
(Intercept)	56.188	6.439	42.212	8.727	0.000	***
Metamorphic	-0.686	5.906	363.381	-0.116	0.908	
Sandstone	-2.341	4.406	566.555	-0.531	0.595	
Centroid distance	-4.413	2.189	42.493	-2.016	0.050	.
Metamorphic : centroid distance	2.904	1.386	635.260	2.096	0.036	*
Sandstone : centroid distance	-0.538	1.488	670.157	-0.362	0.718	

Table C.6: Results of Generalized Mixed Models explaining Remaining Green Canopy (RGC) as a function of soil bedrock and populations distances to the closest point of species niche limit during the reference period 1979-2012 and the interaction between distance and population position in or out of the niche. The model corresponds to the reference period, with plot and species as crossed random effects.

	Estimate	Std. Error	df	t value	Pr(>|t|)	
(Intercept)	30.626	4.664	66.320	6.567	0.000	***
Metamorphic	8.242	3.259	196.478	2.529	0.012	*
Sandstone	-7.656	2.662	140.782	-2.876	0.005	**
Limit distance : in	12.805	3.703	160.670	3.458	0.001	***
Limit distance : out	25.340	9.626	265.609	2.632	0.009	**

Table C.7: Results of Generalized Mixed Models explaining mortality percentage as a function of soil bedrock and population distances to species niche centroid during the reference period 1979-2012, with plot and species as crossed random effects.

	Estimate	Std. Error	z value	Pr(>|z|)	
(Intercept)	-0.553	0.453	-1.221	0.222	
Metamorphic	-0.898	0.218	-4.124	0.000	***
Sandstone	1.033	0.171	6.054	0.000	***
Centroid distance	-0.021	0.150	-0.141	0.888	

Table C.8: Results of Generalized Mixed Models explaining mortality percentage as a function of soil bedrock and populations distances to the closest point of species niche limit during the reference period 1979-2012 and the interaction between distance and population position in or out of the niche during the reference period, with plot and species as crossed random effects.

	Estimate	Std. Error	z	Pr(>|z|)	
(Intercept)	0.200	0.327	0.611	0.541	
Metamorphic	-1.212	0.204	-5.925	0.000	***
Sandstone	0.865	0.170	5.092	0.000	***
Limit distance : in	-0.864	0.198	-4.364	0.000	***
Limit distance : out	-1.881	0.567	-3.316	0.001	***

Table C.9: Results of Generalized Mixed Models explaining Remaining Green Canopy (RGC) as a function of soil bedrock and population climatic suitability estimated with MaxEnt for the extreme drought episode (2013-2014), and the interaction between these two variables, with plot and species as crossed random effects

	Estimate	Std. Error	df	t value	Pr(>|t|)	
(Intercept)	42.182	3.788	54.362	11.136	0.000	***
Metamorphic	4.873	2.510	117.039	1.941	0.055	.
Sandstone	-8.934	2.718	151.633	-3.287	0.001	**
Climatic suitability	27.623	27.315	563.040	1.011	0.312	
Metamorphic : climatic suitability	-64.222	39.044	608.632	-1.645	0.101	
Sandstone : climatic suitability	4.295	26.351	650.332	0.163	0.871	

Table C.10: Results of Generalized Mixed Models explaining Remaining Green Canopy (RGC) as a function of soil bedrock and population climatic suitability estimated with MaxEnt for the reference period 1979-2012 and the interaction between these two variables, with plot and species as crossed random effects.

	Estimate	Std. Error	df	t value	Pr(>|t|)	
(Intercept)	17.567	6.348	70.157	2.767	0.007	**
Metamorphic	13.452	5.367	536.820	2.506	0.012	*
Sandstone	-4.461	5.114	633.276	-0.872	0.383	
Climatic suitability	57.826	12.387	111.003	4.668	0.000	***
Metamorphic : climatic suitability	-29.566	11.390	604.822	-2.596	0.010	**
Sandstone : climatic suitability	-3.462	12.733	540.867	-0.272	0.786	

Table C.11: Result of lsmeans contrast (post-hoc test) between bedrock types in models relating mortality percentage or remaining green canopy with population distances to niche centroid and to the niche limit during the extreme episode (2013-2014).

model	contrast	estimate	SE	df	t.ratio	p.value	
$rgc\ bedrock + centroid\,distance + bedrock : centroid\,distance$	limestone - metamorphic	-7.350	3.180	494	-2.310	0.0553	.
	limestone - sandstone	4.330	3.360	321	1.287	0.4033	
	metamorphic - sandstone	11.680	2.900	2580	4.027	0.0002	***
$rgc\ bedrock + limitdistance : in\ out$	limestone - metamorphic	-12.890	3.270	1290	-3.943	0.0002	***
	limestone - sandstone	-1.440	4.160	636	-0.346	0.9363	
	metamorphic - sandstone	11.450	2.910	1951	3.938	0.0003	***
$mortality\,per\ bedrock + centroid\,distance + bedrock : centroid\,distance$	limestone - metamorphic	0.841	0.261	Inf	3.226	0.0036	**
	limestone - sandstone	-0.937	0.279	Inf	-3.360	0.0022	**
	metamorphic - sandstone	-1.778	0.179	Inf	-9.937	<.0001	***
$mortality\,per\ bedrcok + limit\,distance : in\ out$	limestone - metamorphic	1.608	0.200	Inf	8.042	<.0001	***
	limestone - sandstone	-0.035	0.235	Inf	-0.150	0.9877	
	metamorphic -sandstone	-1.643	0.182	Inf	-9.041	<.0001	***

D

Appendix Chapter 5

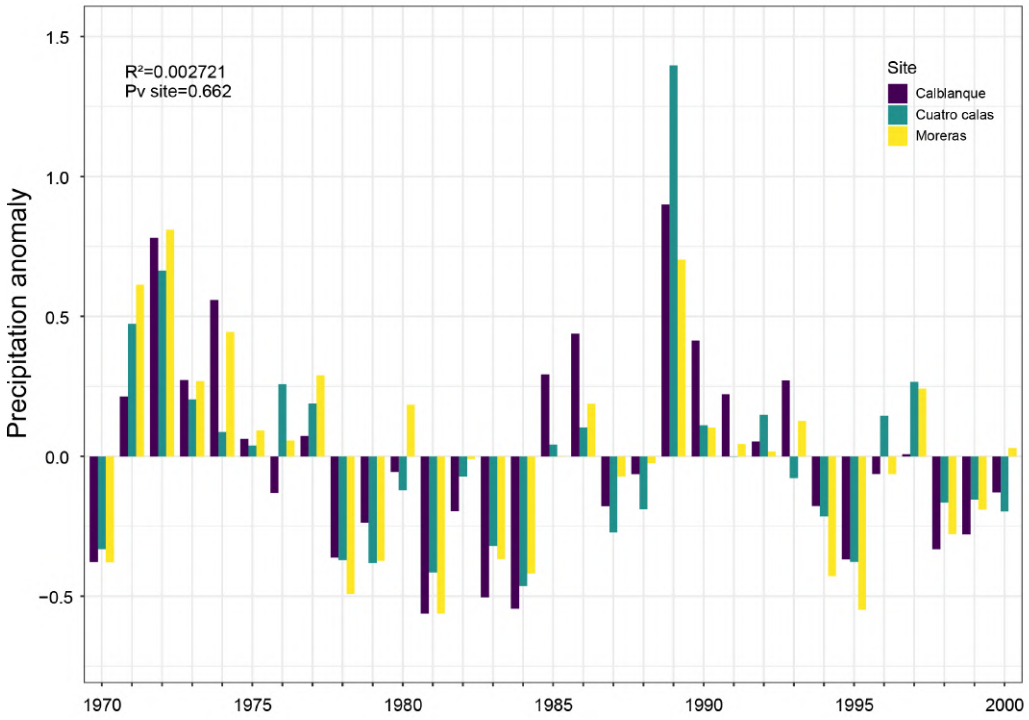

Figure D.1: The graphic shows climatic anomalies for the three studied areas. Red colour represents Moreras Mountain (i.e., limestone bedrock), green colour represents Calblanque Natural Park (i.e. metamorphic bedrock) and blue colour represents Cuatro Calas area (i.e. sandstone bedrock). Yearly anomaly values were calculated as (annual rainfall – mean period rainfall)/ mean period rainfall. Moreover, mix models explaining precipitation anomaly in function of site with year as random effect were performed, showing no significant differences between sites. P value and model marginal R^2 are shown in the bottom left area of the graphic.

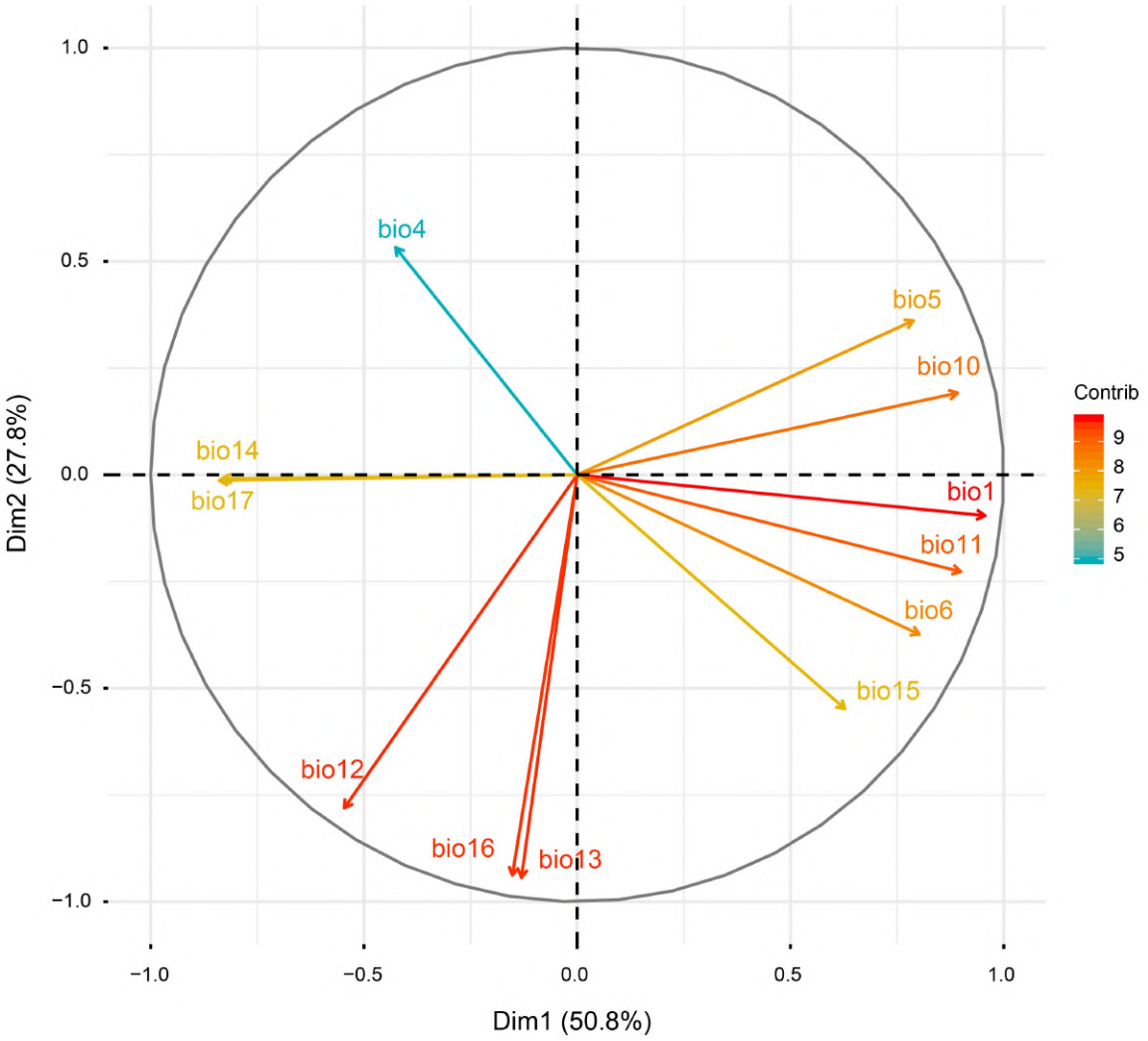

Figure D.2: Correlation circle obtained from PCA from the twelve selected climatic variables. Where BIO1 = Annual Mean Temperature, BIO4 = Temperature Seasonality (standard deviation×100), BIO5 = Max Temperature of Warmest Month, BIO6 = Min Temperature of Coldest Month, BIO10 = Mean Temperature of Warmest Quarter, BIO11 = Mean Temperature of Coldest Quarter, BIO12 = Annual Precipitation, BIO13 = Precipitation of Wettest Month, BIO14 = Precipitation of Driest Month, BIO15 = Precipitation Seasonality (Coefficient of Variation), BIO16 = Precipitation of Wettest Quarter, BIO17 = Precipitation of Driest Quarter. The PCA was calibrated using climatic data from the total filtered 106,876 occurrences from gbif.org for all the 38 sampled species. First and second axes contained 78.5% of explained variability. The variables' colour represents the percentage of each variable' contribution to the PCA.

A)

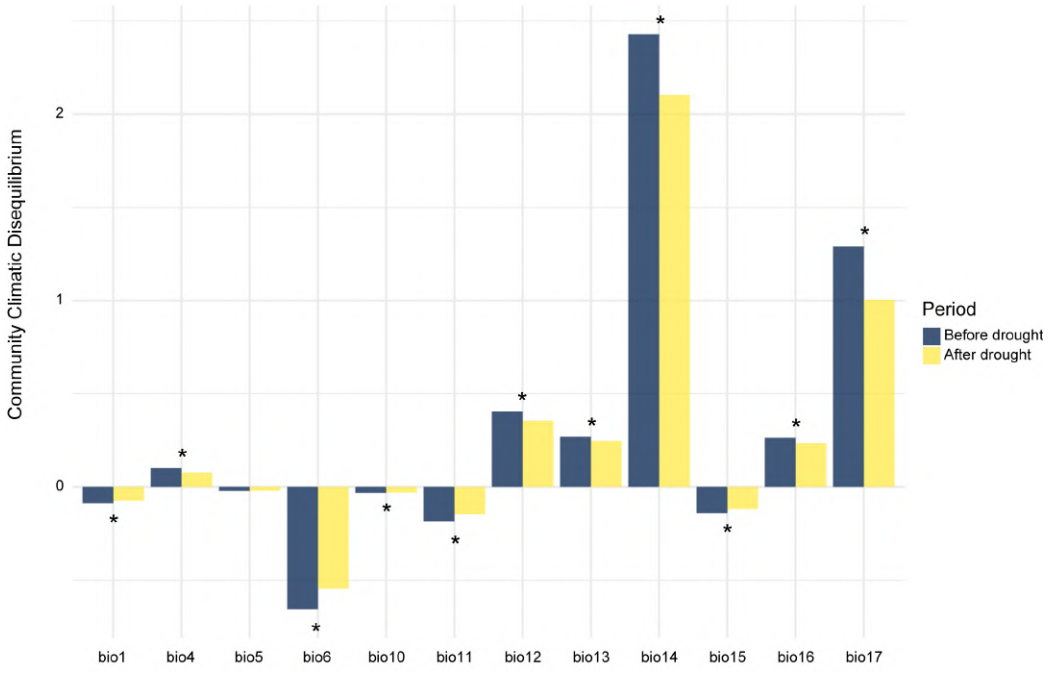
Community Climatic Disequilibrium
2
1
0
bio1
bio4
bio5
bio6
bio10
bio11
bio12
bio13
bio14
bio15
bio16
bio17
Period
Before drought
After drought

B)

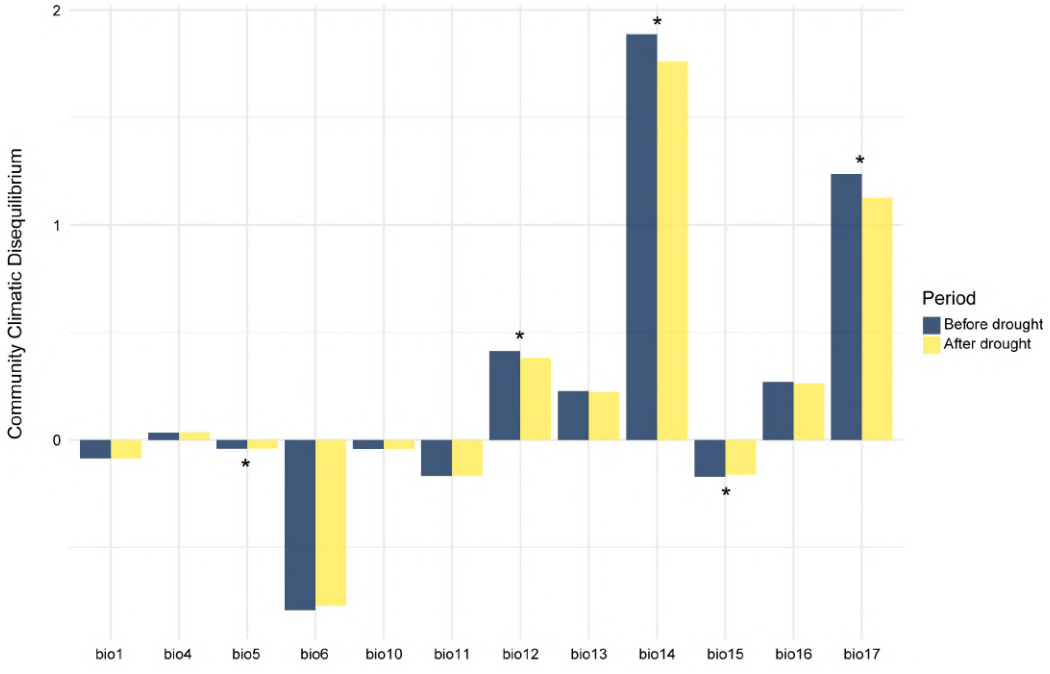
Community Climatic Disequilibrium
2
1
0
bio1
bio4
bio5
bio6
bio10
bio11
bio12
bio13
bio14
bio15
bio16
bio17
Period
Before drought
After drought

C)

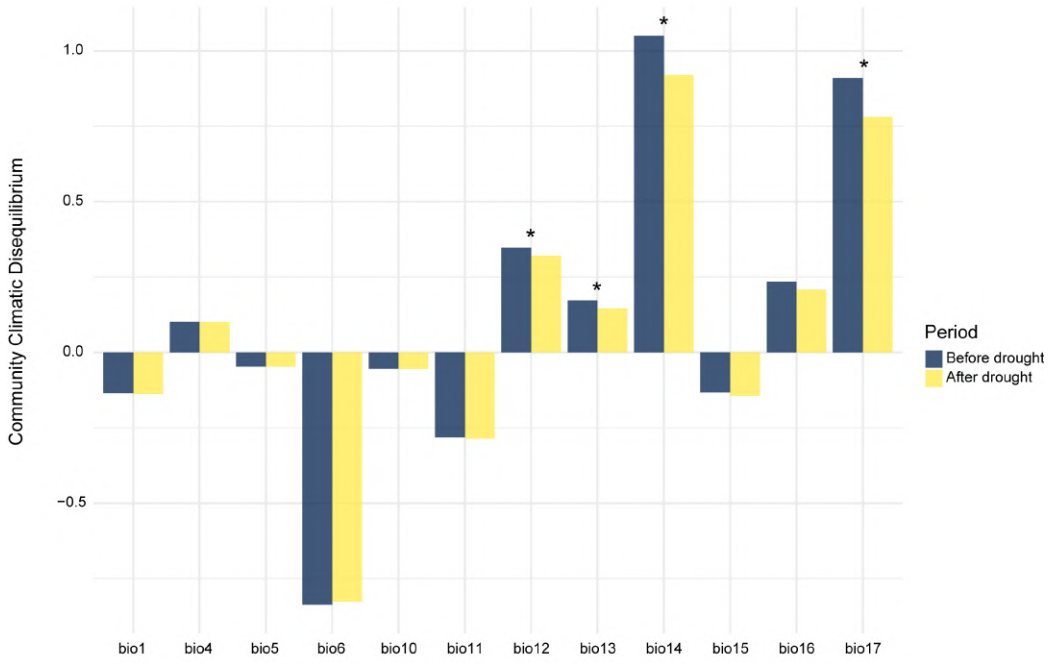

Figure D.3: Univariant community climatic disequilibrium before (average period 1970-2000 Worldclim) and after drought (2013-2014) for each individual climatic variable. Community climatic disequilibrium was estimated as (CIC-OC)/OC per each variable. Variables with * showed significant changes in community disequilibrium after drought. A graphic shows univariant community climatic disequilibrium for sandstone bedrock, B graphic shows univariant community climatic disequilibrium for limestone bedrock and C graphic shows univariant community climatic disequilibrium for metamorphic bedrock.

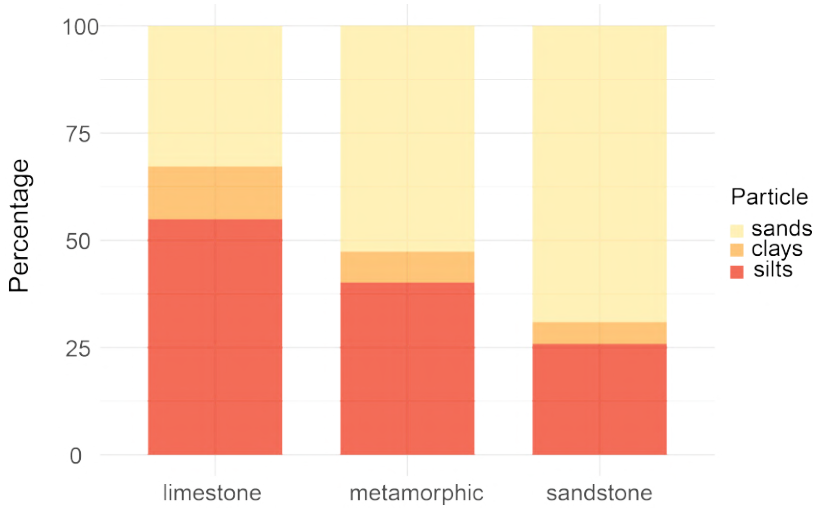

Figure D.4: Soil particle composition of the three different study sites' bedrock (i.e., metamorphic bedrock = Calblanque, limestone bedrock = Moreras Mountain, sandstone bedrock = Cuatro Calas). Yellow colour represents the proportion of sands, orange the proportion of clays and dark orange the proportion of silts.

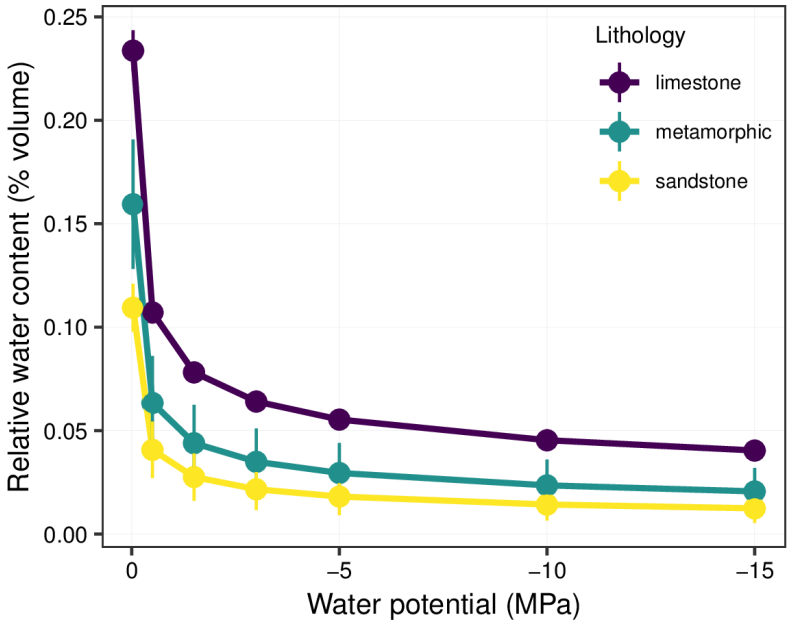

Figure D.5: Soil water content in percentage of volume of different bedrocks under different water potentials, simulated with "medfate" package (Cáceres et al. 2015) using each soil particle composition and organic matter content. In our study we used -0.5 MPa (as field capacity) and -1.5 MPa (as wilting point) but note that regardless of the water potential, limestone bedrock always shows the higher water content, followed by soils in metamorphic and sandstone bedrocks, respectively.

Table D.1: Carbon and nitrogen content of each studied bedrock.

Bedrock	Locality	Replicate	Organic C (g/100g)	Total N (g/100g)	C:N ratio
		C1	1.42	0.19	7.47
Metamorphic	Calblanque	C2	1.22	0.17	7.18
		C3	3.91	0.31	12.61
		H1	0.71	0.06	11.83
Sandstone	Cuatro Calas	H2	0.94	0.09	10.44
		H3	1.09	0.09	12.11
		M1	3.17	0.35	9.06
Limestone	Moreras	M2	1.83	0.22	8.32
		M3	2.52	0.23	10.96

Table D.2: Summary table of analysed species found in the different study sites. The table shows the species codes used in climatic diagrams and the species families, as well as the study area in which they were found. In the latter column, S represents the Cuatro calas area (sandstone bedrock), M the Calblanque area (metamorphic bedrock) and L the Moreras Mountain area (limestone bedrock).

SPECIES NAME	SPECIES CODE	FAMILY	LOCALITY
Anthyllis terniflora	ATER	Leguminosae	S
Artemisia barrelieri	ABAR	Asteraceae	S, M
Asparagus horridus	AHOR	Asparagaceae	S, L, M
Chamaerops humilis	CHUM	Arecaceae	M
Cistus Clusii	CCLU	Cistaceae	S, M
Cistus monspeliensis	CMON	Cistaceae	M
Coronilla juncea	CJUN	Leguminosae	M
Dorycnium pentaphyllum	DPEN	Leguminosae	M
Frankenia corymbosa	FCOR	Frankeniaceae	S, M
Fumana ericoides	FERI	Cistaceae	S, L, M
Fumana laevipes	FLAE	Cistaceae	L, M
Fumana thymifolia	FTHY	Cistaceae	L
Genista valentina	GVAL	Leguminosae	L
Globularia alypum	GALY	Plantaginaceae	L
Helianthemum syriacum	HSYR	Cistaceae	M
Helianthemum violaceum	HVIO	Cistaceae	S, L
Helianthemum viscarium	HVIS	Cistaceae	S
Hyparrhenia hirta	HHIR	Poaceae	L
Launaea arborescens	LARB	Asteraceae	S, L, M
Launaea lanifera	LLAN	Asteraceae	S, L
Lavandula dentata	LDEN	Lamiaceae	S
Lycium intricatum	LINT	Solanaceae	S, M
Lygeum spartum	LSPA	Poaceae	M
Paronychia suffruticosa	PSUF	Caryophillaceae	M
Periploca angustifolia	PANG	Apocynaceae	S, L
Rosmarinus officinalis	ROFF	Lamiaceae	S, L, M
Salsola genistoides	SGEN	Amaranthaceae	S, L
Salsola oppositifolia	SOPP	Amaranthaceae	S
Salsola papillosa	SPAP	Amaranthaceae	M
Satureja obovata	SOBO	Lamiaceae	L
Sideritis ibanyezii	SIBA	Lamiaceae	S, M
Stipa tenacissima	STEN	Poaceae	S, L, M
Teucrium capitatum	TCAP	Lamiaceae	S, M
Teucrium freynii	TFRE	Lamiaceae	L
Teucrium lanigerum	TLAN	Lamiaceae	S, L
Thymelaea hirsuta	THIR	Thymelaeaceae	S, L, M
Thymus hyemalis	THYE	Lamiaceae	S, L, M

Table D.3: Least squared means pairwise test results. These analyses were performed controlling the effect of the rest of the factors.

CONTRAST	ESTIMATE	SE	DF	T.RATIO	P.VALUE
sandstone after - sadstone before	-0.277	0.052	87.00	-5.349	<.0001
limestone after - limestone before	-0.113	0.052	87.00	-2.186	0.0315
metamorphic after - metamorphic before	0.013	0.052	87.00	0.246	0.8064
limestone after - metamorphic after	-0.200	0.142	99.33	-1.410	0.3397
limestone after - sandstone after	0.580	0.142	99.33	4.084	0.0003
metamorphic after -sandstone after	0.781	0.142	99.33	5.494	<.0001
limestone before - metamorphic before	-0.074	0.142	99.33	-0.523	0.8604
limestone before - sandstone before	0.417	0.142	99.33	2.931	0.0116
metamorphic before - sandsone before	0.491	0.142	99.33	3.454	0.0023

Acronyms

AEMET: Agencia Estatal de Meteorología (Spanish Meteorological Agency)

AIC:Akaike Information Criterion

AUC: Area Under ROC (Receiver-Operator Characteristic) Curve

BRT: Boosted Regression Trees

CD: Climatic Disequilibrium

CIC: Community Inferred Climate

CPH: Centre-Periphery Hypothesis (also known as distance-abundance hypothesis)

ECS: Episodic Climatic Suitability

ENM: Ecological Niche Models

GAM: Generalized Additive Models

GBIF: Global Biodiversity Information Facility

GLM: Generalized Linear Models

HCS: Historical Climatic Suitability

IPCC: Intergovernmental Panel on Climate Change

IUSS: International Union of Soil Sciences

MESS: Multivariate Environmental Suitability Surface

OC: Observed climate

PCA: Principal Component Analysis

RGC: Remaining Green Canopy

SDM: Species Distribution Models

VIF: Variance Inflation Factor

References

Abeli, T. et al. 2014. Effects of marginality on plant population performance. - J. Biogeogr. 41: 239–249.

Ackerly, D. D. 2003. Community Assembly , Niche Conservatism , and Adaptive Evolution in Changing Environments. - Int. J. Plant Sci. 164: 164–184.

Ackerly, D. D. et al. 2010. The geography of climate change: Implications for conservation biogeography. - Divers. Distrib. 16: 476–487.

Adler, P. B. et al. 2013. Trait-based tests of coexistence mechanisms. - Ecol. Lett. 16: 1294–1306.

AEMET (Spanish Meteorological Agency) 2014. Avance climatológico mensual mes de septiembre 2014 en la Región de Murcia.

AEMET (Spanish Meteorological Agency) and IP (Portuguese Meteorological Insitute) 2011. Iberian climate atlas. Air temperature and precipitation (1971-2000) (MR y M Ministerio de Medio Ambiente, Ed.).

Aitken, S. N. et al. 2008. Adaptation, migration or extirpation: climate change outcomes for tree populations. - Evol. Appl. 1: 95–111.

Alexander, J. M. et al. 2016. When Climate Reshuffles Competitors: A Call for Experimental Macroecology. - Trends Ecol. Evol. 31: 831–841.

Allen, C. D. and Breshears, D. D. 1998a. Drought-induced shift of a forest – woodland ecotone: Rapid landscape response to climate variation. - Ecology 95: 14839–14842.

Allen, C. D. and Breshears, D. D. 1998b. Drought-induced shift of a forest-woodland ecotone: rapid landscape response to climate variation. - Proc. Natl. Acad. Sci.

U. S. A. 95: 14839–42.

Allen, C. D. et al. 2010. A global overview of drought and heat-induced tree mortality reveals emerging climate change risks for forests. - For. Ecol. Manage. 259: 660–684.

Allen, C. D. et al. 2015. On underestimation of global vulnerability to tree mortality and forest die-off from hotter drought in the Anthropocene. - Ecosphere 6: art129.

Anderegg, W. R. L. et al. 2012. The roles of hydraulic and carbon stress in a widespread climate-induced forest die-off. - Proc. Natl. Acad. Sci. 109: 233–237.

Anderson, R. P. et al. 2002. Using niche-based GIS modeling to test geographic predictions of competitive exclusion and competitive release in South American pocket mice. - Oikos 98: 3–16.

Anne, P. 1945. Carbone organique (total) du sol et de l'humus. - Ann. Agron. 15: 161–172.

Araújo, M. B. and Guisan, A. 2006. Five (or so) challenges for species distribution modelling. - J. Biogeogr. 33: 1677–1688.

Araújo, M. B. and New, M. 2007. Ensemble forecasting of species distributions. - Trends Ecol. Evol. 22: 42–47.

Araújo, M. B. et al. 2013. Heat freezes niche evolution (D Sax, Ed.). - Ecol. Lett. 16: 1206–1219.

Araújo, M. B. et al. 2019. Standards for distribution models in biodiversity assessments. - Sci. Adv. 5: eaat4858.

Ashraf, M. et al. 2011. Drought Tolerance: Roles of Organic Osmolytes, Growth Regulators, and Mineral Nutrients. - Adv. Agron. 111: 249–296.

Austin, M. 1971. The role of regression analysis in plant ecology. - Proc. Ecol. Soc. Aust. 6: 63–75.

Austin, M. P. et al. 1990. Measurement of the Realized Qualitative Niche: Environmental Niches of Five Eucalyptus Species. - Ecol. Monogr. 60: 161–177.

Barbet-Massin, M. et al. 2012. Selecting pseudo-absences for species distribution

models: How, where and how many? - Methods Ecol. Evol. 3: 327–338.

Barry, J. P. et al. 1995. Climate-Related, Long-Term Faunal Changes in a California Rocky Intertidal Community. Science. 267: 672–675.

Barve, N. et al. 2011. The crucial role of the accessible area in ecological niche modeling and species distribution modeling. - Ecol. Modell. 222: 1810–1819.

Belyea, L. R. and Lancaster, J. 1999. Assembly Rules within a Contingent Ecology. - Oikos 86: 402.

Benito Garzón, M. et al. 2011. Intra-specific variability and plasticity influence potential tree species distributions under climate change. - Glob. Ecol. Biogeogr. 20: 766–778.

Bernard-Verdier, M. et al. 2012. Community assembly along a soil depth gradient: Contrasting patterns of plant trait convergence and divergence in a Mediterranean rangeland (H Cornelissen, Ed.). - J. Ecol. 100: 1422–1433.

Bertrand, R. et al. 2012. Disregarding the edaphic dimension in species distribution models leads to the omission of crucial spatial information under climate change: The case of Quercus pubescens in France. - Glob. Chang. Biol. 18: 2648–2660.

Bertrand, R. et al. 2016. Ecological constraints increase the climatic debt in forests. - Nat. Commun. 7: 12643.

Bigler, C. et al. 2006. Drought as an inciting mortality factor in scots pine stands of the Valais, Switzerland. - Ecosystems 9: 330–343.

Blonder, B. et al. 2014. The n-dimensional hypervolume. - Glob. Ecol. Biogeogr. 23: 595–609.

Blonder, B. et al. 2015. Linking environmental filtering and disequilibrium to biogeography with a community climate framework. - Ecology 96: 972–985.

Blonder, B. et al. 2017. Predictability in community dynamics. - Ecol. Lett. 20: 293–306.

Bowler, D. and Böhning-Gaese, K. 2017. Improving the community-temperature index as a climate change indicator. - PLoS One 12: 1–17.

Boyce, M. S. et al. 2002. Evaluating resource selection functions. - Ecol. Modell. 157: 281–300.

Bramer, I. et al. 2018. Advances in Monitoring and Modelling Climate at Ecologically Relevant Scales. - Adv. Ecol. Res. 58: 101–161.

Braun-Blanquet, J. and Bolòs, O. 1957. The plant communities of the Central Ebro Basin and their dynamics. - An. la Estac. Exp. Aula Dei 5: 1–266.

Breiner, F. T. et al. 2017. Including environmental niche information to improve IUCN Red List assessments (B Schröder, Ed.). - Divers. Distrib. 23: 484–495.

Broennimann, O. and Guisan, A. 2008. Predicting current and future biological invasions: both native and invaded ranges matter. - Biol. Lett. 4: 585–9.

Broennimann, O. et al. 2006. Do geographic distribution, niche property and life form explain plants' vulnerability to global change? - Glob. Chang. Biol. 12: 1079–1093.

Broennimann, O. et al. 2012. Measuring ecological niche overlap from occurrence and spatial environmental data. - Glob. Ecol. Biogeogr. 21: 481–497.

Brown, J. H. 1984. On the Relationship between Abundance and Distribution of Species. - Am. Nat. 124: 255–279.

Cáceres, M. De et al. 2015. Coupling a water balance model with forest inventory data to predict drought stress: the role of forest structural changes vs. climate changes. - Agric. For. Meteorol. 213: 77–90.

Cadotte, M. W. and Tucker, C. M. 2017. Should Environmental Filtering be Abandoned? - Trends Ecol. Evol. 32: 429–437.

Carnicer, J. et al. 2011. Widespread crown condition decline, food web disruption, and amplified tree mortality with increased climate change-type drought. - Proc. Natl. Acad. Sci. U. S. A. 108: 1474–8.

Cassel, D. K. and Nielsen, D. R. 1986. Field capacity and available water capacity. - In: Klute, A. (ed), Methods of Soil Analysis: Part 1—Physical and Mineralogical Methods. Agronomy m. Soil Science Society of America, pp. 901–926.

Clark, J. D. et al. 1993. A Multivariate Model of Female Black Bear Habitat Use for a Geographic Information System. - J. Wildl. Manage. 57: 519.

Colwell, R. K. and Rangel, T. F. 2009. Hutchinson's duality: the once and future niche. - Proc. Natl. Acad. Sci. U. S. A. 106 Suppl 2: 19651–8.

Colwell, R. K. et al. 2008. Global Warming, Elevational Range Shifts, and Lowland Biotic Attrition in the Wet Tropics. Science. 322: 258–261.

Cornwell, W. K. and Ackerly, D. D. 2009. Community Assembly and Shifts in Plant Trait Distributions across an Environmental Gradient in Coastal California. - Source Ecol. Monogr. 79.

Coumou, D. and Rahmstorf, S. 2012. A decade of weather extremes. - Nat. Clim. Chang. 2: 491–496.

Csergő, A. M. et al. 2017. Less favourable climates constrain demographic strategies in plants (J Gurevitch, Ed.). - Ecol. Lett. 20: 969–980.

D'Amen, M. et al. 2017. Spatial predictions at the community level: From current approaches to future frameworks. - Biol. Rev. 92: 169–187.

Dallas, T. A. and Hastings, A. 2018. Habitat suitability estimated by niche models is largely unrelated to species abundance. - Glob. Ecol. Biogeogr. 27: 1448–1456.

Dallas, T. et al. 2017a. Species are not most abundant in the centre of their geographic range or climatic niche. - Ecol. Lett. 20: 1526–1533.

Dallas, T. et al. 2017b. Species are not most abundant in the centre of their geographic range or climatic niche. - Ecol. Lett. 20: 1526–1533.

Davis, M. B. 1986. Climatic Instability, Time, Lags, and Community Disequilibrium.: 269–284.

Davis, M. B. and Shaw, R. G. 2001. Range shifts and adaptive responses to quaternary climate change. Science. 292: 673–679.

Davis, K. T. et al. 2019. Microclimatic buffering in forests of the future: the role of local water balance. - Ecography (Cop.). 42: 1–11.

De Frenne, P. et al. 2013. Microclimate moderates plant responses to macroclimate

warming. - Proc. Natl. Acad. Sci. U. S. A. 110: 18561–5. de la Riva, E. G. et al. 2016a. Leaf Mass per Area (LMA) and Its Relationship with Leaf Structure and Anatomy in 34 Mediterranean Woody Species along a Water Availability Gradient. - PLoS One 11: e0148788.

de la Riva, E. G. et al. 2016b. Disentangling the relative importance of species occurrence, abundance and intraspecific variability in community assembly: a trait-based approach at the whole-plant level in Mediterranean forests. - Oikos 125: 354–363.

de la Riva, E. G. et al. 2017. A Multidimensional Functional Trait Approach Reveals the Imprint of Environmental Stress in Mediterranean Woody Communities. - Ecosystems 21: 248–262.

del Cacho, M. and Lloret, F. 2012. Resilience of Mediterranean shrubland to a severe drought episode: The role of seed bank and seedling emergence. - Plant Biol. 14: 458–466.

Devictor, V. et al. 2012. Differences in the climatic debts of birds and butterflies at a continental scale. - Nat. Clim. Chang. 2: 121–124.

Diaz, S. et al. 1998. Plant functional traits and environmental filters at a regional scale. - J. Veg. Sci. 9: 113–122.

Dormann, C. F. 2007. Promising the future? Global change projections of species distributions. - Basic Appl. Ecol. 8: 387–397.

Duchaufour, P. 1970. Pédologie (M& Paris, Ed.).

Duong, T. 2018. Package "ks". ks: Kernel Smoothing. in press.

Duong, T. and Hazelton, M. L. 2005. Cross-validation bandwidth matrices for multivariate kernel density estimation. - Scand. J. Stat. 32: 485–506.

Easterling, D. R. et al. 2000. Climate Extremes: Observations, Modeling, and Impacts. Science. 289: 2068–2074.

Elith, J. 2006. Novel methods improve prediction of species' distributions from occurrence data: Supplement. - Ecography (Cop.). 29: 129–151.

Elith, J. and Leathwick, J. R. 2009. Species Distribution Models: Ecological Explanation and Prediction Across Space and Time. - Annu. Rev. Ecol. Evol. Syst. 40: 677–697.

Elith, J. and Graham, C. H. 2009. Do they? How do they? WHY do they differ? on finding reasons for differing performances of species distribution models. - Ecography (Cop.). 32: 66–77.

Elith, J. et al. 2002. Mapping epistematic uncertainties and vague concepts in predictions of species distribution. - Ecol. Modell. 157: 313–329.

Elith, J. et al. 2008. A working guide to boosted regression trees. - J. Anim. Ecol. 77: 802–813.

Elith, J. et al. 2010. The art of modelling range-shifting species. - Methods Ecol. Evol. 1: 330–342.

Elton, C. S. 1927. Animal ecology. - University of Chicago Press.

Esteve-Selma, M. A. et al. 2010. Effects of climatic change on the distribution and conservation of Mediterranean forests: The case of Tetraclinis articulata in the Iberian Peninsula. - Biodivers. Conserv. 19: 3809–3825.

Esteve-Selma, M. A. et al. 2015. Cambio climático y biodiversidad en el contexto de la Región de Murcia. - In: Consejería de Agua Agricultura y Medio Ambiente (ed), Cambio climático en la Región de Murcia. Evaluación basada en indicadores. pp. 105–132.

Fick, S. E. and Hijmans, R. J. 2017. WorldClim 2: new 1-km spatial resolution climate surfaces for global land areas. - Int. J. Climatol. 37: 4302–4315.

Fielding, A. H. and Bell, J. F. 1997. A review of methods for the assessment of prediction errors in conservation presence/absence models. - Environ. Conserv. 24: 38–49.

Franklin, J. 2010. Mapping species distributions. Spatial inference and prediction. - Cambridge University Press.

Franklin, J. et al. 2013. Modeling plant species distributions under future climates: how fine scale do climate projections need to be? - Glob. Chang. Biol. 19:

473–483.

Franklin, J. et al. 2016. Global change and terrestrial plant community dynamics. - Proc. Natl. Acad. Sci. 113: 3725–3734.

Franks, S. J. et al. 2014. Evolutionary and plastic responses to climate change in terrestrial plant populations. - Evol. Appl. 7: 123–139.

Freckleton, R. P. et al. 2002. Phylogenetic Analysis and Comparative Data: 160: 712–726.

Fridley, J. 2009. Downscaling Climate over Complex Terrain: High Finescale (<1000 m) Spatial Variation of Near-Ground Temperatures in a Montane Forested Landscape (Great Smoky Mountains)*. - J. Appl. Meteorol. Climatol. 48: 1033–1049.

Fridley, J. D. et al. 2011. Soil heterogeneity buffers community response to climate change in species-rich grassland. - Glob. Chang. Biol. 17: 2002–2011.

Galiano, L. et al. 2010. Drought-Induced Multifactor Decline of Scots Pine in the Pyrenees and Potential Vegetation Change by the Expansion of Co-occurring Oak Species. - Ecosystems 13: 978–991.

Gause, G. F. (Georgiĭ F. 1934. The struggle for existence (Williams & Wilkin, Ed..

Gaüzère, P. et al. 2018. Empirical Predictability of Community Responses to Climate Change. - Front. Ecol. Evol. 6: 186.

GBIF.org (18 January 2019), GBIF Occurrence Download `https://doi.org/10.15468/dl.er7c3e`

Gee, G. W. and Bauder, J. W. 1986. Particle size analysis. - In: Klute, A. (ed), Methods of Soil Analysis: Part 1—Physical and Mineralogical Methods. Soil Science Society of America, pp. 383–411.

Geiger, R. et al. 1995. The Climate Near the Ground. - Vieweg+Teubner Verlag.

Giorgi, F. and Lionello, P. 2008. Climate change projections for the Mediterranean region. - Glob. Planet. Change 63: 90–104.

Gotelli, N. J. et al. 2010. Macroecological signals of species interactions in the Danish avifauna. - Proc. Natl. Acad. Sci. U. S. A. 107: 5030–5.

Graae, B. J. et al. 2018. Stay or go – how topographic complexity influences alpine plant population and community responses to climate change. - Perspect. Plant Ecol. Evol. Syst. 30: 41–50.

Graham, C. H. et al. 2004. Integrating phylogenetics and environmental niche models to explore speciation mechanisms in dendrobatid frogs. - Evolution 58: 1781–93.

Grant, P. R. et al. 2016. Evolution caused by extreme events. - Philos. Trans. R. Soc. Lond. B. Biol. Sci. 372: 20160146.

Greenwood, S. et al. 2017. Tree mortality across biomes is promoted by drought intensity, lower wood density and higher specific leaf area. - Ecol. Lett. 20: 539–553.

Grinnell, J. 1917. The Niche-Relationships of the California Thrasher. - Auk 34: 427–433.

Guiot, J. and Cramer, W. 2016. Climate change: The 2015 Paris Agreement thresholds and Mediterranean basin ecosystems. Science. 354: 4528–4532.

Guisan, A. and Zimmermann, N. E. 2000. Predictive habitat distribution models in ecology. - Ecol. Modell. 135: 147–186.

Guisan, A. and Thuiller, W. 2005. Predicting species distribution: Offering more than simple habitat models. - Ecol. Lett. 8: 993–1009.

Guisan, A. et al. 2013. Predicting species distributions for conservation decisions (H Arita, Ed.). - Ecol. Lett. 16: 1424–1435.

Guisan, A. et al. 2014. Unifying niche shift studies: insights from biological invasions. - Trends Ecol. Evol. 29: 260–269.

Guisan, A. et al. 2017. Habitat Suitability and Distribution Models (Cambridge University Press, Ed.). - Cambridge University Press.

Guisan, A. et al. 2019. Scaling the linkage between environmental niches and functional traits for improved spatial predictions of biological communities (A Hampe, Ed.). - Glob. Ecol. Biogeogr.: geb.12967.

Hamerlynck, E. P. and McAuliffe, J. R. 2008. Soil-dependent canopy die-back and

plant mortality in two Mojave Desert shrubs. - J. Arid Environ. 72: 1793–1802.

Hampe, A. and Petit, R. J. 2005. Conserving biodiversity under climate change: the rear edge matters. - Ecol. Lett. 8: 461–467.

Hanley, A. J. and McNeil, J. B. 1982. The Meaning and Use of the Area under a Receiver Operating Characteristic (ROC) Curve. - Radiology 143: 29–36.

Hannah, L. et al. 2007. Protected area needs in a changing climate. - Front. Ecol. Environ. 5: 131–138.

Hanski, I. 1999. Metapopulation ecology. - Oxford University Press.

Hewitt, G. 2000. The genetic legacy of the Quaternary ice ages. - Nature 405

Hijmans, R. J. et al. 2005. Very high resolution interpolated climate surfaces for global land areas. - Int. J. Climatol. 25: 1965–1978.

Hijmans, R. J. et al. 2011. Package 'dismo .' - October: 55.

Hijmans, A. R. J. et al. 2016. Package 'dismo' Species Distribution Modeling. - `https://cran.r-project.org/web/packages/dismo/dismo.pdf`: (accesed 11.01.2016).

HilleRisLambers, J. et al. 2012. Rethinking Community Assembly through the Lens of Coexistence Theory. - Annu. Rev. Ecol. Evol. Syst. 43: 227–248.

Hirzel, A. H. et al. 2006. Evaluating the ability of habitat suitability models to predict species presences. - Ecol. Modell. 199: 142–152.

Holt, R. D. 2009. Bringing the Hutchinsonian niche into the 21st century: Ecological and evolutionary perspectives. - Proc. Natl. Acad. Sci. U. S. A. 106: 19659–19665.

Holt, R. D. et al. 2005. Theoretical models of species' borders: single species approaches. - Oikos 108: 18–27.

Hubbell, S. P. 2001. The unified neutral theory of biodiversity and biogeography. - Princeton University Press.

Huberty, C. J. 1994. Applied discriminant analysis. - Wiley.

Huntley, B. and Webb, T. 1989. Migration: Species' Response to Climatic Variations Caused by Changes in the Earth's Orbit. - J. Biogeogr. 16: 5.

Hutchinson, G. E. 1957. Concluding Remarks - The Demographic Symposium as a Heterogeneous Unstable Population. 53: 415–427.

Hutchinson, G. E. (George E. 1978. An introduction to population ecology. - Yale University Press.

IPCC Working Group 1 2014. IPCC Fifth Assessment Report (AR5) - The physical science basis (VB and PMM (eds. . Stocker, T.F., D. Qin, G.-K. Plattner, M. Tignor, S.K. Allen, J. Boschung, A. Nauels, Y. Xia, Ed.).

IUSS Working Group WRB 2015. World Reference Base for Soil Resources 2014, update 2015. International soil classification system for naming soils and creating legends for soil maps. - World Soil Resour. Reports No. 106.

Jackson, S. T. 2009. Introduction. - In: (editor), S. T. J. (ed), Essay on the Geography of Plants. The University of Chicago Press, pp. 1–52.

Jackson, S. T. and Sax, D. F. 2010. Balancing biodiversity in a changing environment: extinction debt, immigration credit and species turnover. - Trends Ecol. Evol. 25: 153–160.

Jaime, L. et al. 2019. Scots pine (Pinus sylvestris L.) mortality is explained by the climatic suitability of both host tree and bark beetle populations. - For. Ecol. Manage. 448: 119–129.

Jentsch, A. et al. 2007. A new generation of events , not trends experiments. - Front. Ecol. Environ. 5: 365–374.

Jump, A. S. and Woodward, F. I. 2003. Seed production and population density decline approaching the range-edge of Cirsium species. - New Phytol. 160: 349–358.

Jump, A. S. et al. 2006. Rapid climate change-related growth decline at the southern range edge of Fagus sylvatica. - Glob. Chang. Biol. 12: 2163–2174.

Jump, A. S. et al. 2009. The altitude-for-latitude disparity in the range retractions of woody species. - Trends Ecol. Evol. 24: 694–701.

Karger, D. N. et al. 2017. Climatologies at high resolution for the earth's land surface areas. - Sci. Data 4: 170122.

Kearney, M. 2006. Habitat , en v ironment and niche: what are we modelling? - Oikos 115: 186–191.

Kearney, M. and Porter, W. 2009. Mechanistic niche modelling: Combining physiological and spatial data to predict species' ranges. - Ecol. Lett. 12: 334–350.

Keddy, P. A. 1992. Assembly and response rules: two goals for predictive community ecology. - J. Veg. Sci. 3: 157–164.

Kreyling, J. et al. 2011. Stochastic trajectories of succession initiated by extreme climatic events. - Ecol. Lett. 14: 758–764.

Kruckeberg, A. R. 2002. Geology and plant life: the effects of landforms and rock types on plants. - University of Washington Press.

Kuussaari, M. et al. 2009. Extinction debt: a challenge for biodiversity conservation. - Trends Ecol. Evol. 24: 564–571.

Kuznetsova, A. et al. 2017. lmerTest Package: Tests in Linear Mixed Effects Models. - J. Stat. Softw. 82: 1–26.

Lázaro, R. et al. 2001. Analysis of a 30-year rainfall record (1967–1997) in semi–arid SE Spain for implications on vegetation. - J. Arid Environ. 48: 373–395.

Leathwick, J. R. 1998. Are New Zealand's Nothofagus species in equilibrium with their environment? - J. Veg. Sci. 9: 719–732.

Lembrechts, J. J. et al. 2019a. Comparing temperature data sources for use in species distribution models: From in-situ logging to remote sensing. - Glob. Ecol. Biogeogr.: geb.12974.

Lembrechts, J. J. et al. 2019b. Incorporating microclimate into species distribution models. - Ecography (Cop.). 42: 1267–1279.

Lenoir, J. and Svenning, J.-C. 2015. Climate-related range shifts - a global multidimensional synthesis and new research directions. - Ecography (Cop.). 38: 15–28.

Lenoir, J. et al. 2008. A Significant Upward Shift in Plant Species Optimum Elevation

During the 20th Century. Science. 320: 1768–1771. Lenoir, J. et al. 2013. Local temperatures inferred from plant communities suggest strong spatial buffering of climate warming across Northern Europe. - Glob. Chang. Biol. 19: 1470–1481.

Lenth, R. V. 2016. Least-Squares Means: The R Package lsmeans. - J. Stat. Softw. 69: 1–33.

Lesica, P. and Crone, E. E. 2016. Arctic and boreal plant species decline at their southern range limits in the Rocky Mountains. - Ecol. Lett.: 166–174.

Lévesque, M. et al. 2016. Soil nutrients influence growth response of temperate tree species to drought (R Jones, Ed.). - J. Ecol. 104: 377–387.

Li, Y. and Shipley, B. 2018. Community divergence and convergence along experimental gradients of stress and disturbance. - Ecology 99: 775–781.

Li, Y. et al. 2018. Habitat filtering determines the functional niche occupancy of plant communities worldwide. - J. Ecol. 106: 1001–1009.

Lloret, F. and Granzow-de la Cerda, I. 2013. Plant competition and facilitation after extreme drought episodes in Mediterranean shrubland: Does damage to vegetation cover trigger replacement by juniper woodland? - J. Veg. Sci. 24: 1020–1032.

Lloret, F. and García, C. 2016. Inbreeding and neighbouring vegetation drive drought-induced die-off within juniper populations (K Field, Ed.). - Funct. Ecol. 30: 1696–1704.

Lloret, F. and Kitzberger, T. 2018. Historical and event-based bioclimatic suitability predicts regional forest vulnerability to compound effects of severe drought and bark beetle infestation. - Glob. Chang. Biol. in press.

Lloret, F. et al. 2012. Extreme climatic events and vegetation: The role of stabilizing processes. - Glob. Chang. Biol. 18: 797–805.

Lloret, F. et al. 2016. Climatic events inducing die-off in Mediterranean shrublands: are species responses related to their functional traits? - Oecologia 180: 961–973.

Lomolino, M. V. et al. 2004. Foundations of biogeography: classic papers with commentaries. - University of Chicago Press.

Macarthur, R. and Levins, R. 1967. The Limiting Similarity, Convergence, and Divergence of Coexisting Species. - Am. Nat. 101: 377–385.

Maestre, F. T. and Cortina, J. 2002. Spatial patterns of surface soil properties and vegetation in a Mediterranean semi-arid steppe. - Plant Soil 241: 279–291.

Maggini, R. et al. 2011. Are Swiss birds tracking climate change?: Detecting elevational shifts using response curve shapes. - Ecol. Modell. 222: 21–32.

Maguire, B. and Jr. 1973. Niche Response Structure and the Analytical Potentials of Its Relationship to the Habitat. - Am. Nat. 107: 954 (213–246).

Martinez-Meyer, E. et al. 2013. Ecological niche structure and rangewide abundance patterns of species. - Biol. Lett. 9: 20120637–20120637.

Martínez-Vilalta, J. and Lloret, F. 2016. Drought-induced vegetation shifts in terrestrial ecosystems: The key role of regeneration dynamics. - Glob. Planet. Change 144: 94–108.

Mauri, A. et al. 2016. Pinus halepensis and Pinus brutia in Europe: distribution, habitat, usage and threats. - In: European Atlas of Forest Tree Species. in press.

Mauri, A. et al. 2017. EU-Forest, a high-resolution tree occurrence dataset for Europe. - Sci. Data in press.

Mcdowell, N. et al. 2008. Mechanisms of Plant Survival and Mortality during Drought: Why Do Some Plants Survive while Others Succumb to Drought? - New Phytol. 178: 719–739.

McDowell, N. et al. 2019. Mechanisms of a coniferous woodland persistence under drought and heat. - Environ. Res. Lett. in press.

Mellert, K. H. et al. 2011. Hypothesis-driven species distribution models for tree species in the Bavarian Alps. - J. Veg. Sci. 22: 635–646.

Merow, C. et al. 2013. A practical guide to MaxEnt for modeling species' distributions: what it does, and why inputs and settings matter. - Ecography (Cop.). 36: 1058–1069.

Merow, C. et al. 2014. What do we gain from simplicity versus complexity in species

distribution models? - Ecography (Cop.). 37: 1267–1281.

Miriti, M. N. et al. 2007. Episodic death across species of desert shrubs. - Ecology 88: 32–36.

Morueta-Holme, N. and Svenning, J.-C. 2018. Geography of Plants in the New World: Humboldt's Relevance in the Age of Big Data. - Ann. Missouri Bot. Gard. 103: 315–329.

Mouillot, F. et al. 2002. Simulating climate change impacts on fire frequency and vegetation dynamics in a Mediterranean ecosystem. - Glob. Chang. Biol. 8: 423–437.

Murphy, H. T. et al. 2006. Distribution of abundance across the range in eastern North American trees. - Glob. Ecol. Biogeogr. 15: 63–71.

Niehaus, A. C. et al. 2012. Predicting the physiological performance of ectotherms in fluctuating thermal environments. - J. Exp. Biol. 215: 694–701.

Ninyerola, M. et al. 2000. A methodological approach of climatological modelling of air temperature and precipitation through GIS techniques. - Int. J. Climatol. 20: 1823–1841.

Ninyerola, M. et al. 2007. Monthly precipitation mapping of the Iberian Peninsula using spatial interpolation tools implemented in a Geographic Information System. - Theor. Appl. Climatol. 89: 195–209.

Osorio-Olvera, L. et al. 2019. On population abundance and niche structure. - Ecography (Cop.). 42: 1415–1425.

Parmesan, C. 2006. Ecological and Evolutionary Responses to Recent Climate Change. - Annu. Rev. Ecol. Evol. Syst. 37: 637–669.

Parmesan, C. and Yohe, G. 2003. A globally coherent fingerprint of climate change impacts across natural systems. - Nature 421: 37–42.

Pausas, J. G. and Bond, W. J. 2018. Humboldt and the reinvention of nature. - J. Ecol. in press.

Pearman, P. B. et al. 2008. Niche dynamics in space and time. - Trends Ecol. Evol.

23: 149–158.

Pearson, R. G. and Dawson, T. P. 2003. Predicting the Impacts of Climate Change on the Distribution of Species: Are Bioclimate Envelope Models Useful? - Glob. Ecol. Biogeogr. 12: 361–371.

Pearson, R. G. et al. 2006. Model-based uncertainty in species range prediction. - J. Biogeogr. 33: 1704–1711.

Pearson, D. E. et al. 2018. Community Assembly Theory as a Framework for Biological Invasions. - Trends Ecol. Evol. 33: 313–325.

Peñuelas, J. et al. 2001. Severe drought effects on mediterranean woody flora in Spain. - For. Sci. 47: 214–218.

Pérez-Ramos, I. M. et al. 2017. Climate variability and community stability in Mediterranean shrublands: the role of functional diversity and soil environment (A Zanne, Ed.). - J. Ecol. 105: 1335–1346.

Pérez Navarro, M. Á. et al. 2018. Climatic Suitability Derived from Species Distribution Models Captures Community Responses to an Extreme Drought Episode. - Ecosystems: 1–14.

Peterson, A. T. 2011. Ecological Niches and Geographic Distributions (Princeton University Press, Ed.).

Peterson, A. T. and Vieglais, D. A. 2001. Predicting Species Invasions Using Ecological Niche Modeling: New Approaches from Bioinformatics Attack a Pressing Problem. - Bioscience 51: 363–371.

Peterson, A. T. (Andrew T. et al. 2011. Ecological Niches and Geographic Distributions.

Petitpierre, B. et al. 2012. Climatic Niche Shifts Are Rare Among Terrestrial Plant Invaders. Science. 335: 1344–1348.

Phillips, S. J. and Dudík, M. 2008a. Modeling of species distribution with Maxent: new extensions and a comprehensive evalutation. - Ecography (Cop.). 31: 161–175.

Phillips, S. J. and Dudík, M. 2008b. Modeling of species distributions with Maxent: new extensions and a comprehensive evaluation. - Ecography (Cop.). 31: 161–175.

Piedallu, C. et al. 2013. Soil water balance performs better than climatic water variables in tree species distribution modelling. - Glob. Ecol. Biogeogr. 22: 470–482.

Pironon, S. et al. 2015. Do geographic, climatic or historical ranges differentiate the performance of central versus peripheral populations? - Glob. Ecol. Biogeogr. 24: 611–620.

Pironon, S. et al. 2016. Geographic variation in genetic and demographic performance: new insights from an old biogeographical paradigm. - Biol. Rev.: 000–000.

Pironon, S. et al. 2017. The 'Hutchinsonian niche' as an assemblage of demographic niches: implications for species geographic ranges. - Ecography (Cop.). in press.

Prentice, I. C. et al. 1992. A Global Biome Model Based on Plant Physiology and Dominance, Soil Properties and Climate. - J. Biogeogr. 19: 117.

Pulliam, H. R. 1988. Sources, Sinks, and Population Regulation. - Am. Nat. 132: 652–661.

Pulliam, H. R. 2000. On the relationship between niche and distribution. - Ecol. Lett. 3: 349–361.

Randin, C. F. et al. 2009. Climate change and plant distribution: local models predict high-elevation persistence. - Glob. Chang. Biol. 15: 1557–1569.

Ricklefs, R. E. 2008. Disintegration of the ecological community. - Am. Nat. 172: 741–750.

Rivas-Martínez, S. et al. 2011. Worldwide bioclimatic classification system. - Glob. Geobot. 1: 1–638.

Rivas-Martínez, S. et al. 2017. Bioclimatology of the Iberian Peninsula and the Balearic Islands. - In: Springer, Cham, pp. 29–80.

Sangüesa-Barreda, G. et al. 2018. Delineating limits: Confronting predicted climatic suitability to field performance in mistletoe populations (A Satake, Ed.). - J. Ecol.

106: 2218–2229.

Sapes, G. et al. 2017. Species climatic niche explains drought-induced die-off in a Mediterranean woody community. - Ecosphere 8: e01833.

Schurr, F. M. et al. 2012. How to understand species' niches and range dynamics: A demographic research agenda for biogeography. - J. Biogeogr. 39: 2146–2162.

Segurado, P. and Araújo, M. B. 2004. An evaluation of methods for modelling species distributions. - J. Biogeogr. 31: 1555–1568.

Serra-Diaz, J. M. et al. 2013. Geographical patterns of congruence and incongruence between correlative species distribution models and a process-based ecophysiological growth model (R Pearson, Ed.). - J. Biogeogr. 40: 1928–19338.

Sexton, J. P. et al. 2009. Evolution and Ecology of Species Range Limits. - Annu. Rev. Ecol. Evol. Syst 40: 415–36.

Sexton, J. P. et al. 2014. Genetic isolation by environment or distance: which pattern of gene flow is most common? - Evolution (N. Y). 68: 1–15.

Shantz, H. L. 1927. Drought Resistance and Soil Moisture. - Ecology 8: 145–157.

Sheffield, J. and Wood, Æ. E. F. 2008. Projected changes in drought occurrence under future global warming from multi-model , multi-scenario , IPCC AR4 simulations. - Clim. Dyn. 31: 79–105.

Simpson, A. H. et al. 2016. Soil–climate interactions explain variation in foliar, stem, root and reproductive traits across temperate forests. - Glob. Ecol. Biogeogr. 25: 964–978.

Soberón, J. 2007. Grinnellian and Eltonian niches and geographic distributions of species. - Ecol. Lett. 10: 1115–1123.

Soberón, J. and Nakamura, M. 2009. Niches and distributional areas: Concepts, methods, and assumptions. - Proc. Natl. Acad. Sci. 106: 19645–19650.

Solarik, K. A. et al. 2018. Local adaptation of trees at the range margins impacts range shifts in the face of climate change. - Glob. Ecol. Biogeogr. 27: 1507–1519.

Svenning, J.-C. and Skov, F. 2004. Limited filling of the potential range in European

tree species. - Ecol. Lett. 7: 565–573.

Svenning, J.-C. and Skov, F. 2007. Could the tree diversity pattern in Europe be generated by postglacial dispersal limitation? - Ecol. Lett. 10: 453–460.

Svenning, J. C. and Sandel, B. 2013. Disequilibrium vegetation dynamics under future climate change. - Am. J. Bot. 100: 1266–1286.

Takahashi, K. and Tanaka, S. 2016. Relative importance of habitat filtering and limiting similarity on species assemblages of alpine and subalpine plant communities. - J. Plant Res. 129: 1041–1049.

Thibault, K. M. and Brown, J. H. 2008. Impact of an extreme climatic event on community assembly. - Proc. Natl. Acad. Sci. 105: 3410–3415.

Thomas, C. D. et al. 2004. Extinction risk from climate change. - Nature 427: 145–148.

Thornthwaite, C. W. and Mather, J. R. 1957. Instructions and tables for computing potential evapotranspiration and the water balance,. - Publ. Climatol. 10: 185–311.

Thuiller, W. 2004. Patterns and uncertainties of species' range shifts under climate change. - Glob. Chang. Biol. 10: 2020–2027.

Thuiller, W. 2013. On the importance of edaphic variables to predict plant species distributions - limits and prospects. - J. Veg. Sci. 24: 591–592.

Thuiller, W. et al. 2005a. Niche properties and geographical extent as predictors of species sensitivity to climate change. - Glob. Ecol. Biogeogr. 14: 347–357.

Thuiller, W. et al. 2005b. Climate change threats to plant diversity in Europe. - Proc. Natl. Acad. Sci. U. S. A. in press.

Thuiller, W. et al. 2010. Variation in habitat suitability does not always relate to variation in species' plant functional traits. - Biol. Lett. 6: 120–123.

Thuiller, W. et al. 2014. Does probability of occurrence relate to population dynamics? - Ecography (Cop.). 37: 1155–1166.

Tulloch, A. I. T. et al. 2016. Conservation planners tend to ignore improved accu-

racy of modelled species distributions to focus on multiple threats and ecological processes. - Biol. Conserv. 199: 157–171.

Ulrich, W. et al. 2014. Climate and soil attributes determine plant species turnover in global drylands. - J. Biogeogr. 41: 2307–2319.

Valladares, F. et al. 2004. CAPÍTULO 6 Estrés hídrico: ecofisiología y escalas de la sequía. - In: Valladares, F. (ed), Ecologia del bosque mediterráneo en un mundo cambiante. Ministerio. pp. 163–190.

Valladares, F. et al. 2008. Functional traits and phylogeny: What is the main ecological process determining species assemblage in roadside plant communities? - J. Veg. Sci. 19: 381–392.

Valladares, F. et al. 2014a. Global change and Mediterranean forests: current impacts and potential responses. - In: Forests and Global Change. pp. 47–75.

Valladares, F. et al. 2014b. The effects of phenotypic plasticity and local adaptation on forecasts of species range shifts under climate change. - Ecol. Lett. 17: 1351–1364.

van der Maaten, E. et al. 2017. Species distribution models predict temporal but not spatial variation in forest growth. - Ecol. Evol. 7: 2585–2594.

van Mantgem, P. J. et al. 2009. Widespread Increase of Tree Mortality Rates in the Western United States. Science. 323: 521–524.

VanDerWal, J. et al. 2009. Abundance and the environmental niche: environmental suitability estimated from niche models predicts the upper limit of local abundance. - Am. Nat. 174: 282–91.

Vellend, M. 2010. Conceptual synthesis in community ecology. - Q. Rev. Biol. 85: 183–206.

Vicente-Serrano, S. M. et al. 2013. Response of vegetation to drought time-scales across global land biomes. - Proc. Natl. Acad. Sci. U. S. A. 110: 52–57.

Volterra, V. 1926. Fluctuations in the Abundance of a Species considered Mathematically1. - Nature 118: 558–560.

von Humboldt, A. and Bonpland, A. 1807 (2009). Essay on the geography of plants. Reprint, translated by Sylvie Romanowski, edited with an introduction by S. T. Jackson. in press.

Walther, G.-R. et al. 2009. Alien species in a warmer world: risks and opportunities. - Trends Ecol. Evol. 24: 686–693.

Wan, Z. 2008. New refinements and validation of the MODIS Land-Surface Temperature/Emissivity products. - Remote Sens. Environ. 112: 59–74.

Wang, J. and Maintainer, L. S. C. 2016. Package "MixRF." in press.

Webb, T. 1986. Is vegetation in equilibrium with climate? How to interpret late-Quaternary pollen data. - Vegetatio 67: 75–91.

Webb, C. O. and Donoghue, M. J. 2005. Phylomatic: Tree assembly for applied phylogenetics. - Mol. Ecol. Notes 5: 181–183.

Webb III, T. 1992. Global Changes During the Last 3 Million Years: Climatic Controls and Biotic Responses. - Annu. Rev. eclogy Syst. 23: 141–173.

Weber, M. M. et al. 2016. Is there a correlation between abundance and environmental suitability derived from ecological niche modelling? A meta-analysis. - Ecography (Cop.). 40: 817–828.

Weiher, E. et al. 2011. Advances, challenges and a developing synthesis of ecological community assembly theory. - Philos. Trans. R. Soc. B Biol. Sci. 366: 2403–2413.

Wessels, K. J. et al. 1998. An evaluation of the gradsect biological survey method. - Biodivers. Conserv. 7: 1093–1121.

Wiens, J. J. and Graham, C. H. 2005. Niche Conservatism: Integrating Evolution, Ecology, and Conservation Biology. - Annu. Rev. Ecol. Evol. Syst. 36: 519–539.

Wiens, J. A. et al. 2009. Niches, models, and climate change: Assessing the assumptions and uncertainties. - Proc. Natl. Acad. Sci. 106: 19729–19736.

Woodward, F. I. 1987. Climate and plant distribution. - Cambridge University Press.

Wright, J. W. et al. 2006. Experimental verification of ecological niche modeling in a heterogeneous environment. - Ecology 87: 2433–2439.

Zavaleta, E. S. et al. 2003. Grassland Responses To Three Years of Elevated Temperature, Co 2 , Precipitation, and N Deposition. - Ecol. Monogr. 73: 585–604.

Zimmermann, N. E. et al. 2009. Climatic extremes improve predictions of spatial patterns of tree species. - Proc. Natl. Acad. Sci. U. S. A. 106 Suppl: 19723–8.

Zunzunegui, M. et al. 2005. To live or to survive in Doñana dunes: Adaptive responses of woody species under a Mediterranean climate. - Plant Soil 273: 77–89.